Studies of genome maintenance mechanisms using gene-editing technology

遺伝子改変細胞を用いたゲノム維持機構に関する研究 (英文)

Masato Ooka

Department of chemistry, Graduate school of science and engineering, Tokyo Metropolitan University.

2020

首都大学東京　博士（理学）学位論文（課程博士）

論 文 名
Studies of genome maintenance mechanisms using gene-editing technology

著　者
大岡　正人

審査担当者

主　査

委　員

委　員

委　員

上記の論文を合格と判定する

平成　　年　　月　　日

首都大学東京大学院理工学研究科教授会

研究科長

DISSERTATION FOR A DEGREE OF
DOCTOR OF PHILOSOPHY IN SCIENCE
TOKYO METROPOLITAN UNIVERSITY

TITLE :
Studies of genome maintenance mechanisms using gene-editing technology

AUTHOR :
Masato Ooka

EXAMINED BY

Examiner in chief

Examiner

Examiner

Examiner

QUALIFIED BY THE GRADUATE SCHOOL
OF SCIENCE AND ENGINEERING
TOKYO METROPOLITAN UNIVERSITY

Dean

Date

Index

Abbreviations

ALC	Amplified in Liver Cancer 1
AP site	apurinic/apyrimidinic site
ATP	Adenosine triphosphate
BER	Base excision repair
DDR	DNA damage repair
DDT	DNA damage tolerance
DDX11	DEAD/H-Box Helicase 11
DNA	Deoxyribonucleic acid
DSB	DNA double strand break
ER	Estrogen receptor
FA	Fanconi Anemia
FANC proteins	Fanconi Anemia complementation proteins
H_2O_2	Hydrogen peroxide
HR	Homologous Recombination
ICL	Interstrand cross link
MMS	Methyl methanesulfonate
mRNA	messenger RNA
NCATS	National center for advancing translational science
NHEJ	Non Homologous End Joining
NIH	National institute of Health
PAR	Poly ADP ribose
PARP	Poly (ADP-ribose) polymerase
PCNA	Proliferating cell nuclear antigen
Pol	polymerase
PTM	Post-translational modification
qHTS	quantitative high throughput screening
ROS	Reactive oxygen species
RT	Room temperature
SSB	Single Strand Break
TLS	Translesion DNA synthesis
Top1	Topoisomerase I
Top1-cc	Topoisomerase I DNA Covalent Complexes
TS	Template Switch
UV	Ultra Violet
XRCC1	X-ray repair cross-complementing protein 1
TAM	Tamoxifen

学位論文要旨（博士（理学））

理工学研究科　分子物質化学専攻

大岡　正人

論文題名：Studies of genome maintenance mechanisms using gene-editing technology

邦題：遺伝子改変細胞を用いたゲノム維持機構に関する研究（英文）

Introduction

A genome is a complete set of an organism's genetic information written in chromosomal DNA. Genome information includes all living species' genes. Our body is built and maintained according to the genome information. The genome maintenance system is strictly controlled by a variably of enzymes. This highly organized regulation can be destroyed even by a single nucleotide mutation in our genome, leading to cancer or other severe diseases. Advancements in genome sequencing technology has allowed us to clarify the relationships between diseases and genes. We believe that cancer is caused by genome mutations. The genome DNA is not only damaged by external factors (*eg*. UV and ionizing radiation), but also internal factors caused by our own metabolism. Cells are equipped with several DNA repair pathways to prevent our genome from such DNA damage. Cells use proper repair enzymes and mechanisms according to the type of DNA damage and the cell cycle phase. However, the repair mechanism is not perfect, and cells occasionally fail to repair DNA damage properly. When cells fail to repair DNA damage, unrepaired damage causes mutations, translocation, or other genome instabilities. Although numerous researchers have studied DNA repair mechanisms, there are still many pieces missing. In this study, I analyze the role played by ALC1 chromatin remodeling enzyme in base excision repair (BER), DDX11 helicase enzyme in DNA damage tolerance system, and identify several previously unknown synthetic relationships between genes in genome maintenance. In addition, I have created a high throughput drug screening system, based on DNA damage in cells, to potentially create a novel cancer chemotherapy through synthetic lethality using specific inhibitors for DNA repair enzymes.

The most common DNA damage type is base damage DNA. To repair this damage, base excision repair (BER) is required. Generally, BER consists of three enzymatic-steps: (1) Removal of damaged bases by glycosylase-enzyme, leading the formation of abasic (AP) site. (2) Incision of the DNA backbone at the 5' end of AP site by AP endonuclease-enzyme, yielding single strand breaks (SSBs). (3) The repair of SSBs, which is the slowest enzymatic step in BER and SSBs, can be detected as a BER intermediates. In this process, Poly(ADP-ribose) polymerase (PARP) accumulates at SSBs which causes PARP to induce Poly ADP-ribosylation in PARP itself and chromatin proteins. XRCC1 recognizes this modification and recruits Polβ-enzyme and Lig3-enzyme to the damage site. Polβ-enzyme induces incision of 3' end of AP site and removes the resultant 5'-deoxyribose. DNA polymerase(s) performs gap-filling DNA synthesis leaving a DNA nicked substrate for DNA ligation by Lig3-enzyme. Recently, ALC1, a chromatin remodeling-enzyme, was found to have Poly(ADP-ribose) interacting domain and catalyze PARP-stimulated nucleosome sliding. However, the role played by ALC1 in genome maintenance system has not been elucidated.

Warsaw breakage syndrome, a developmental disorder, is caused by mutations in DDX11 helicase enzyme. This disease shows cellular features of genome instability similar to Fanconi anemia (FA). The

common feature of FA cells is hypersensitivity to interstrand-crosslink (ICL). It is believed that the enzymes mutated in FA are implicated in ICL repair. ICL repair employs several distinct repair pathways such as excision repair, homologous recombination (HR) and translesion DNA synthesis (TLS), which are believed to be orchestrated by the FA enzymes. Generally, helicase enzyme catalyzes the separation of double-stranded DNA into single strands during DNA replication and DNA repair. However, the way DDX11 helicase contributes to ICL repair remains unclear. Moreover, the relationship between DDX11 helicase and FA pathway has been largely unknown.

1. Analysis of the role played by ALC1 in DNA damage repair

I explored ALC1's role in DNA repair. Because ALC1 has Poly(ADP-ribose) interacting domain, I first focused on BER and a genetic relationship with PARP1. In viability assay, *ALC1*$^{-/-}$ mutant shows hypersensitivity to MMS and H_2O_2, which cause base damages. I identified the epistatic relationship between *ALC1*$^{-/-}$ and *PARP1*$^{-/-}$ in cellular resistance to MMS and H_2O_2. I performed alkaline-comet assay, which measures single strand break (SSB), an intermediate of BER. *ALC1*$^{-/-}$ cells showed slower repair-kinetics of SSB than wild-type cells. This data suggests that ALC1 promotes BER after SSB formation. I found that ALC1 contributes to the PARP-dependent promotion of BER without affecting the recruitment of XRCC1 and Polβ to DNA lesions. I thus conclude that ALC1 plays a key role in BER repair coupled with PARP but independent of both of the key repair proteins in BER, XRCC1 and Polβ.

To identify other role(s) of ALC1 in DNA repair, I treated *ALC1*$^{-/-}$ mutant with various DNA damaging agents and measured the sensitivity. Unexpectedly, *ALC1*$^{-/-}$ mutant showed higher sensitivity to Camptothecin (CPT) than wild-type did. CPT induces single-strand breaks covalently attaching to Top1 with its 3' terminus (TOP1-DNA cleavage complex *(TOP1cc)*). To suppress DSB formation, replication fork slows via PARP-mediated fork reversal. Strikingly, *ALC1*$^{-/-}$ cells showed impaired fork slowing. Moreover, *PARP1*$^{-/-}$ and *PARP1*$^{-/-}$/ *ALC1*$^{-/-}$ cells show similar sensitivity to CPT. This epistatic relationship suggests that ALC1 plays roles in PARP-mediated fork-reversal.

2. Analysis of the role played by DDX11 in DNA damage repair

I sought the role of DDX11 in DNA repair and DNA replication and the functional relationship between DDX11 and FA proteins. Both *DDX11*$^{-/-}$ and *FANCC*$^{-/-}$ mutants showed less capability to repair DNA interstrand crosslinks (ICL) than wild type did. FA deficient mutant showed much higher sensitivity to ICL inducer than *DDX11*$^{-/-}$ mutant. *DDX11*$^{-/-}$/*FANCC*$^{-/-}$ mutant showed higher sensitivity to ICL inducer than each single mutant. I concluded DDX11 works as a critical back-up pathway for FA pathway to repair ICL. *DDX11*$^{-/-}$ mutant showed higher sensitivity to DNA replication stress. DNA replication stress is often bypassed by Trans lesion DNA synthesis (TLS) or HR dependent template-switch. To test if DDX11 has a role to tolerate DNA replication stress, I measured the frequency of TLS and HR dependent gene-conversion in Immunoglobulin variable (*IgV*) gene during IgV diversification. This assay allows us to measure the frequency of both TLS and HR. *DDX11*$^{-/-}$ mutant showed less frequency of both TLS and HR at *IgV* locus, suggesting the pivotal role of DDX11 to tolerate DNA replication stress.

3. Development of high throughput drug screening system using image analysis of DNA damages in cells

I identified synthetic effects of concurrent loss of DDX11 and FA factor on genome maintenance and cell proliferation. Thus, the rapid proliferation of FA cancer cells might be largely supported by the complementary working DDX11. Similarly, genes related to DNA damage repair pathways are generally mutated in cancer cells and thus the survival of the cancer cells is maintained by alternative and complementary DNA repair pathways. The inhibition of such complementary system results in cell growth defect or cell death. To establish the novel cancer chemotherapy based on such genetic synthetic-relationship, I wish to establish a high throughput drug screening system based on imaging analysis of DNA damages in cells.

To find a better cell-based high-throughput assay system to quickly identify DNA double strand break (DSB) in cells, I optimized and validated an immunostaining assay using a quantitative high-throughput and high-content imaging method. To validate this assay, MCF7 cells were plated in a 1536-well plate. The MCF7 cells were treated with bleomycin, a known DNA damage inducer, which causes phosphorylation on H2AX in a concentration-dependent manner. Phospho-H2AX was used as a biomarker for DNA damage. In the screening, the number of foci per cell was used for quantitative image analysis of phospho-H2AX induction using Operetta High Content Imaging System. The immunostaining assay was validated in 1536-well formats using Bleomycin with average signal-to-background (S/B) ratio, coefficient of variation (CV) value, and Z' factor of 26.7, 10.1%, and 0.62, respectively.

I screened 907 compounds from Tox21-10K chemical library at the National Center for Advancing Translational Science/ National Institutes of Health (NCATS/NIH). These compounds were directly or indirectly related to DSB from previous screenings done at NCATS/NIH. The average CV value, S/B ratio, and Z' factor from the primary screen of 21 assay plates were 14.85%, 5.53, and 0.32, respectively. The compounds, with efficacy of >3SD from the negative control (DMSO), were considered active and potential phospho-H2AX inducers. A total of 128 potential inducers were identified from the primary screening.

In this study, I achieved three things. First, that ALC1 works as a chromatin remodeler together with PARP in BER. ALC1 also works in the repair of Camptothecin-induced DNA damage. Second, that DDX11 works as a backup of Fanconi anemia pathway in the repair of DNA interstrand crosslink. Furthermore, I identified DDX11's role in DNA replication and the relationship between DDX11 and other proteins which work to tolerate DNA replication stress. Finally, I optimized a high throughput imaging analysis to measure the amount of DNA damage in cells caused by environmental chemicals.

Introduction

Genome and Cancer

A genome is a complete set of an organism's genetic information including all of genes. Our body is built according to the genome information. Human's genetic information consists of more than 3 billion ATCG letters written in DNA molecules. The gigantic molecules form a compactly folded structure called chromatin to be fit into the nuclei. Chromatin is a complex of DNA and histones (Figure 1). DNA wraps around histones, forming a nucleosome. Nucleosomes condense into a more compact structure. The roles of chromatin are 1) compact the DNA, 2) regulating gene expression and DNA replication and 3) preventing DNA damage (Venkatesh and Workman, 2015). These functions are strictly controlled by many enzymes. Once the control is disrupted, there would be severe health problems.

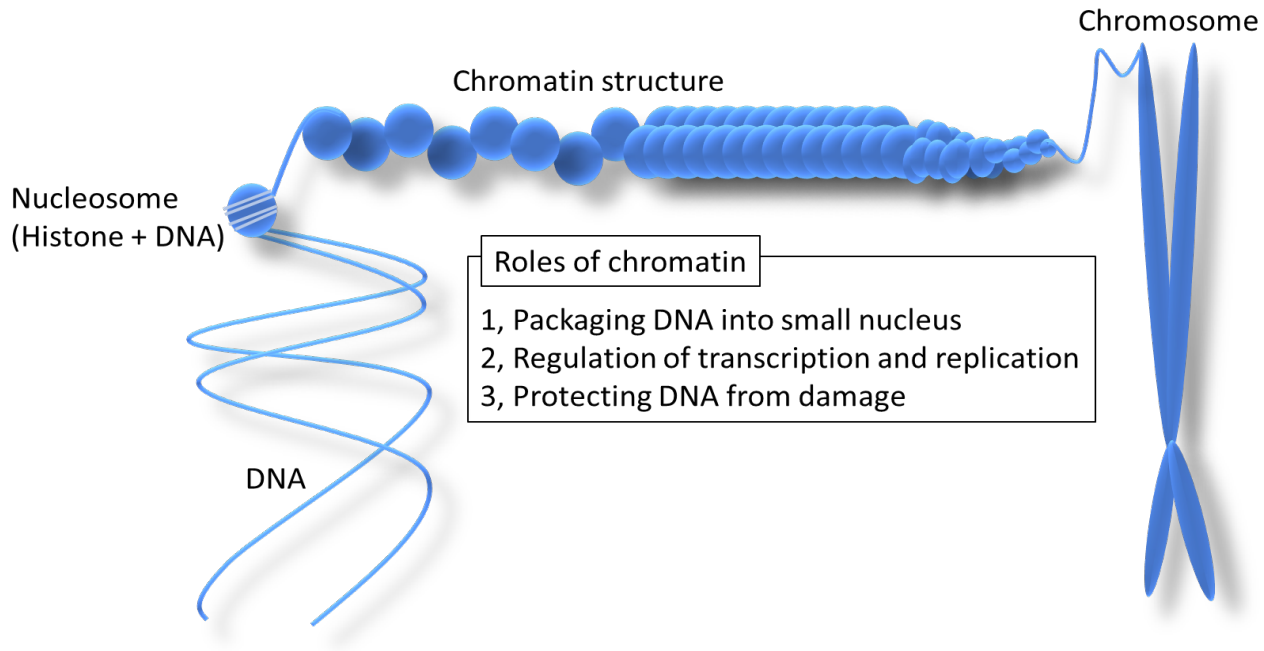

Figure 1

Chromatin structure and the roles.

Improvement of genome sequencing technology allows us to clarify the relationships between disease and genes. We have an idea that cancer is a disease of the genome. The function of our body consists of numerous numbers of cells. Each cell has a role to maintain our life. The roles are strictly controlled by tens of thousands of enzymes. This highly organized regulation can be destroyed even by a single nucleotide mutation in our genome, leading to cancer or other severe diseases. Our genome is inherited from parents. If the parents have mutations in their genome, the same mutation can be found in the genome of the children according to the Mendelian inheritance. Another way of occurrence of mutation is a result of DNA damage. Our genome is continuously damaged by many factors, such as reactive oxygen species, environmental hormones, UV, *etc* (Carol Bernstein, Anil R. Prasad, Valentine Nfonsam and Harris Bernstein, 2012, the book" New Research Directions in DNA Repair"). There are several DNA repair pathways (Kelley and Fishel, 2016). Once our DNA is damaged, the DNA repair mechanism works to protect the genome. Proper repair enzymes and mechanisms are used depending on a type of DNA damage. However, the repair mechanism is not perfect. Cells occasionally fail to repair them properly. When cells make mistakes to repair DNA damages, it causes mutations, translocation or other genome instabilities (Ganem and Pellman, 2012). The most common DNA damage is DNA base damages by reactive oxygen species, which are produced endogenously (Carol Bernstein, Anil R. Prasad, Valentine Nfonsam and Harris Bernstein, 2012, the book" New Research Directions in DNA Repair"). Such DNA damages arise more than 10,000 times a day. This type of DNA damage is repaired by a repair mechanism referred to as base excision repair.

Base Excision Repair and Single Strand Break Repair

Base excision repair (BER) is one of the DNA repair mechanisms (Figure 2) (Liu et al., 2007). As the name suggests, it eliminates damaged bases by oxidation, alkylation, and hydrolysis. Since reactive oxygen species are a by-product of a metabolic reaction in cells, these damages are inevitable. Several enzymes are involved in the BER process. A typical BER is initiated by enzymatic removal of the damaged base, leading to the formation of apurinic/apyrimidinic (AP) sites, followed by incision of the DNA backbone at the AP sites, yielding single-strand breaks (SSBs) (Liu et al., 2007). Since SSB repair and BER share many repair factors, such as Poly (ADP-ribose) polymerase (PARP) 1 and 2, SSB repair is considered as a BER sub-pathway. PARP1 and PARP2 accumulate quickly at SSB sites, and

poly ADP-ribosylate themselves as well as chromatin proteins around the SSB site (Chaudhuri et al., 2012). Poly (ADP-ribose) facilitates the recruitment of x-ray-repair cross-complementing group 1 (XRCC1). XRCC1 plays a key role in SSB repair by providing docking sites for critical effector molecules, polynucleotide kinase 3'-phosphatase (PNKP), DNA polymerase β (Polβ), and ligase 3. PNKP and Polβ restore hydroxyl and phosphorylation residues at the 3' and 5' ends, respectively, of the SSBs. Polβ incorporates a single nucleotide, a process called short-patch repair synthesis, for subsequent ligation of SSBs. Polβ, Polδ, and Polθ, on the other hand, undergo long-patch repair synthesis, involving 2±12 nucleotide incorporation, by strand-displacement synthesis, generating a 5' flap. The Fen-1 endonuclease removes the 5' flap for subsequent ligation (Chaudhuri et al., 2012).

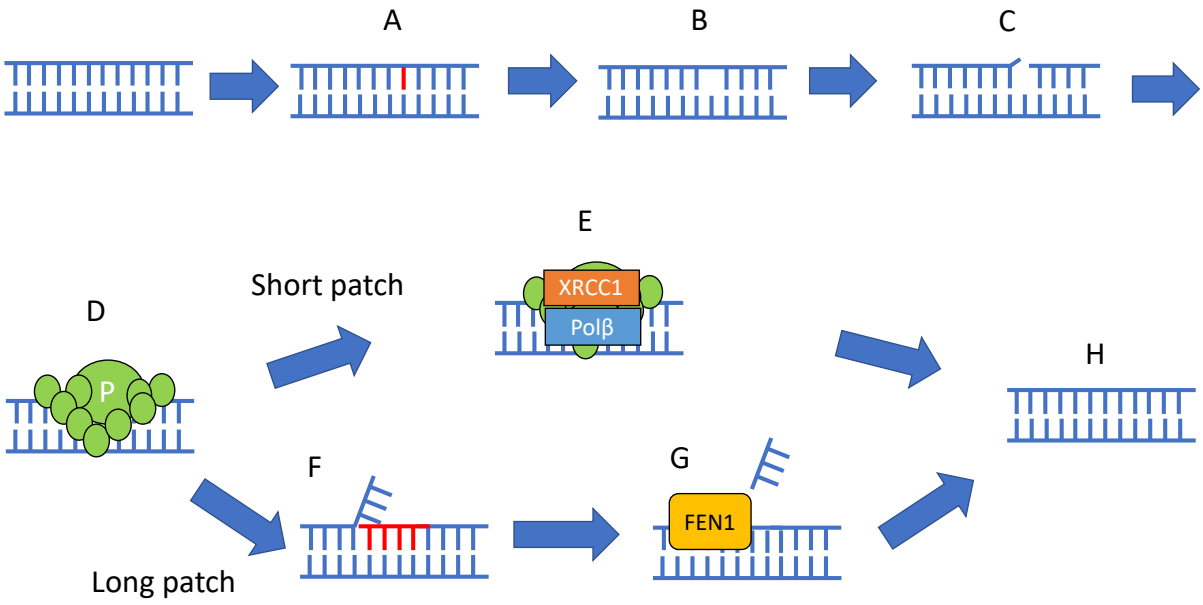

Figure 2

The scheme of Base excision repair. When base damage occurs (A), DNA glycosylase removes the DNA, leaving AP site (B). After the AP site is cleaved by AP endonuclease (C), a single-strand break (SSB) remains. PARP recognizes the SSB and Poly-ADP ribosylates histone proteins and PARP itself (D). In short patch pathway, XRCC1 binds to poly ADP ribose and works as a scaffold protein for other BER proteins such as Pol β. In the long patch pathway, DNA polymerases incorporate DNA. Flip endonuclease (FEN1) removes the

flipped DNA. DNA ligase 3 completes the repair by ligating the DNA ends (H).

DNA Double Strand Break Repair

DNA double-strand break (DSB) is the most toxic type of DNA damage. DSB is the DNA damage which shows breaks at the same position in the duplex DNA. Unrepaired breaks can lead to cell death and improper repair can cause toxic genetic rearrangement. DSBs are repaired mainly by two repair pathways. One is non-homologous end joining (NHEJ) and the other is homologous recombination (HR) (Ceccaldi et al., 2016a). Many researchers tried to reveal the repair mechanisms. We have the detail, still not perfect, mechanism of the repairs.

NHEJ pathway is the commonest DSB repair pathway in human cells (Figure 3). NIHEJ is active throughout the cell cycle (Ceccaldi et al., 2016a). NHEJ is triggered by a binding of the Ku70-Ku80 heterodimer to DSB ends. Ku70-Ku80 complex works as a scaffold to recruit other NHEJ factors, including DNA-dependent protein kinase catalytic subunit (DNA-PKcs), DNA ligase4 (LIG4), X-ray repair cross-complementing protein 4 (XRCC4), etc. Once DNA-PKcs is recruited to the DSB site, it phosphorylates several NHEJ factor and itself. XRCC4-LIG4 complex ligates the broken DNA ends. Because NHEJ seals the two edges without applying homology, it can induce unscheduled insertion, deletion, or chromosome translocation.

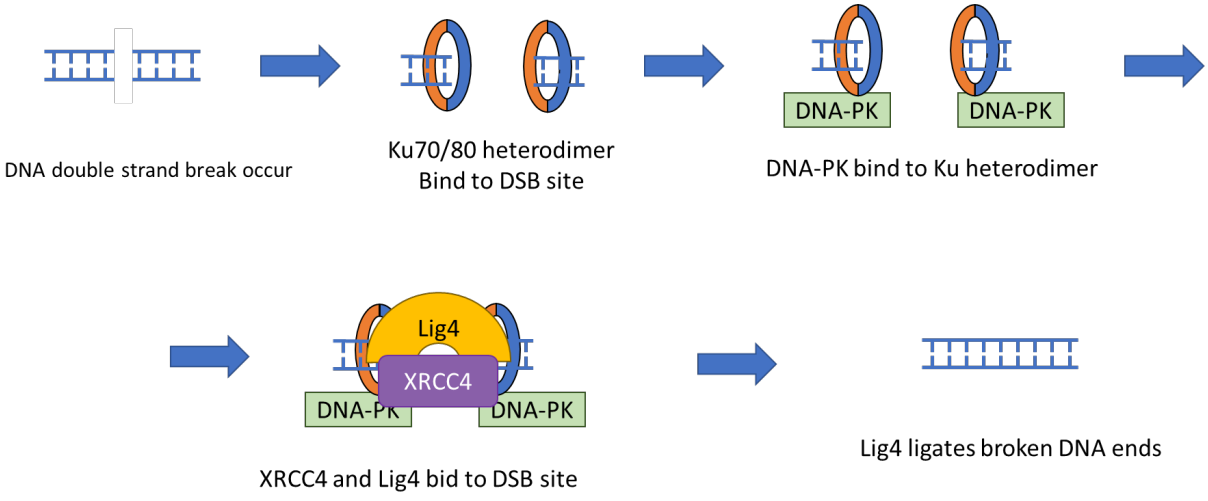

Figure 3
The scheme of Non-Homologous End Joining.

HR is the second most common DSB repair pathway in human cells (Figure 4). It is an error-free pathway that uses a homologous sequence in the sister chromosome to copy the damaged sequence(Ceccaldi et al., 2016a). It is activated usually in S/G2 phase. In this pathway, when DSB occurs, CtIP and Mre11-Rad50-Nbs1(MRN) complex binds to DSB sites and resects the DNA end, resulting in 3' overhang. After the resection, Rad51 forms nucleoprotein filaments around 3' overhang to find a homologous sequence. Once the homologous sequence is found, the 3' overhang strand invades into the homologous DNA, forming a D-loop structure. After this invasion, DNA polymerases synthesis DNA according to the template sequence.

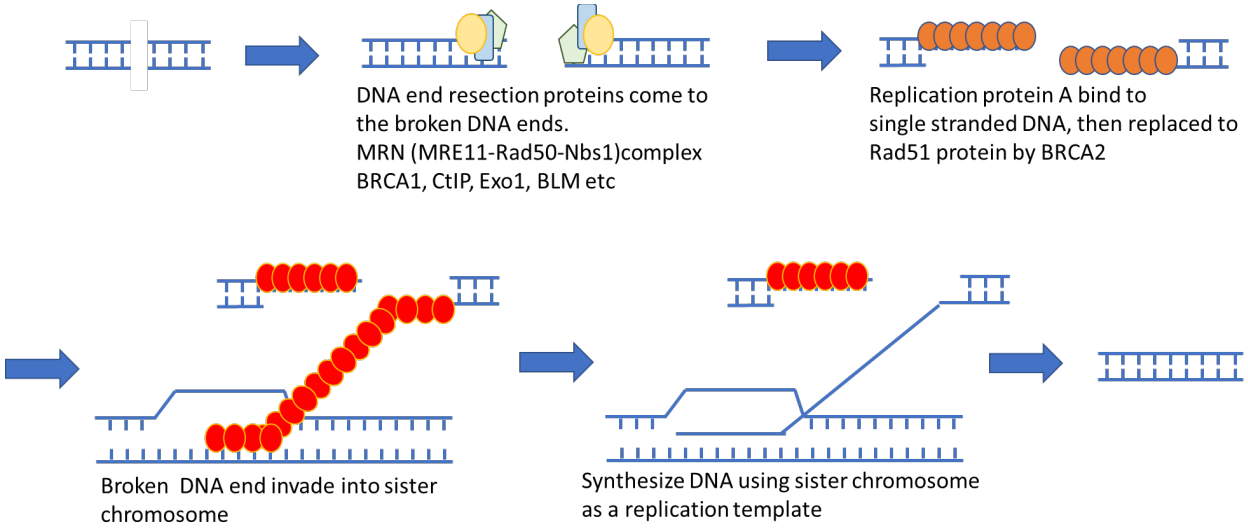

Figure 4

The scheme of homologous recombination.

These two pathways are regulated by the balance between breast cancer type 1 susceptibility protein (BRCA1) and p53 binding protein 1(53BP1) (Fig5). While 53BP1 prevents DNA resection by keeping CtIP from accessing DNA ends and promotes NHEJ, BRCA1 promotes the removal of 53BP1 in S-phase and directs HR (Daley and Sung, 2014). In the absence of BRCA1, DSB end resection is not carried properly, leading to embryonic lethality. This lethality is suppressed by knockout of 53BP1 in mouse, suggesting BRCA1 plays an

important role in the removal of 53BP1 and regulation in the DSB repair pathway choice (Bunting et al., 2010).

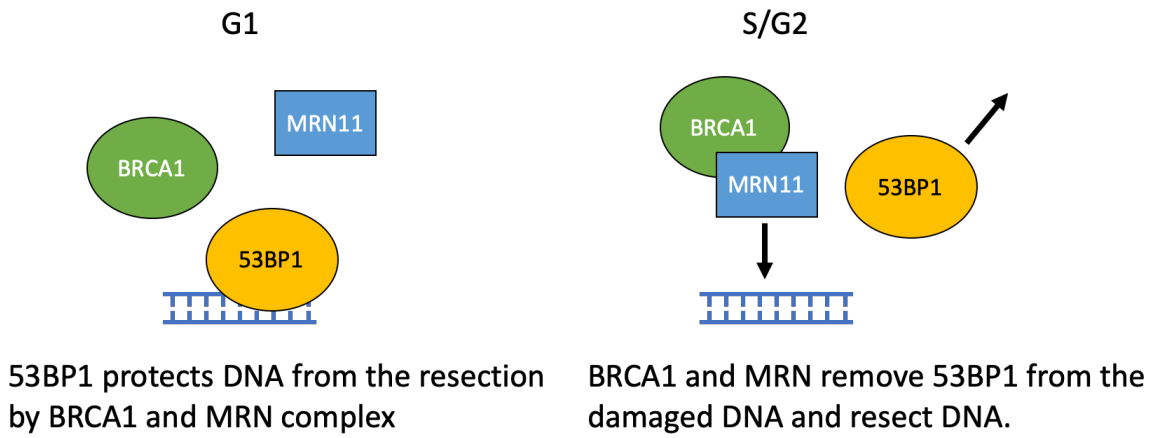

Figure 5 Model for DSB repair choice in G1 and S/G2
(Left) In G1 cells, 53BP1 localizes at the break. Other NHEJ proteins RIF1 are recruited to the damaged DNA and block the resection. (Right) In S/G2 cells, BRCA1 and MRN form complex and displace 53BP1 leading to the initiation of end- resection.

DNA Replication Stress

DNA polymerases synthesize DNA by inserting nucleotides, which are complementary to template strand. DNA replication frequently stalls at the DNA damage site. Stalled replication fork causes replication fork collapse. Cells have evolved DNA damage tolerance (DDT) mechanisms (Figure 6), including trans-lesion DNA synthesis (TLS), template switching (TS) to tolerate replication stress (Abe et al., 2018). DDT prevents replication fork collapse. These two mechanisms are regulated by ubiquitylation on proliferating cell nuclear antigen (PCNA) on the stalled replication fork by ubiquitin ligases (Arakawa et al., 2006).

TLS is initiated by a mono-ubiquitylation on PCNA. When PCNA is ubiquitylated, DNA replicative polymerases are replaced with TLS polymerases (TLS pols), which are specialized for TLS. TLS pols include polymerase ζ, η, κ, *etc*. DNA damages often distort

DNA or make DNA bulky. Since replicative DNA polymerases have a narrow nucleotide pocket for accurate insertion of a nucleotide, the distorted or bulky DNA cannot be accommodated in the pocket. On the other hand, TLS Pols have a broad nucleotide pocket. Therefore, they can synthesize DNA over damaged template with low fidelity (Vaisman and Woodgate, 2017).

TS is initiated by polyubiquitylation on PCNA. TS employs many HR-related proteins. Stalled newly synthesized DNA invades the sister chromatid and continues synthesizing by using sister chromatid as a template. Since the correct DNA sequence is used as a template in this process, TS is error-free.

In addition to TLS and TS, cells have developed another tolerance mechanism called re-priming (Figure 6). In this process, the DNA primer is generated from downstream of the damaged template. With this manner, cells can skip the replication of damaged template DNA. DNA primase-polymerase (PrimPol) plays a central role in this process (Bailey and Doherty, 2017; Kobayashi et al., 2016).

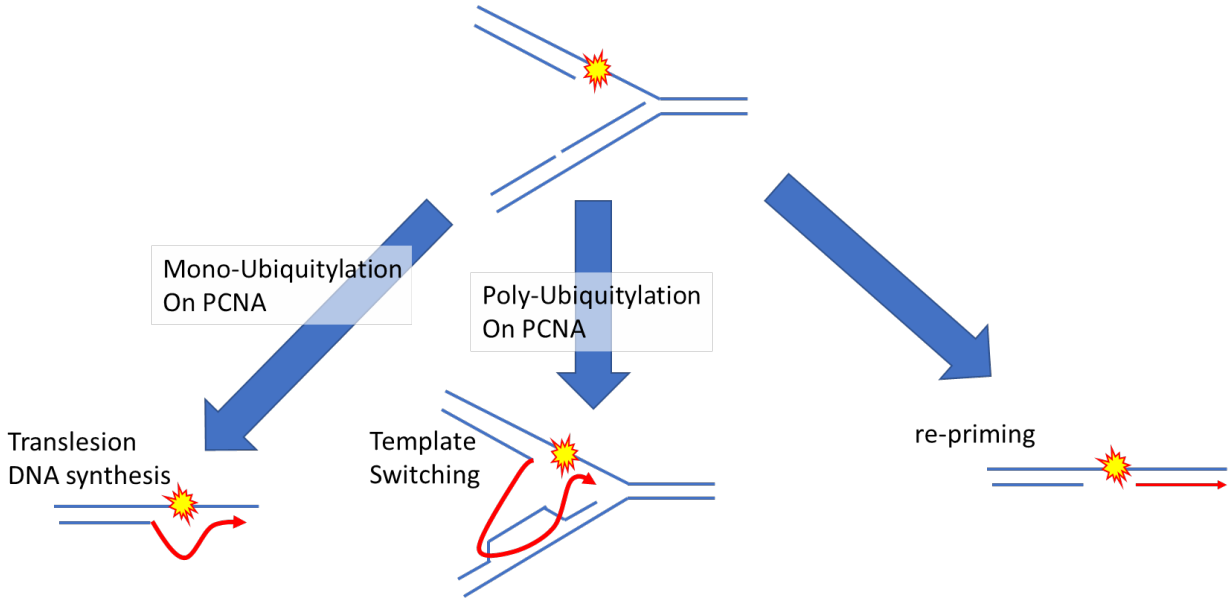

Figure 6 DNA damage tolerance mechanism

The scheme of DNA damage tolerance mechanism. Cells utilize translesion DNA synthesis, Template Switching and re-priming.

Cancer Chemotherapy

DNA damage happens not only in daily life but also by therapeutic drugs. Since most cancer cells are less tolerant of DNA replication stress or DNA damage, current cancer chemotherapies apply DNA damaging reagents. They damage DNA in healthy (non-cancer) cells as well. The genetic study allows us to understand the relationship between two or more genes. Due to the high frequency of targeted integration rate, gene knockout system in Chicken B lymphocyte DT40 cells was established for genetic study in a vertebrate in the early ’90s (Buerstedde and Takeda, 1991). In 2013, gene-editing technology using CRISPR-Cas9 is established for genetic study in a mammal cell lines (Cong et al., 2013). These genetic studies contributed to the understanding of genetic relationships between two or more. We have the idea that when two or more genes are disrupted at the same time, even if cells can proliferate properly under the loss of every single gene, the cell shows lethality. This phenomenon is referred to as ‘synthetic lethality’. Cancer cells often lack the function of a certain protein related to the genome maintenance, DNA repair and replication. We can selectively kill cancer cells by disrupting or inhibiting certain proteins that are in a synthetic lethal relationship with the protein lost in cancer.

To identify the synergistic relationship, genetic studies are important. Moreover, many enzymes work not only in one pathway but also work in several pathways. Inhibition of one enzyme can lead to deficiencies in several pathways. Selecting enzymes to inhibit is very important to reduce unexpected side effects in cancer-chemotherapy. Therefore, understanding of molecular networks in the genome maintenance, DNA repair and replication is critical to establish better molecular-targeting chemotherapy.

PARP inhibitors, for example, are the most successful targeting cancer chemotherapy drugs (Murai et al., 2012; Tutt et al., 2010). PARP inhibitors inhibit the enzymatic activity of PARP enzymes responsible for SSB repair, and thereby resulting in accumulated unrepaired SSB. Replication across the unrepaired SSB induces DSB during S-phase. Since HR exclusively contributes to the repair of this type of lesion, PARP inhibitors selectively kills HR defective cancer cells such as *BRCA* negative cancer. Since non-cancer cells have a normal HR pathway, use of PARP inhibitors has limited side effect for patients. Although many companies or institutes try to find molecular targeting drugs like PARP inhibitors, few drugs were established. This suggests there are further needs for understanding molecular networks.

Toxicological Study

DNA damage can cause mutation on the genome, leading to disfunction of enzymes. Since cellular reactions are strictly controlled by the combination of many enzymes, single mutation can induce severe diseases. DNA damage can be caused by many factors, including daily products or drugs. We need more information about chemical compounds' toxicity to live safe life. Toxicology is a research field that studies the harmful effects of chemicals. Zillions of chemical compounds are produced for clinical use, commercial use, food, *etc*. Some of them can be very toxic. Understanding how chemicals can be toxic is important to keep our health safe.

Bruce Ames has developed the first genotoxicity assessment system. This assay system uses bacteria, which is usually *Salmonella Typhimurium*. This assay can find out if tested compounds have a mutagenic effect or not. Although it is still used for the first screening to test compounds' genotoxicity, it has a high rate of false-positives or false-negatives (Kirkland et al., 2014). Since the structure of nuclei and biological systems are deferent between bacteria and eukaryotic cells, applying the Ames test for safety tests for the human has been a matter of debate. To resolve this problem, a genotoxicity assessment system using gene-edited chicken B lymphocyte (DT40) was established (Ji et al., 2009). Mutant cells, which lack certain DNA repair pathways, and Wild-Type cell (WT) are used in this assay. By comparing the sensitivity of each mutant and WT cells, we can assess whether or not tested compounds induce DNA lesion. Moreover, if tested compounds are judged to have genotoxic potential, we can estimate the type of DNA damages induced by the tested compounds. Since this assay applies WT as a negative control, the false-positive and false-negative rate is very low. The same assessment system has been developed with human cells (Saha et al., 2018). Moreover, we can generate gene-edited cell, which has the same mutation in patients. This assay helps us to understand the toxicity to individual person carrying a specific somatic mutation.

Quantitative High Throughput Screening in National Institutes of Health

Since numerous chemicals are in the world, we cannot test all of them. To understand the toxicity of such an amount of chemicals, we need a great method for prediction of the toxicity. To predict the toxicity, we need a better assay system to collect a big amount of the toxicological data. The U.S tox 21 program in National Institutes of Health (NIH) aims to evaluate hundreds and thousands of chemicals quickly and efficiently. This program has utilized a quantitative high throughput screening (qHTS) approach to assess a numerous number of chemicals by a series of biologically relevant in vitro assays.

Chapter 1:

Analysis of the role of ALC1 in Base Excision repair

1-1 Introduction

1-1-1 The Biological roles of Poly ADP Ribose Polymerase

Proteins are translated from messenger RNA (mRNA). After the translation, some proteins are modified on their amino acids. This modification is referred to as post-translational modifications (PTM). PTM contributes to the regulation of protein function, protein degradation and protein localization. There are more than 300 types of PTM, including phosphorylation, ubiquitylation, SUMOylation, *etc*. Each PTM is involved in a range of essential cellular and biological process. Thus, unregulated PTM loss or gain can cause diseases as well as mutations in the genome.

One of the well known PTMs is Poly ADP-ribosylation (PARylation). PARylation is carried by Poly(ADP-ribose) polymerase (PARP)(Burkle, 2001). PARP is one of the target protein in cancer chemotherapy, because PARP inhibition has synthetic lethal effect in HR defective (or reduced) cancer such as *BRCA* negative cells. PARP family comprises 17 members. In human cells, most of the PARP activity is mefdiated by PARP1 and PARP2 (Yelamos et al., 2011). The simultaneous depletion of PARP1 and PARP2 causes cell death (Yelamos et al., 2011). PARP possesses 4 domains, DNA binding domain, a caspase-cleaved domain, an auto-modification domain, and a catalytic domain (Desroches et al., 2019). When DNA damage occurs, especially single-strand breaks, DNA binding domain bind to the DNA and leads the conformational shift of PARP itself (Mansoorabadi et al., 2014). This shift allows PARP to synthesize PAR by using NAD^+ as a substrate. PAR acts as a signal for SSB repair enzymes, such as XRCC1, and contributes to the recruitment of repair factors.

Although it has been believed PARylation by PARP is important during the single-strand break repair or base excision repair, other roles of PARP have been uncovered. PARP is not only a base excision repair factor but also involved in transcription (Schiewer and Knudsen, 2014), DNA double-strand break repair or cell cycle regulation (Maya-Mendoza et al., 2018;

Wang et al., 2006). For this reason, inhibiting PARP for chemotherapy can cause an unexpected side effect. Identifying the genetic network around PARP helps us to understand the side effects caused by PARP inhibition. I focused on identifying a roles of PARP enzyme in DNA repair.

1-1-2 ALC1 and Base excision repair

ALC1(Amplified in Liver Cancer 1, also known as CHD1L [chromodomain helicase-DNA-binding protein 1-like]) is a member of the SNF2 superfamily of ATPases(Ahel et al., 2009). ALC1 possesses a helicase domain and macro domain (Figure 7). ALC1 is preserved well in higher eukaryotes. The homology of the sequence is around 60 - 85% in mouse, chicken, zebrafish, and turtle (Table 1). Helicase domain and macrodomain are preserved in all of those species (Figure 8). This suggests the importance of ALC1 for all higher organisms. Helicase domain functions as chromatin remodeling enzymes (chromatin remodelers). Chromatin remodelers induce local reluxation of chromatin structure via eviction or sliding of nucleosome. This chromatin configuration changes (tight or reluxed form of chromatin) contributes to the regulation of all DNA-related reaction such as transcription and DNA repair. Macrodomain recognizes Poly(ADP-ribose) (PAR) *in vitro* and *in vivo* (Ahel et al., 2009; Karras et al., 2005). The domatin structure of ALC1 suggests a potential role of ALC1 as chromtin demodeler working in the downstream of PARP signal pathway. PAR is generated by Poly(ADP-ribose) polymerase (PARP), which is activated by single-strand DNA breaks (SSB) and gaps. SSB is created during base-excision repair (BER), which removes base damage, including oxidation and alkylation on bases. Formation of PAR at chromatin proteins in the vicinity of SSB facilitates the recruitment of BER factors to damaged-base sites. PARP1 stimulates the chromatin-repositioning enzyme activity of ALC1. Collaboration between ALC1 and PARP was also reported in the nucleotide-excision repair of ultraviolet light (UV) - induced DNA damage (Pines et al., 2012). Although there are several studies reporting the role of ALC1, the genetic relationship between PARP and ALC1 has not been elucidated.

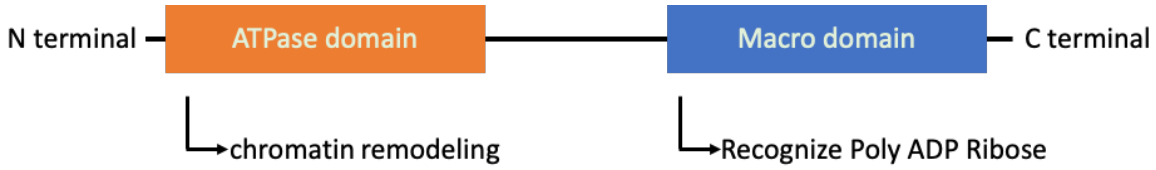

Figure 7

The domain structure of ALC1. ALC1 possesses the ATPase domain and the Macro domain. ATPase domain is required for chromatin remodeling activity. Macrodomain recognizes Poly ADP ribose.

common name	scientific name	homology with ALC1 sequence in human
Human	Homo sapiens	
Mouse	Mus Musculus	63.30%
Chicken	Gallus Gallus	71.00%
Green sea turtle	Chelonia Mydas	84.80%
Zebrafish	Danio Retio	72.80%
Pacific purple sea urchin	S.Purpuratus	49.20%

Table 1

ALC1 is well conserved in Human, Mouse, Chicken, Green sea turtle, Zebrafish and Pacific purple sea urchin.

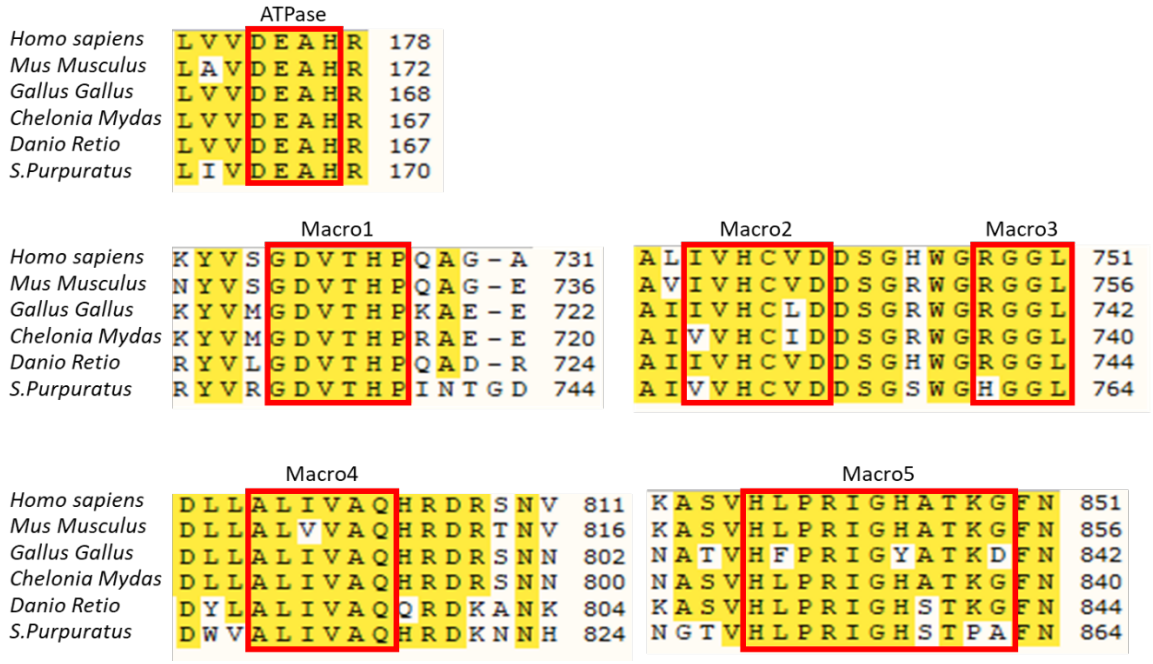

Figure 8

ATPase domain and Macro domain are well conserved in higher eukaryote. Consensus sequences for each domain are in red square. The identical amino acids with a human sequence are highlighted with yellow. Red boxes indicate the consensus sequence in the ATPase domain and Macrodomain.

1-1-3 PARP works together with Tyrosyl DNA Phosphodiesterase 1

Another remarkable role of PARP is in the tolerance to Camptothecin (CPT)-induced damage (Chaudhuri et al., 2012; Sugimura et al., 2008). CPT is a Topoisomerase1 (Top1) poison. Each cell has huge genomic DNA sequences (totally approximate 2 meters of DNA). Chromatin structure allows DNA to be fit in a small nucleus, the diameter of which is about 10 μm. During DNA replication, DNA helicases unzip double-strand DNA. Because DNA is highly compacted in the nucleus, unzipping by replication machinery causes topological stress of DNA. This topological stress needs to be relaxed because replication fork should be arrested by this stress. DNA topological stress is resolved by Topoisomerase1 (Top1) during DNA replication. Top1 binds to DNA and induces SSB by forming a covalent bond with 3' end of SSB. Top1 mediates DNA nicking, rotation and resealing to resolve DNA topological

stress. CPT inhibits resealing step of Top1 mediated reaction and stabilizes Top1-DNA covalent complex (Top1-cc) (Figure 9). Since actively replicating cancer cells generally show hyper-sensitivity to CPT, this drug is used for cancer chemotherapy.

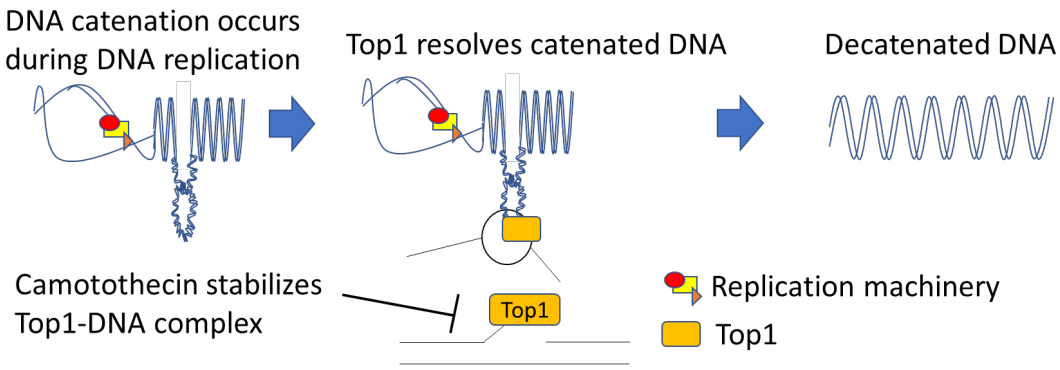

Figure 9
The scheme of TOP1-mediated DNA decatenation. Camptothecin stabilizes the Top1-DNA complex during DNA replication.

During replication, progression of replication forks at Top1-cc induces DSB. To suppress this CPT mediated DSB formation, replication fork slows via PARP-mediated fork reversal mechanism (Figure 10) (Chaudhuri et al., 2012). By fork reversal mechanism, DSB converts into SSB and resultant SSB associated with Top1-cc is repaired by Tyrosyl DNA Phosphodiesterase1 (Tdp1) and SSB repair pathway (Das et al., 2014). PARP acts with Tdp1 to remove Top1-cc (Das et al). In the absence of PARP, DNA replication does not slow upon CPT treatment, leading to a replication fork collapse (Sugimura et al Chaudhuri et al) . Although CPT is approved for cancer chemotherapy, the mechanism of cellular tolerance to Top1-cc has not been completely understood. In this study, I also focused on the role of ALC1 in CPT tolerance, because ALC1 possesses macrodomain and PARP works in the tolerance to CPT-induced DNA damage.

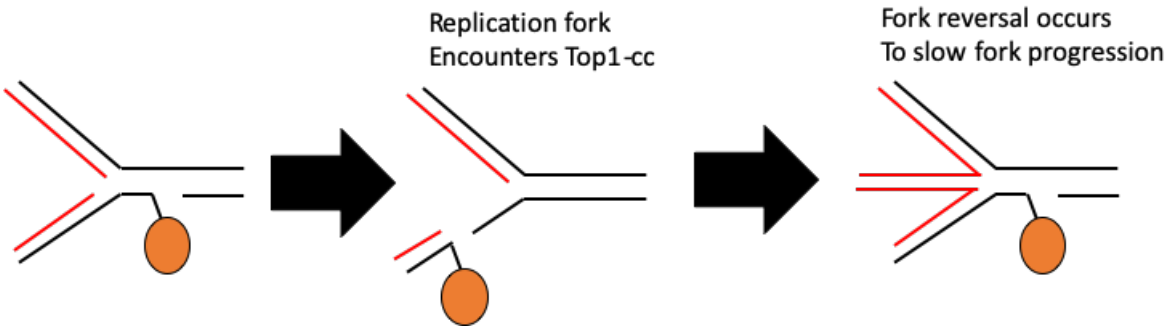

Figure 10

The scheme of fork reversal mechanism to slow replication fork progression at Top1-cc.

1-2 Materials

・DT40 strains

WT

ALC1$^{-/-}$

ALC1$^{E165Q/-}$ (ATPase dead mutant)

PARP1$^{-/}$

ALC1$^{-/-}$*/PARP1*$^{-/}$

RNF8$^{-/-}$

・TK6 strains

WT

ALC1$^{-/-}$

・Genotoxic reagents

H_2O_2 (Nacalai, Japan), MMS (Nacalai, Japan), Camptothecin (TopoGEN, Inc.), olaparib (AZD-2281, Astrazeneca), etoposide (VP16, Funakoshi), ICRF-193 (Funakoshi) and cis-diamminedichloroplatinum (II) (cisplatin, Nippon Kayaku)

Cell culture medium

・DT40

DT40 cell line was obtained from Takeda lab (Kyoto University, Japan). DT40 cells were cultured in an RPMI 1640 medium (Nacalai Tesque, Kyoto, Japan) supplemented with 10% heat-inactivated fetal bovine serum (FBS), 1% chicken serum, 0.05 mM β-mercaptoethanol, L-glutamine (Nacalai Tesque), 50 U/mL penicillin, and 50 μg/mL streptomycin (Nacalai Tesque).

・TK6

TK6 cell line was purchased from JCRB cell bank (http://cellbank.nibiohn.go.jp/english/). TK6 cells were cultured in an RPMI 1640 medium (Nacalai Tesque, Kyoto, Japan) supplemented with 10% heat-inactivated horse serum (HS) (GIBCO), 0.1 mM sodium

pyruvate, L-glutamine (Nacalai Tesque), 50 U/mL penicillin, and 50 μg/mL streptomycin (Nacalai Tesque).

1-3 Experimental Method

・ATPase assay

10^6 DT40 cells were exposed to H_2O_2 and MMS for 1 h in 1 ml culture medium and PBS containing 1% fetal bovine serum, respectively. 3 x 10^4 DT40 cells were exposed to UV in 30 μl PBS containing 1% fetal bovine serum. TK6 cells were exposed to the two DNA-damaging agents in the same manner. 10 μl of cell suspensions (containing 10^4 cells) of the exposed DT40 or TK6 cells were plated in duplicate onto 24-well cluster plates containing 1 ml of the complete medium and were incubated for 48 h (for DT40) and 72 h (for TK6). 1 x 10^4 DT40 cells were cultured in 1ml culture medium containing olaparib, etoposide, ICRF-193 and cis-diamminedichloroplatinum (II) for 48 h. To measure the number of living cells, I transferred 100 μl cell suspensions to the individual wells of 96-well plates and measured the amount of ATP in the cellular lysates using Cell Titer-Glo (Promega). Luminescence was measured with Fluoroskan Ascent FL (Thermo Fisher Scientific Inc., Pittsburgh, PA).

・Colony formation assay

Cells were cultured in DMEM Ham's F12 medium supplemented with 15% FBS, 1% chicken serum, L-glutamine, 1.5% methylcellulose. DNA damaging reagents were mixed with the medium one night before the experiment. Cells were transferred to pre-warmed medium and cultured for 1 week. After the formation of colonies, the number of colonies was counted by a black marker.

・si-RNA treatment

HeLa and U2OS cells were cultured in DMEM supplemented with 10% fetal calf serum at 37 °C. si-RNAs for the depletion of ALC1 and the control were purchased from Thermo Scientific (Dhamacon si-RNA, PA). 3×10^5 cells were transfected with 250 pmol si-RNA using 10μl Lipofectamine RNAi MAX (Invitrogen, CA).

・Detection of GFP-XRCC1 at the site of SSBs induced by *Neurospora crassa* UV-damage endonuclease (UVDE)

U2OS cells expressing *Neurospora crassa* UV-damage endonuclease (UVDE) and GFP-XRCC1 or GFP-Polβ were used. UV irradiation causes cyclobutane-pyrimidine Dimer (CPD). UVDE converts CPD into SSB. After the irradiation, cells were observed under a fluorescent microscope.

・Partial digestion of chromatin DNA with micrococcal nuclease (MNase)

5×10^7 DT40 cells were pulse-labeled with 20 μM BrdU for 10 min. Cells were then harvested and washed and resuspended in medium either with CPT (20 μM) or without CPT and further cultured for 15 min. Partial digestion of chromatin DNA with Micrococcal nuclease (MNase) was performed as described previously(Hirota et al., 2008), with slight modifications. Briefly, the abovementioned BrdU-labeled cells were suspended in 0.5 ml of lysis buffer (18% Ficoll 400, 10 mM KH_2PO_4, 10 mM K_2HPO_4, 1 mM $MgCl_2$, 0.25 mM EGTA, 0.25 mM EDTA) containing a proteinase inhibitor cocktail (Complete, Roche). After centrifugation at 14,000 rpm for 30 min at 4 °C, the crude chromatin fraction was resuspended in 0.3 ml of buffer A (10 mM Tris-HCl [pH 8.0], 150 mM NaCl, 5 mM KCl, and 1 mM EDTA) containing a proteinase inhibitor cocktail (Complete, Roche). After the addition of $CaCl_2$ (5 mM final concentration), 0.1 ml aliquots of crude chromatin suspension were digested with several different amounts of MNase (0, 5, 10, and 20 U/ml) at 37 °C for 5 min. The reaction was terminated by adding 25 mM EDTA, and DNA was purified. DNA samples were resolved in 2% agarose gel electrophoresis followed by membrane transfer and immunodetection using anti-BrdU antibody (Roche).

Lysis buffer	
18%	Ficol 400
10mM	KH2PO4
10mM	K2HPO4
1mM	MgCl2
0.25mM	EGTA
0.25mM	EDTA

Buffer A

10mM Tris-HCl [pH 8.0]

5mM KCl

・Isolation of nuclear-soluble and chromatin-bound fractions from DT40 Cells

I isolated the nuclear soluble fraction from DT40 cells using the Subcellular Protein Fractionation Kit for Cultured Cells (Thermo, PA). Histone and Top1 were detected using following specific antibodies (anti-Histone H3 from MBL, MABI0301 and anti-Top 1 from BD PharmingenTM, 556597).

・Measuring the amount of single-strand breaks by Alkaline comet assay

For the chicken DT40 cells, the tail DNA percentage, reflecting the number of SSBs (% DNA in tail), was measured for cells that had been exposed to 25 μM H_2O_2 for 20 min on ice, and cells that had been exposed to 25 μM H_2O_2 for 20 min on ice followed by a 30 min repair period at 39.5 °C. Human TK6 cells were treated with 80 μM H_2O_2 on ice for 30 min or with MMS at 37 °C for 15 min and subsequently released in drug-free, pre-warmed culture medium. Cells were harvested at the indicated time after release.

After the chemical treatment, individual cells are embedded in a thin agarose gel on a microscope slide. After embedding, I lysed the cell to remove all cellular proteins in buffer (2.5M NaCl, 100mM EDTA, 10mM Tris-HCl (pH 10), 1% Triton, 0.5% Sarcosine) at 4°C for 90 min. Then, I treated the cells under alkaline condition to let DNA unwind. Finally, I separated DNA based on the size of DNA by electrophoresis. Electrophoresis was carried out by applying 25 volts at 4 °C in running buffer (0.3M NaOH, 1mM EDTA (pH 13)) for 50 min using a submarine gel electrophoresis machine (Cat. NB-1012, NIHON EIDO CO. Ltd.) filled with 1850 ml running buffer. The broken DNA fragments or damaged DNA migrates away from the nucleus. After staining with ethidium bromide, a DNA-specific fluorescent dye, I took several pictures of DNA. The resulting image looks like a comet as the name of the assay indicates. Each comet has a distinct head and tail. The head is composed of intact DNA, while the tail consists of single-strand broken DNA. I analyzed the images by using Comet Analyzer software.

・Chromosomal aberration analysis

DT40 clones were treated with 0.06% colcemid (Gibco BRL) for 2.5 h to arrest cells in the M-phase. Cells were pelleted by centrifugation, resuspended in 1 ml of 75 mM KCl for 15 min at room temperature, and fixed in 5 ml of a freshly prepared 3:1 mixture of methanol and acetic acid (Carnoy's solution). The pelleted cells were then resuspended in 5 ml of Carnoy's solution, dropped onto clean glass slides and air-dried. The slides were stained with a 5% HARLECO Giemsa stain solution (Nacalai Tesque) for 10 min, rinsed with water and acetone, and dried. All chromosomes in each mitotic cell were scored at 1000 × magnification.

・DNA fiber assay

Cells (5 x 10^5 in 1 mL of medium) were pulse-labeled with 25 μM chlorodeoxyuridine (CldU; Sigma) and then sequentially pulse-labeled with 250 μM iododeoxyuridine (IdU; Sigma). Cells were resuspended in ice-cold PBS and then dropped onto glass slides (MATSUNAMI). Cells were lysed with DNA fiber lysis buffer (0.5% SDS, 200 mM Tris-HCl, pH 7.4, 50 mM EDTA), and then glass slides were tilted to extend DNA. For fixation, glass slides were immersed in Carnoy solution (MeOH: AcOH, 3:1) for 3 min, then 70% EtOH for 1 h to overnight. After washing with PBS, glass slides were immersed in 2.5 M HCl for 30 min to denature DNA molecules and subsequently in 0.1 M sodium tetraborate for 3 min to neutralize the acid. After washing with PBS, the slides were treated with rat anti-BrdU antibody (1:200; Abcam) and mouse anti-BrdU antibody (1:50; BD Biosciences), which reacted against CldU and IdU, respectively. Cy3- conjugated anti-rat IgG (1:400; Jackson Immunoresearch) and Alexa Fluor 488 antimouse IgG (1:100; Invitrogen) were used as the secondary antibodies. The first and second antibodies were incubated for 1 h at room temperature, respectively. Washing of antibodies was performed with 0.05% Tween 20 in PBS. Coverslips were mounted with Shandon* PermaFluor (Invitrogen). Images were captured with a fluorescence microscope. Fiber lengths were measured using ImageJ, and micrometer values were expressed in kilobases using the following conversion factor: 1 μm = 2.59 kb. Measurements were recorded from areas of the slides with untangled DNA fibers to prevent the possibility of recording labeled patches from tangled bundles of fibers.

Fiber length was measured using Image J (https://imagej.nih.gov/ij/), and the CldU/IdU ratio was calculated.

1-4 Results

1-4-1 Analysis of sensitivity profile of ALC1 mutant

To investigate the role played by ALC1 in BER, I measured sensitivity to base damaging reagents, hydrogen peroxide (H_2O_2) and Methyl MethaneSulfonate (MMS). Once cells incorporate H_2O_2, H_2O_2 produces hydroxyl radical (•OH) as a result of Fenton's reaction (see below).

$$Fe^{2+} + H_2O_2 \rightarrow Fe^{3+} + OH^- + \bullet OH$$

The hydroxyl radical is one of the most reactive oxygen species (ROS). It bonds to DNA and causes DNA base damages. It is a by-product of many biological reactions such as metabolization. MMS is an alkylating reagent. It mainly binds to guanine or adenine and causes base damage as well as H_2O_2.

ALC1$^{-/-}$ cells were hypersensitive to both H_2O_2 and MMS (Figure 10). *PARP1*$^{-/}$ cells showed higher sensitivity than *wild-type* does, as reported previously. To learn more about ALC1 as a chromatin-remodeling factor, I generated an ATPase-dead ALC1 mutant. The ATPase activity is inactivated by mutating the essential E165 to Q of the endogenous wild-type ALC1 allelic gene in *ALC1*$^{-/+}$ cells. *ALC1*$^{-/E165Q}$ and *ALC1*$^{-/-}$ cells displayed virtually the same phenotype (Figure 11). This suggests that ALC1 may promote DNA repair as a chromatin remodeler.

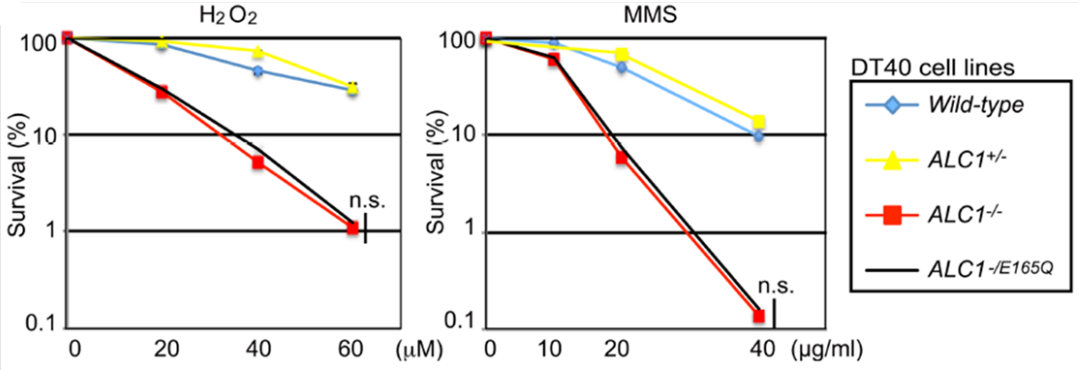

Figure 11

The sensitivity profile of WT and ALC1 mutants to H2O2 (left) and MMS (right). Y-axis indicates the survival % and X-axis indicate the dose.

1-4-2 The epistatic analysis between ALC1 and PARP

To analyze the functional relationship between ALC1 and PARP1, I generated *ALC1*$^{-/-}$*/PARP1*$^{-/-}$ cells by disrupting the ALC1 gene in *PARP1*$^{-/-}$ DT40 cells. I analyzed cellular sensitivity to H_2O_2 and MMS by comparing the sensitivity among *Wild-type*, *PARP1*$^{-/-}$, *ALC1*$^{-/-}$, and *ALC1*$^{-/-}$*/PARP1*$^{-/-}$ clones. While the sensitivity of *ALC1*$^{-/-}$ and *PARP*$^{-/-}$ to H_2O_2 was higher than that of *Wild-type* clones, it was very similar in *ALC1*$^{-/-}$ and *ALC1*$^{-/-}$*/PARP1*$^{-/-}$ clones, indicating an epistatic relationship between ALC1 and PARP1(Figure 12). Moreover, ALC1 and PARP1 have an epistatic relationship, as sensitivity to MMS was very similar for *PARP1*$^{-/-}$ and *ALC1*$^{-/-}$*/ PARP1*$^{-/-}$ clones(Figure 12). These observations indicate that ALC1's role in cellular tolerance to H_2O_2 and MMS depends at least partially on the functionality of PARP1. In conclusion, given that PARP1 contributes to H_2O_2 and MMS tolerance by promoting BER, ALC1 may play a role in BER in the chicken DT40 cell line.

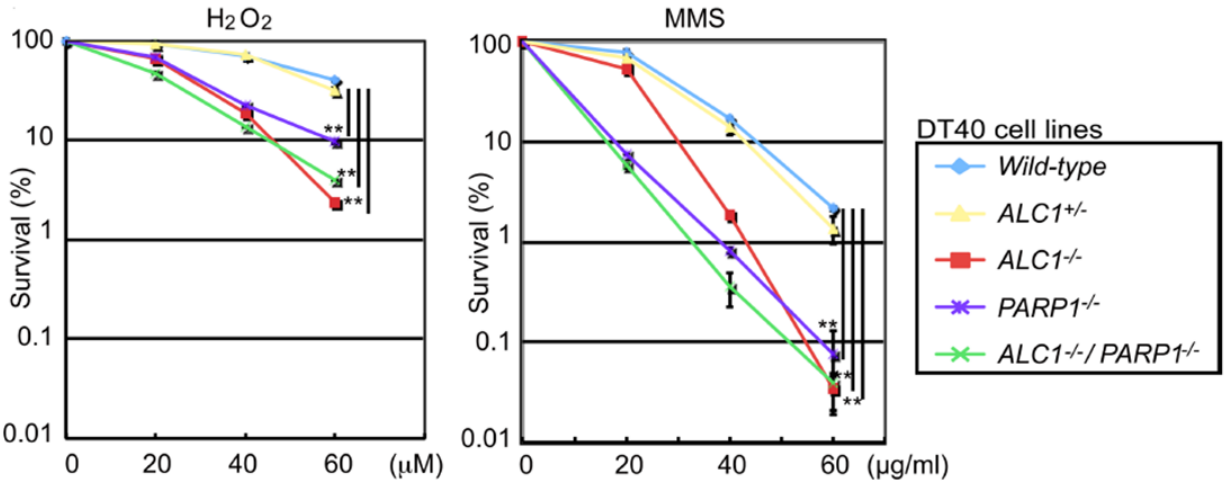

Figure 12
The sensitivity profile of indicated cell lines to H_2O_2 (left) and MMS (right). Y-axis indicates the survival % and x-axis indicates the dose.

1-4-3 The role of ALC1 in Base Excision Repair

The sensitivity data suggest that ALC1 may facilitate BER cooperating with PARP. I thus monitored ongoing BER by measuring the number of SSBs, which are BER intermediates. After 20 min of H_2O_2 treatment on ice, I performed the alkaline-comet assays. Alkaline Comet Assay (i.e. single cell gel electrophoresis), is a sensitive technique to quantify DNA single-strand breaks in individual cells (Braafladt et al., 2016). Immediately after H_2O_2 pulse-treatment, tail sizes in *wild-type* and *ALC1*$^{-/-}$ cells were very similar (Figure 13 middle). At 30 min after treatment, tails in the wild-type cells had decreased to nearly normal size, while tails in the *ALC1*$^{-/-}$ cells were significantly longer (Figure 13 right). Importantly, *ALC1*$^{-/-}$, *PARP1*$^{-/-}$, and *ALC1*$^{-/-}$*/PARP1*$^{-/-}$ clones all showed similar kinetics in SSB repair. These data demonstrate that ALC1 and PARP1 collaborate in SSB repair in chicken DT40 cells.

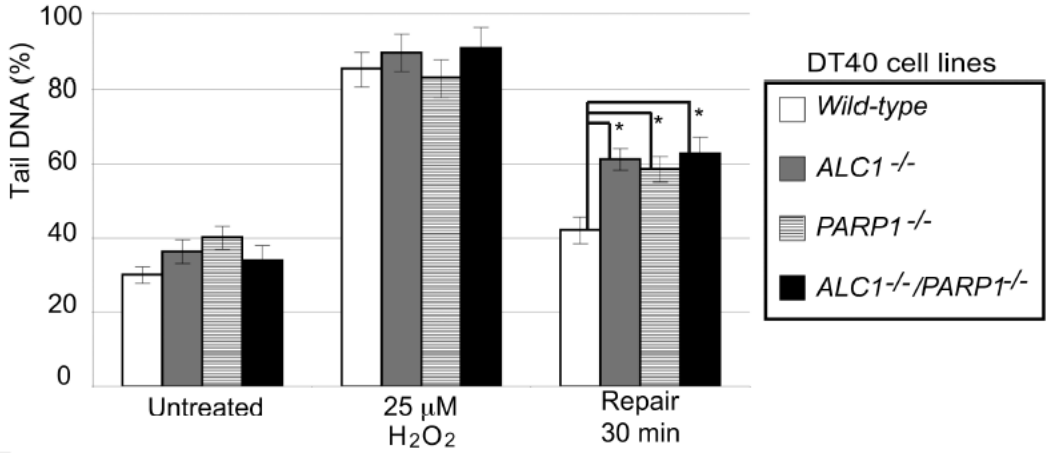

Figure 13

Alkaline comet assay to detect SSBs. Indicated cell lines were tested in untreated cells, immediately after exposure to 25 μM H_2O_2 on ice, and after a further 30 min incubation (repair period). Error bars represent standard deviations from three independent experiments. Tail-DNA percentage, defined as the percentage of damaged DNA (% DNA in the tail), was calculated as described in Materials and Methods. Tail-DNA% is displayed on the y-axis on a linear scale.

To examine ALC1's role in BER in human cells, I created *ALC1*$^{-/-}$ clones from the human TK6 cell line and analyzed SSB-repair kinetics by performing an alkaline-comet assay in *Wild-type* and *ALC1*$^{-/-}$ TK6 cells. *ALC1*$^{-/-}$ TK6 cells were more sensitive to MMS than *Wild-type* cells (Figure.15). Unlike the DT40 cells, *ALC1*$^{-/-}$ TK6 cells showed similar H_2O_2 sensitivity compared to *Wild-type* cells (Figure 14). It is possible that the oxidative stress decreased cellular viability through mechanisms other than DNA damage in this cell line.

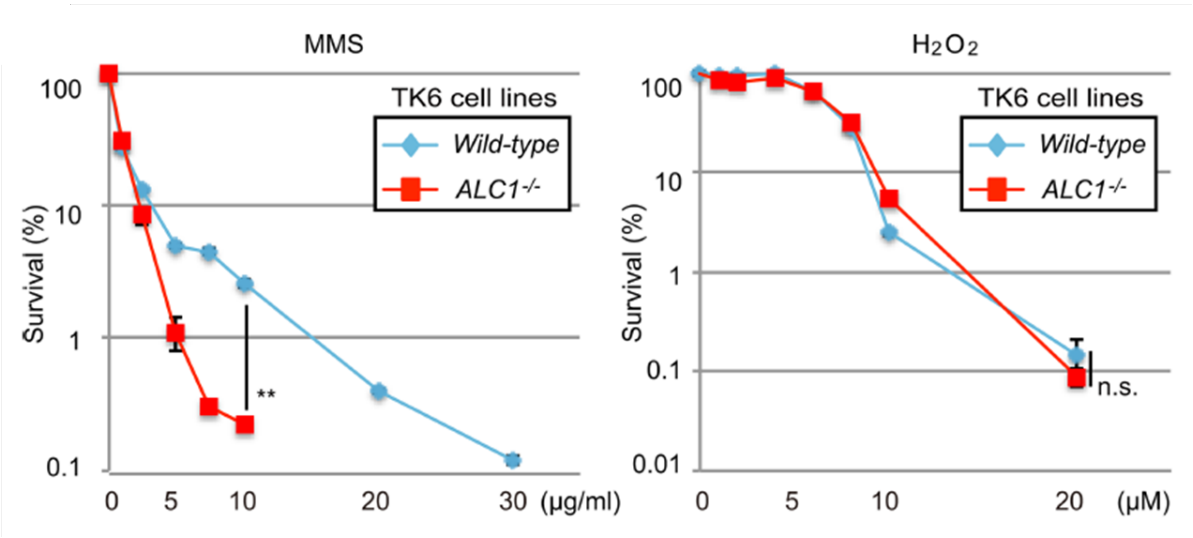

Figure 14
The sensitivity profile of indicated cell lines to MMS (left) and H2O2 (right). Y-axis indicates the survival % and x-axis indicates the dose.

Nonetheless, delayed SSB repair at 5 min following pulse-exposure to H_2O_2 was reproducibly seen in *ALC1*$^{-/-}$ TK6 cells (Figure 15A). Moreover, when the pulse-exposed cells were subsequently treated with the chemotherapeutic PARP poison, olaparib, which stabilizes the PARP-DNA complex, the delay in SSB repair in *ALC1*$^{-/-}$ TK6 cells was more pronounced than in the wild-type cells (Figure 15 B). I thus conclude that ALC1 contributes to SSB repair in the human TK6 cell line as well as in the chicken DT40 cells. I examined the kinetics of BER following pulse-exposure to MMS. Note that pulse-exposure to MMS has to be done at 37 °C, at which temperature base damage and repair occur in parallel. Alkaline-comet tails were longer in *ALC1*$^{-/-}$ than in *Wild-type* cells after pulse-exposure to MMS, suggesting a BER defect in the *ALC1*$^{-/-}$ cells. To examine the actual BER kinetics, I pulse-exposed *Wild-type* and *ALC1*$^{-/-}$ cells to MMS and released them in a drug-free medium. Repair in *ALC1*$^{-/-}$ cells was significantly delayed during the chase period. I thus conclude that ALC1 promotes BER in both chicken DT40 and human TK6 cell lines.

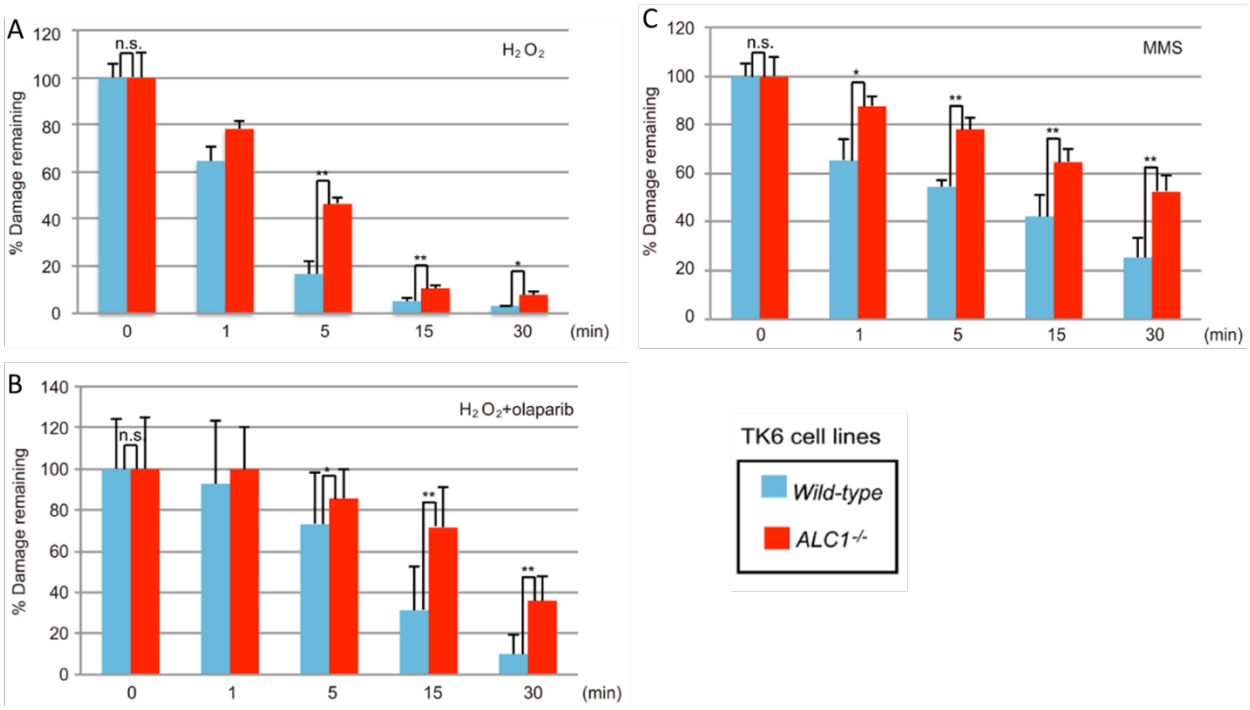

Figure 15

Alkaline-comet assay to detect unrepaired SSBs in human TK6 cells. The percentage of DNA strand breaks remaining at the indicated time points is displayed on the y-axis on a linear scale. Error bars represent standard deviations from three independent experiments. (A) Human TK6 cells of the indicated genotype were exposed to 80 μM H_2O_2 on ice for 30 min. The cells were released in drug-free, pre-warmed culture medium and further cultured for the indicated time. (B) TK6 cells treated with H_2O_2 as in (A) were released in culture medium containing 1 μM olaparib then cultured for the indicated time. (C) Wild-type and *ALC1*$^{-/-}$ TK6 cells were treated with 0.1 and 0.075 mg/ml MMS, respectively, for 15 min. Cells were then released in drug-free, pre-warmed culture medium and further cultured for the indicated time. p-value was calculated by a student's t-test: p (**) <0.01, (*) <0.05, and n.s. (not significant).

1-4-4 ALC1 promote BER independently of XRCC1

I confirmed that ALC1 and PARP1 have an epistatic relationship in BER in chicken DT40

cells. I next aimed to define the role played by ALC1 in the promotion of BER by PARP. To test whether ALC1 controls PARP-mediated PARylation, I measured intracellular NAD(P)H during continuous exposure to H_2O_2 and MMS. This assay monitors PARP-mediated PARylation, since the reduction of NAD^+, a major substrate of PARP, results in depletion of cellular NAD(P)H. I found that the amount of NAD(P)H was reduced in wild-type and *ALC1*$^{-/-}$ DT40 cells with very similar kinetics (Figure 16), indicating that ALC1 does not affect PARylation by PARP.

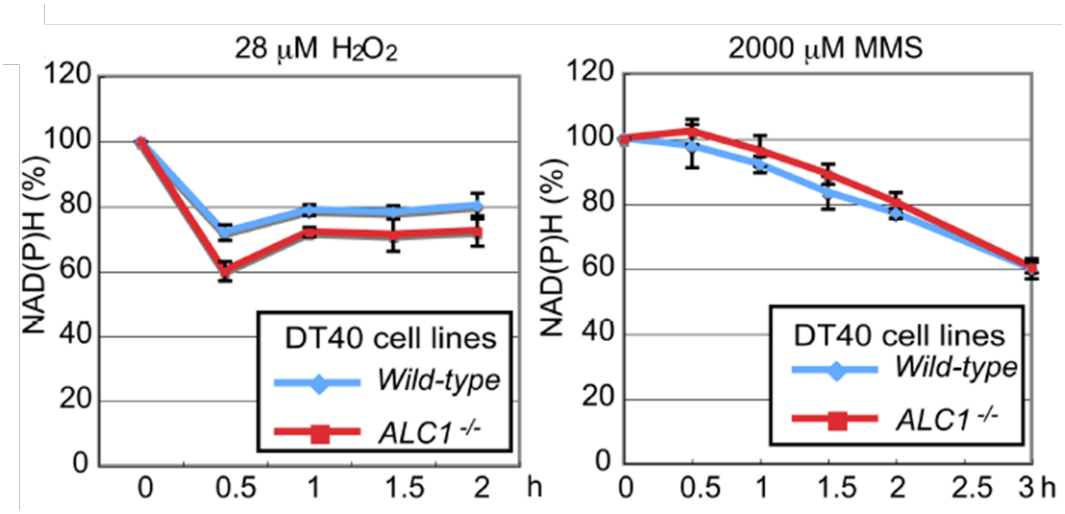

Figure 16

DT40 clones of the indicated genotypes were treated with H2O2 or MMS and harvested at the indicated times after treatment. To evaluate the activation of the PARylation event by PARP1 at SSB sites, I measured the cellular concentration of NAD(P)H, the major substrate for PARP. Time after treatment with H_2O_2 or MMS is displayed on the x-axis, while the relative cellular NAD(P)H concentration is displayed on the y-axis.

I considered that ALC1 might control PARP-mediated recruitment of XRCC1 to damage sites. To test this hypothesis, I induced SSBs selectively in subnuclear areas and examined the kinetics of XRCC1 re-localization to SSB sites. To induce SSBs, I employed a nucleotide

excision repair-deficient xeroderma pigmentosum group A (XPA) U2OS cells expressing Neurospora crassa UV-damage endonuclease (UVDE), which generates SSBs at UV photoproducts. I depleted ALC1 using si-RNA in HeLa and U2OS cells and monitored the recruitment of BER factors to induced SSB sites after UV irradiation. As with the *ALC1*$^{-/-}$ DT40 cells, the ALC1-depleted HeLa cells showed a higher sensitivity to H_2O_2 than did the si-control-RNA-treated cells (Figure 17A). On the other hand, the depletion of ALC1 did not impair the recruitment of XRCC1 to induced SSB sites (Figure 17C). Similarly, GFP-XRCC1 was efficiently recruited to laser-induced DNA damage sites in ALC1-depleted and control cells. Moreover, recruited XRCC1 seemed to be functional since GFP-Polβ also accumulated at DNA-damage sites (Figure 17C). I thus conclude that ALC1 contributes to BER independently of the recruitment of XRCC1 or Polβ.

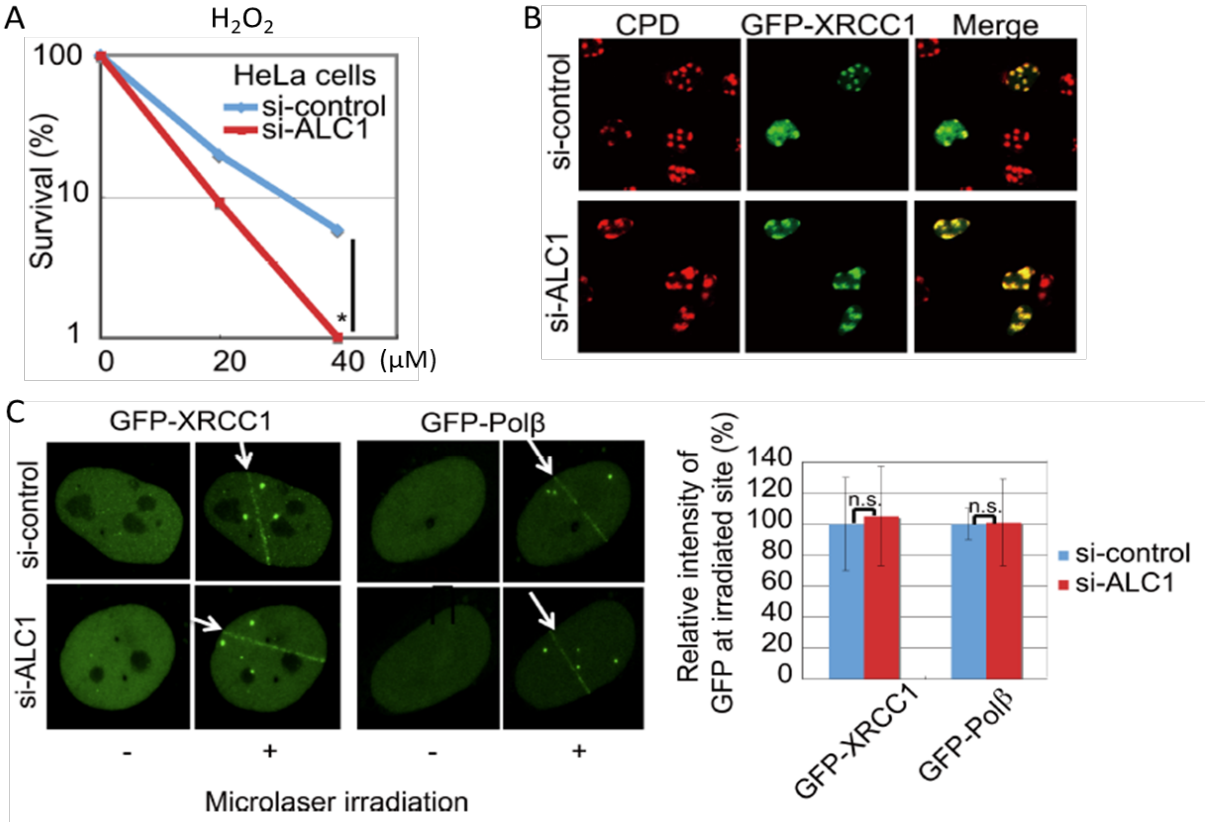

Figure 17

(A) H_2O_2 sensitivity of ALC1-depleted or control si-RNA-treated HeLa cells. The dose of H2O2 is displayed on the x-axis on a linear scale, while the percentage of cell survival is displayed on the y-axis on a logarithmic scale. (B) U2OS cells deficient in nucleotide excision repair, xeroderma pigmentosum group A^- (XPA^-) expressing Neurospora crassa UV-damage endonuclease (UVDE) were exposed to 100 J/m2 UV through micropores in membrane filters. DNA single-strand breaks were produced at the UV-irradiated region, where GFP-XRCC1 accumulated independently of ALC1 expression. Representative image of XPA-UVDE cells displaying GFP-XRCC1 and UV damage (CPD) signals. (C) GFP-XRCC1 and GFP-Polβ accumulate immediately at DNA damage sites after exposure to a 405 nm pulse laser in U2OS cells, which have been treated with siRNA against ALC1 or control siRNA for 48 h. GFP-signal intensity for GFP-XRCC1 and GFP-Polβ is displayed in the histogram. Error bars represent standard deviations from three independent experiments. p-value was calculated by a student's t-test: p (*) <0.05, and n.s. (not significant).

1-4-5 ALC1 promotes BER by inducing chromatin remodeling through histone eviction

The above conclusion led me to consider that ALC1 might promote chromatin relaxation at DNA-damage sites to facilitate DNA repair. To monitor the extent of chromatin compaction, I performed the MNase chromatin digestion assay. MNase tends to digest nucleosomes that have reluxed (open) chromatin structure, resulting in a single nucleosome (mononucleosome). I exposed chicken DT40 cells to H_2O_2, then partially digested chromatin DNA with MNase, and quantified the fraction of the mononucleosome. Five min after treatment with 5mM H_2O_2, the amount of partially digested product, ~146 bp DNA, was significantly increased in *Wild-type* cells, but not in *ALC1*$^{-/-}$ cells(Figure 18A). The data suggest that the configuration of chromatin changes into open status in *Wild-type* but not in *ALC1*$^{-/-}$ cells by H_2O_2-induced DNA damage presumably through inducing histone eviction. To further examine this possibility, I measured the amount of histone H3 released from the chromatin after DNA damage. After H_2O_2 treatment, histone proteins translocate to nuclear soluble from chromatin fraction. The amount of histone H3 in the nuclear soluble fraction was increased in wild-type cells after H_2O_2 treatment(Figure 18B), suggesting that DNA-damage induces histone eviction from chromatin. However, histone eviction was not observed in *ALC1*$^{-/-}$ cells(Figure 18B). These results suggest that ALC1 promotes BER by inducing chromatin remodeling through histone eviction and facilitating the access of BER factors to DNA-damage sites.

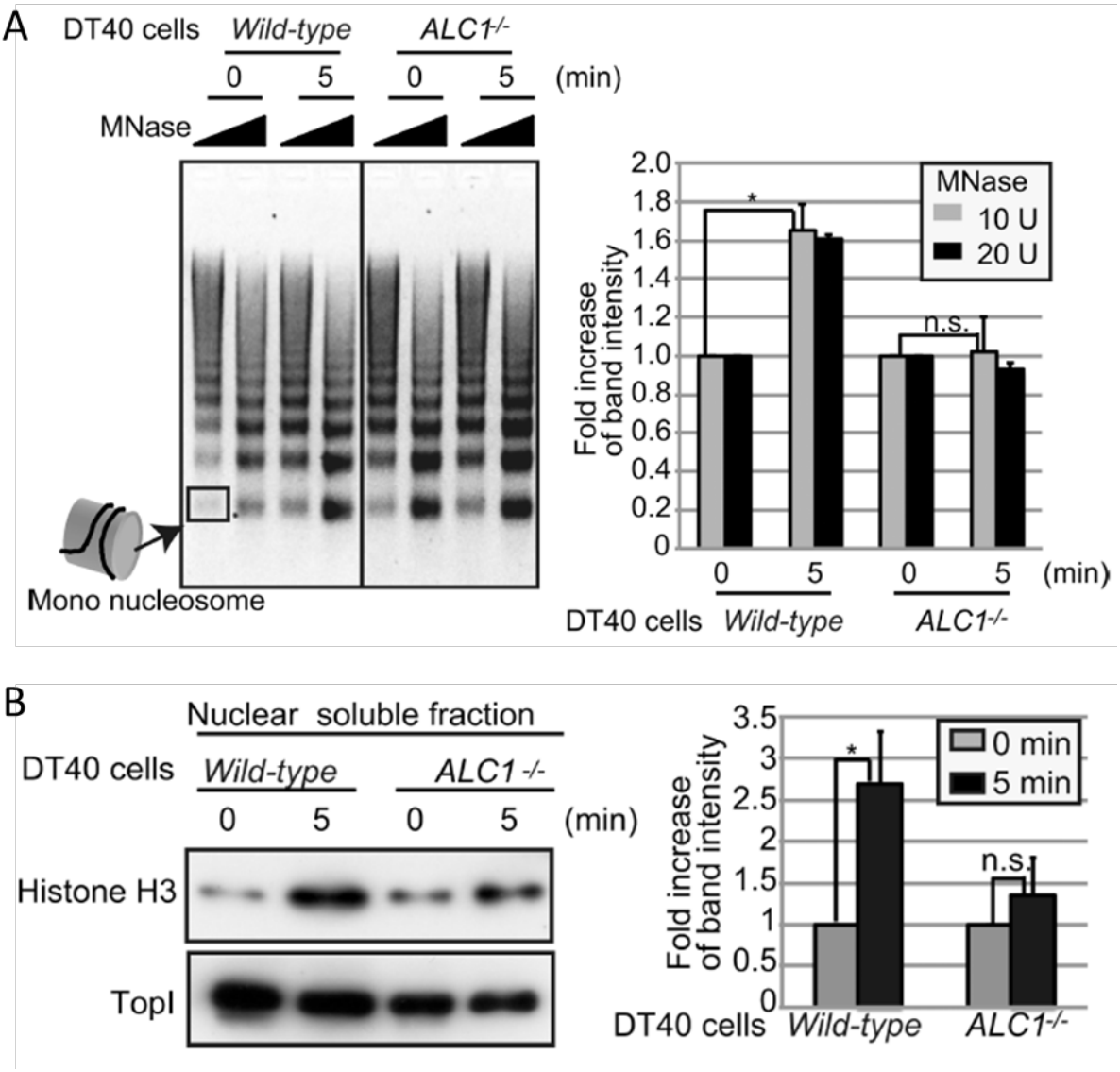

Figure 18

(A) DT40 cells of the indicated genotypes were treated with H_2O_2, and cells were harvested at the indicated times after H_2O_2 treatment. The chromatin fraction was digested with 10 and 20 U/ml MNase. Digested genomic DNA products were analyzed by gel electrophoresis. The relative intensity of the band corresponding to the mono-nucleosome (146 bp, indicated by arrow) was quantified. (B) Histone H3 present in the nuclear soluble fraction was detected by western blot. The blot was probed with anti-Topoisomerase I (TopI) antibody as a loading control. The relative intensity of the band corresponding to histone H3 was quantified and normalized for the level of TopI. p-value was calculated by a student's t-test: p (*) <0.05, and n.s. (not significant).

From the above data, I conclude ALC1 promotes chromatin relaxation at DNA-damage sites to facilitate base excision repair to tolerate base damage.

1-4-6 The role of ALC1 to tolerate CPT-induced DNA damage

To investigate the further role of ALC1 in various DNA-repair mechanisms, I measured cell survival after exposure to a wide variety of known DNA-damaging agents. *ALC1*$^{-/-}$ and wild-type cells exhibited an indistinguishable sensitivity to cisplatin, UV, VP16, ICRF-193, and olaparib, but the *ALC1*$^{-/-}$ cells were moderately more sensitive to CPT than wild-type cells. *PARP1*$^{-/-}$ cells were critically more sensitive to CPT than wild-type and ALC1$^{-/-}$ cells, (Figure 19). Moreover, *ALC1*$^{-/E165Q}$ and *ALC1*$^{-/-}$ cells showed a virtually identical CPT sensitivity, indicating that the chromatin-remodeling activity of ALC1 is required for cellular tolerance to CPT(Figure 19). These data indicate that ALC1 is involved in the cellular tolerance to CPT as well as PARP. Olaparib is a PARP poison. It stabilizes PARP on the DNA during SSB repair and makes PARP toxic. *PARP*$^{-/-}$ mutant showed less sensitivity to olaparib than wild-type cells. This is because there is no PARP in *PARP*$^{-/-}$ mutant.

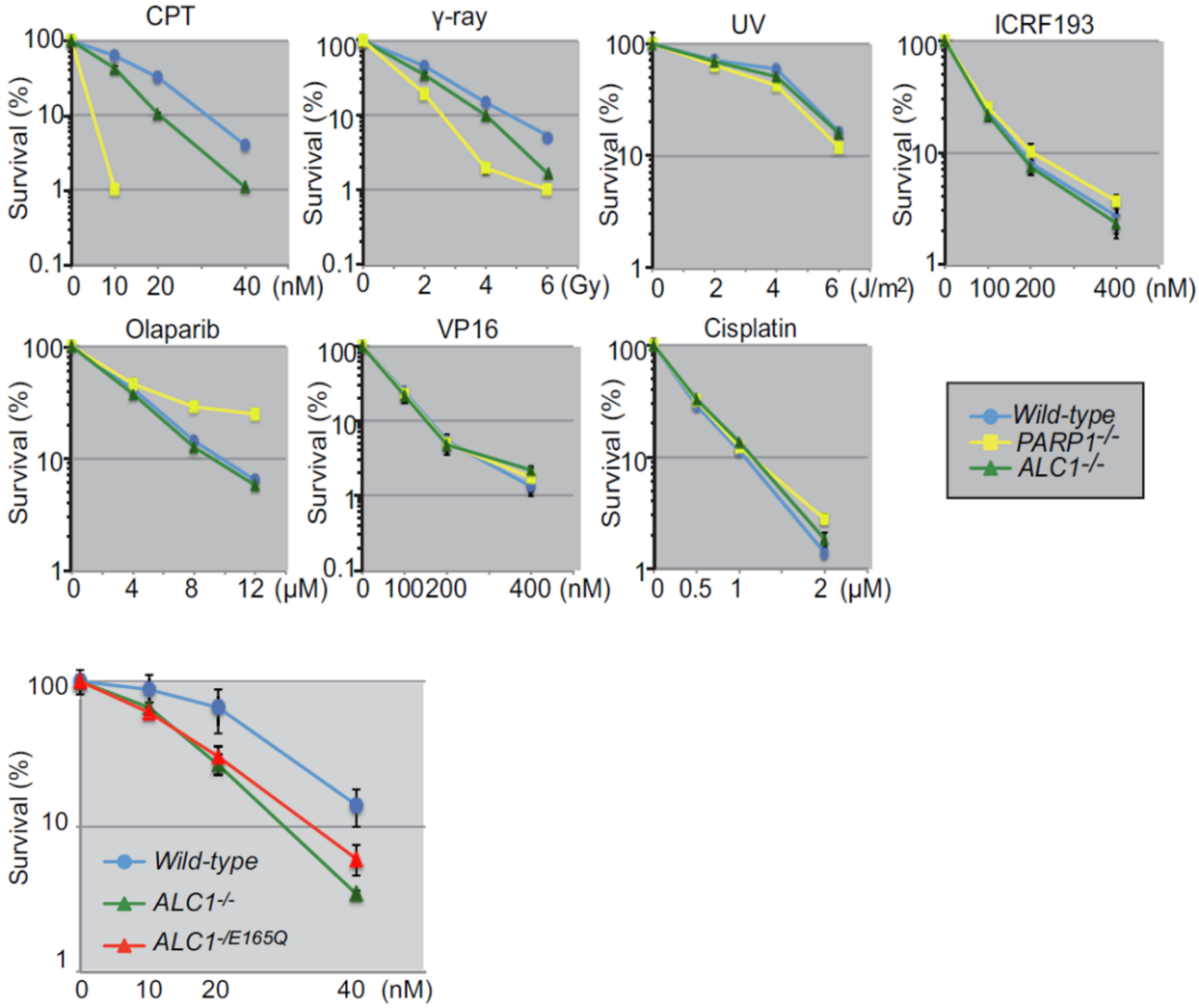

Figure 19

The sensitivity profile of *Wild-type* and *ALC1*$^{-/-}$ and *PARP*$^{-/-}$ mutants to indicated compounds and irradiations (upper 7 panels). The sensitivity profile of WT and *ALC1* null mutants and *ALC1* helicase dead mutant to CPT (lower panel). Y-axis indicates the survival % and X-axis indicate the dose.

I next compared the sensitivity to CPT among *Wild-type*, *ALC1*$^{-/-}$, *PARP1*$^{-/-}$, and *ALC1*$^{-/-}$*/PARP1*$^{-/-}$ cells. The *ALC1*$^{-/-}$ cells were less sensitive than the *PARP1*$^{-/-}$ cells, with the *PARP1*$^{-/-}$ and *ALC1*$^{-/-}$*/PARP1*$^{-/-}$ cells exhibiting a similar sensitivity (Figure 20). Therefore, I conclude

that ALC1 and PARP1 collaborate in contributing to cellular tolerance to CPT as well as DNA base damaging agents.

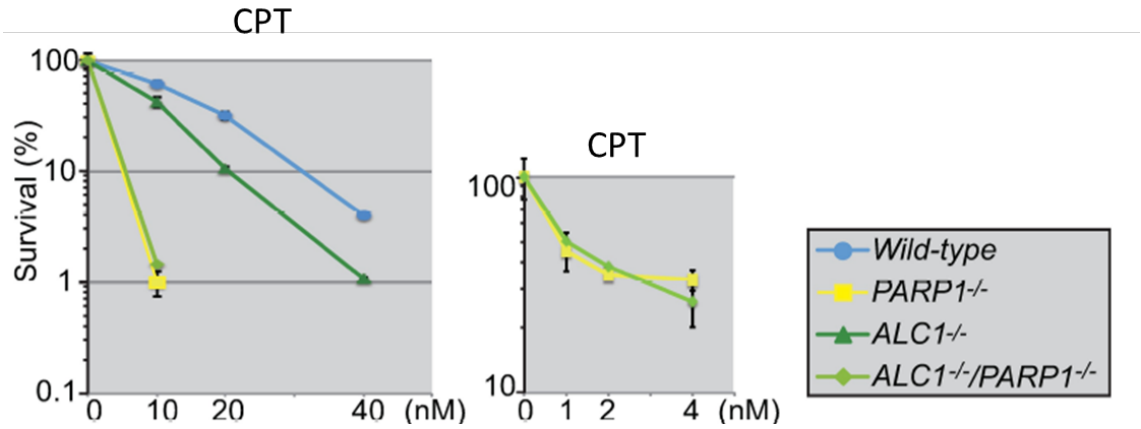

Figure 20

The sensitivity profile of indicated cell lines to CPT. Y-axis indicates the survival % and x-axis indicates the dose.

The sensitivity data suggest that ALC1 has a role to tolerate CPT induced DNA damage. To confirm the epistatic relationship between ALC1 and PARP to repair CPT-induced DNA damage, I conducted chromosome analysis. In this assay, I can see the DNA damage as breaks or gaps in chromosomes under microscopy. *ALC1*$^{-/-}$, *PARP1*$^{-/-}$, and *ALC1*$^{-/-}$/*PARP1*$^{-/-}$ cells all showed an increase in the number of chromosome breaks after exposure to CPT, with the *PARP1*$^{-/-}$ and *ALC1*$^{-/-}$/*PARP1*$^{-/-}$ cells exhibiting a very similar number of chromosome aberrations (Figure 21). Note that loss of PARP1 in *ALC1*$^{-/-}$ cells changed the type of chromosome aberrations and resulted in an increase of iso-chromatid breaks (i.e., breaks at the same site of both sister chromatids.) This type of break is likely caused by the defective resolution of recombination intermediates and thus implying a possible involvement of PARP1 in the resolution of recombination intermediates.

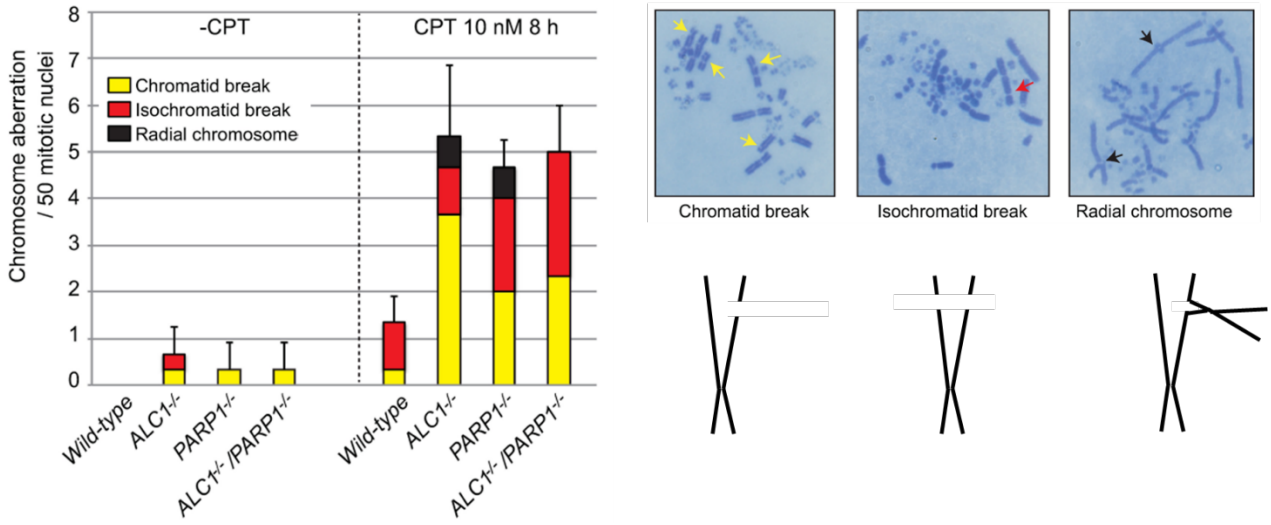

Figure 21

(right) Representative images showing DT40 chromosomes. The yellow, red and black arrows indicate chromatid breaks, isochromatid breaks and radial chromosomes, respectively. (left) The number of chromatid breaks, isochromatid breaks, and radial chromosomes in 50 mitotic cells. Chicken DT40 cells were exposed to CPT (10 nM) for 8 h with colcemid added 2.5 h before harvest to accumulate mitotic cells. Error bars represent standard deviations from three independent experiments.

1-4-7 ALC1 promotes chromatin relaxation around DNA replication to tolerate CPT-induced DNA damage

The requirement of ALC1's ATPase activity for tolerance to CPT suggests that ALC1 might induce chromatin relaxation around Top1-cc. To examine this hypothesis, I analyzed the degree of chromatin condensation around the replication forks stalled at Top1-cc using an MNase digestion assay. I modified this assay to see the event around replication fork. I labeled newly replicated DNA with BrdU for 10 min and I treated the cells with CPT for 15 min, then detected it with an anti-BrdU antibody. The partially digested product corresponding to mono-nucleosomes was quantified. Following treatment with 20 μM CPT, MNase sensitivity was significantly increased and mono-nucleosomes were more efficiently

digested in wild-type cells (Figure 22), suggesting a change of chromatin state into a more open configuration. In marked contrast, MNase sensitivity in *ALC1*$^{-/-}$ cells was slightly reduced by the CPT treatment (Figure 22), suggesting that chromatin relaxation around the Top1-cc site cannot be maintained in the absence of ALC1. I thus conclude that CPT induces chromatin de-condensation and that ALC1 might be required for this process. This conclusion is consistent with the recently demonstrated pivotal role played by ALC1 in chromatin remodeling at DNA damages induced by laser micro irradiation.

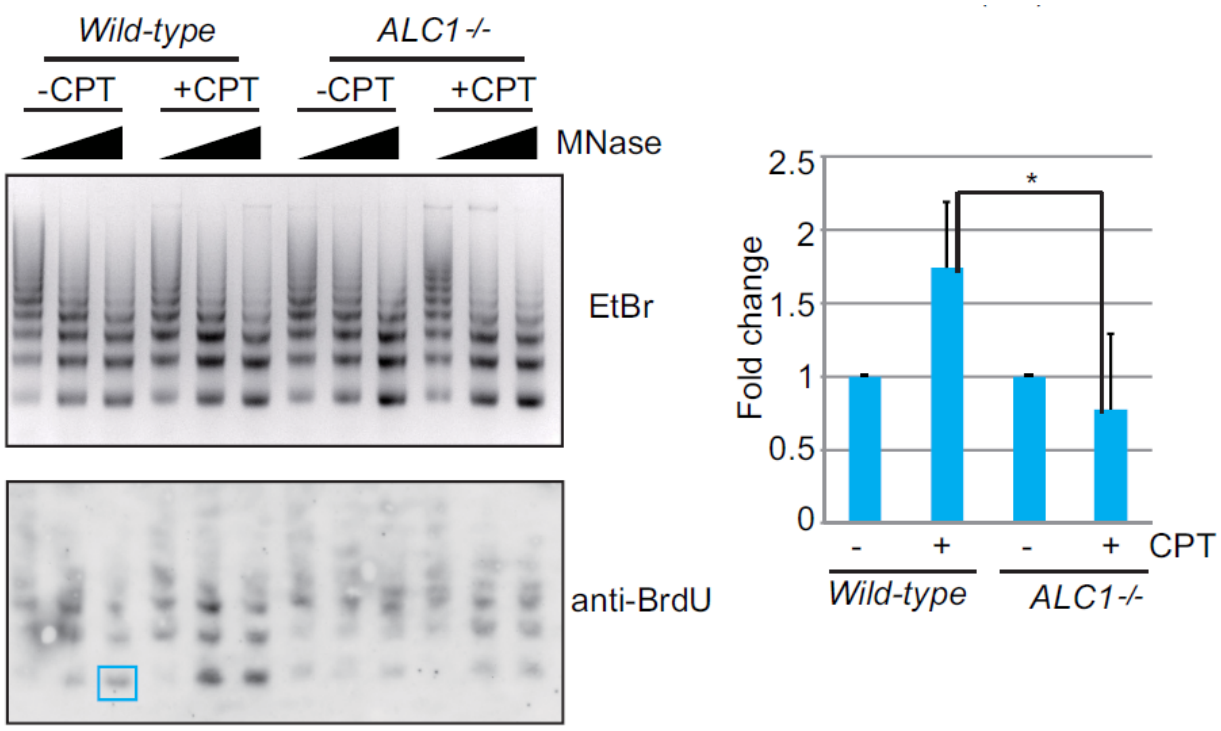

Figure 22

Nucleosome assembly near Top1-cc. 5 ×10^7 wild-type and *ALC1*$^{-/-}$ cells were pulse-labeled with BrdU for 10 min followed by treatment with CPT (20 μM) for 15 min. Nuclei were prepared and treated with 5, 10, and 20 units/ml MNase for 5 min. DNA was resolved in 2% agarose gel and stained with ethidium bromide (EtBr) (upper left panel), transferred onto a membrane, and detected with an anti-BrdU antibody (lower left panel). The blue box indicates the quantified band corresponding to the mono-nucleosomes. P-value was calculated by Student's t-test (*P<0.05).

1-4-8 ALC1 does not suppress toxic NHEJ above CPT

RNF8$^{-/-}$ cells showed a higher sensitivity to CPT than *Wild-type* cells as well as *ALC1*$^{-/-}$ and *PARP1*$^{-/-}$. It is reported that RNF8 suppresses toxic non-homologous end-joining (NHEJ), as evidenced by the increased number of radial chromosomes in the *RNF8*$^{-/-}$ cells. This phenomenon occurs mainly because of aberrant NHEJ, as the number of radial chromosome events in NHEJ-deficient *KU70*$^{-/-}$ cells is lower than that in *Wild-type* cells. To examine whether the collaborative ALC1-PARP pathway also contributes to CPT tolerance by suppressing toxic NHEJ, I measured the number of radial chromosomes. Radial chromosomes are a result of toxic NHEJ. There was no increase in radial chromosomes in either *ALC1*$^{-/-}$ or *PARP1*$^{-/-}$, whereas the number of radial chromosomes in *RNF8*$^{-/-}$ was two times higher than in wild-type cells (Figure 23), consistent with the previous report. I thus conclude that the ALC1-PARP pathway contributes to CPT tolerance by some other mechanism(s) than the suppression of toxic NHEJ. This conclusion is consistent with a previous study, which showed that RNF8 and RAD18 collaboratively suppress toxic NHEJ following CPT damage, while PARP1 contributes to cellular tolerance to CPT independently of RAD18.

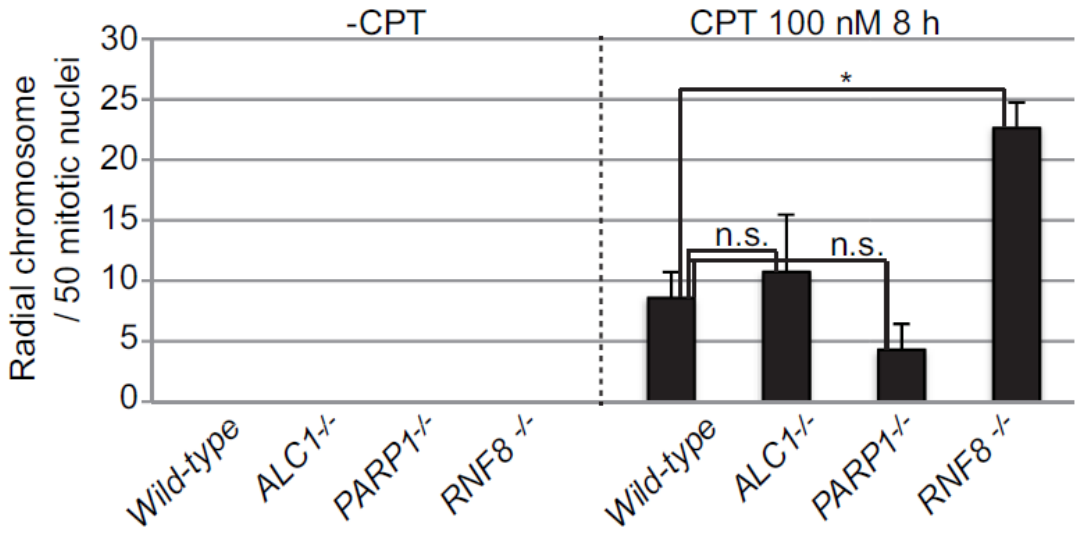

Figure 23

The number of radial chromosomes in 50 mitotic cells. DT40 cells were exposed to CPT (100nM) for 8 h with colcemid added 2.5 h before harvest to accumulate mitotic cells. Error bars represent standard deviations from three independent experiments. P-value was calculated by a Student's t-test (*P<0.05); n.s. = not significant.

1-4-9 ALC1 prevents replication-fork collapse by slowing fork progression

Since CPT induces replication-fork slowing, I next examined roles played by ALC1 in fork slowing upon CPT. To observe the replication fork progression, I carried the DNA fiber assay. In this assay, I added two types of nucleotide analogs, CldU and IdU in culture medium. Replicating cells incorporate them in replicated tracts, and the replicated tracts can be separately stained by specific antibodies. I measured the length of the replicated tracks before (CldU) and after (IdU) CPT treatment in *ALC1*$^{-/-}$, *PARP1*$^{-/}$, and wild-type cells, then compared the CldU/IdU ratios (Figure 24). Consistent with the previous study (Chaudhuri et al., 2012; Sugimura et al., 2008), replication tracts in the wild-type cells were significantly shortened following CPT exposure, with a median CldU/IdU ratio of 2.29± 0.15. In *ALC1*$^{-/-}$ cells, replication-fork slowing was partially impaired, with a median CldU/IdU ratio of 1.77± 0.08. *PARP1*$^{-/-}$ cells showed an even more pronounced defect in replication-fork slowing (median CldU/IdU ratio of 1.29± 0.01) (Figure 24). These results indicate that ALC1 is involved in the replication-fork slowing at Top1-cc.

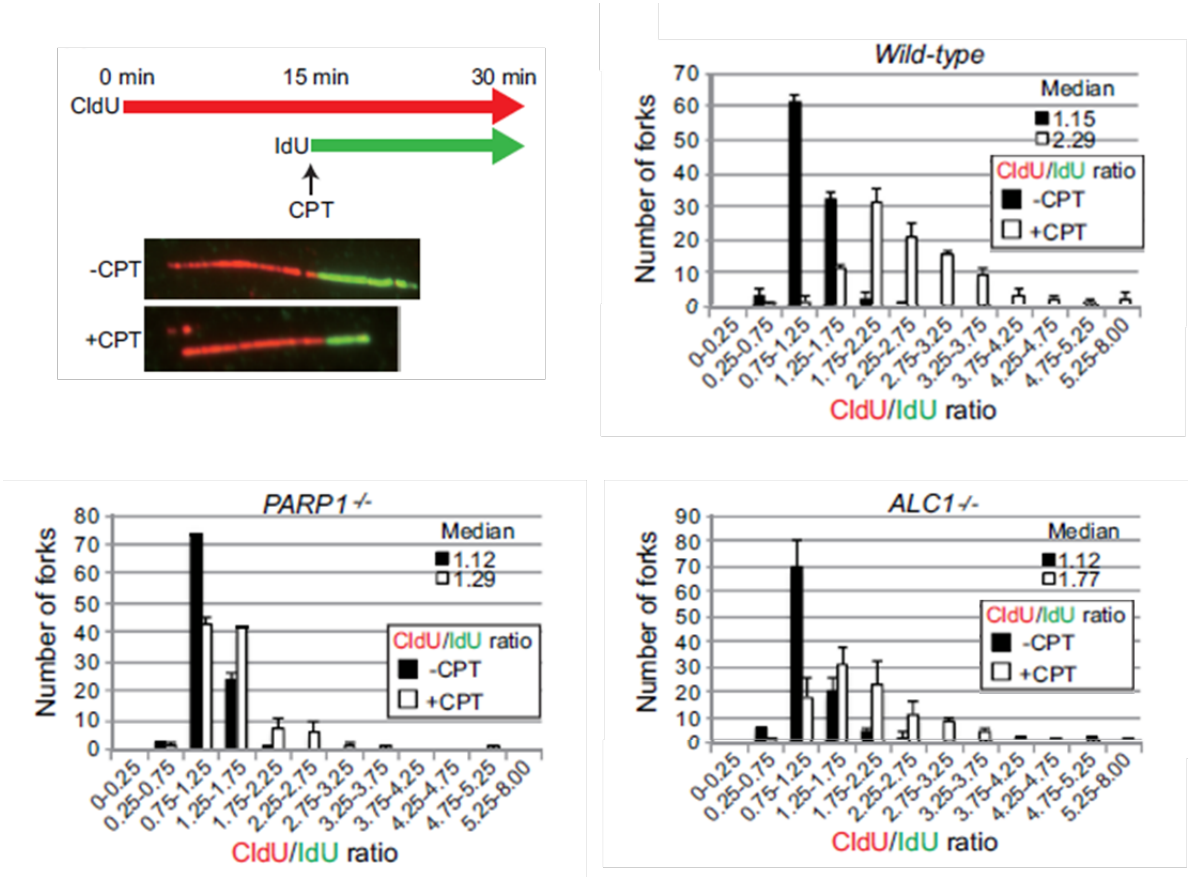

Figure 24

(upper left) Representative images showing stained DNA fibers. DT40 cells were labeled sequentially with CldU and IdU with or without CPT treatment after CldU labeling. Distribution of CldU/IdU ratios for replication forks in cells exposed to CPT. Indicated cells were incubated in medium containing CldU (25 μM) for 15 min, then incubated in medium containing IdU (250 μM) with CPT (10 μM) or without CPT for 15 min. The CldU/IdU ratios are shown on the x-axis. The number of fibers in each section is shown on the y-axis. 100 forks from each cell line were analyzed. Error bars represent standard deviations from three independent analyses.

The critical role played by the PARP pathway in safe fork slowing and the data showing an epistatic relationship between ALC1 and PARP1 in CPT tolerance combine to suggest that

ALC1 collaborates with the PARP pathway in the regulation of replication forks at Top1-cc sites.

1-5 Discussion

1-5-1 ALC1 works with PARP as a chromatin remodeler in the base excision repair but independent of XRCC1

During the past decade, roles played by ALC1 in the regulation of DNA repair, as well as its PARP1 stimulated chromatin-repositioning enzyme activity, have been well determined (Ahel et al., 2009; Pines et al., 2012). 12 proteins are found to have macrodomain so far. ALC1 is the only protein that possesses both macrodomain and ATPase domain, suggesting the uniqueness of ALC1.

In this study, I explored ALC1's possible role in BER in the chicken DT40 and human TK6 cell lines and a genetic relationship with PARP. In viability assay, *ALC1*$^{-/-}$ cells show high sensitivity to both MMS and H_2O_2. I demonstrated the epistatic relationship between *ALC1*$^{-/-}$ and *PARP1*$^{-/-}$ mutants in cellular resistance to H_2O_2 and MMS in chicken DT40 cells. The epistatic relationship between *ALC1*$^{-/-}$ and *PARP1*$^{-/-}$ is consistent with the previous reports showing that ALC1 is recruited to the site of DNA damage and activated through PARylation. Since PARP1 plays a role in BER, this epistatic relationship further supports the conclusion that ALC1 plays a role in BER. In Alkaline-comet assays, which measures SSB which is an intermediate of BER, *ALC1*$^{-/-}$ showed higher amount of SSB than *wild-type* cells in both chicken and human cells. It suggests that ALC1 promotes BER after SSB formation. The results were consistent with the previously suggested possible roles of ALC1 in DNA repair. However, in human cells, *ALC1*$^{-/-}$ cells did not show a higher sensitivity to H_2O_2. Even so, *ALC1*$^{-/-}$ TK6 cells showed a higher amount of SSB at 5min after H_2O_2 pulse treatment. Given that *ALC1*$^{-/-}$ almost complete SSB repair at 15min after H_2O_2 treatment, base excision repair is a very quick reaction and ALC1 may works within 5 minutes after SSB occurs. This is possible that another repair mechanism can repair H_2O_2-induced DNA damage in long term repair. This may be the reason *ALC1*$^{-/-}$ TK6 cells did not show sensitivity in viability assay.

The data reveal that ALC1 contributes to the PARP-dependent promotion of BER without affecting the recruitment of XRCC1 or Polβ to DNA lesions. I thus conclude that ALC1 plays

a key role in BER repair, independent of both XRCC1 and Polβ. How ALC1 contribute to BER is still controversial. A significant delay in the repair of SSBs, which are BER intermediates, indicates that ALC1 contributes to promoting the sealing of SSBs downstream of PARylation. ALC1 facilitates chromatin relaxation, most likely at DNA damage sites. This is consistent with the fact that attenuation of ALC1's ATPase activity by the E165Q mutation completely inactivates its functions, which is shown as a viability assay. There are two choices after SSB formation during BER. One is short-patch BER and long-patch BER. One possible explanation is that chromatin remodeling by ALC1 might facilitate long-patch repair by removing nucleosomes for DNA-repair synthesis by DNA polymerases. Future research is indicated to clarify ALC1's role in BER by conducting in vitro BER in a chromatin context.

1-5-2 ALC1 prevents replication-fork collapse by slowing fork progression

I also uncovered a previously unappreciated function of ALC1 in the regulation of DNA replication, wherein ALC1 slows replication-fork progression at Top1-cc under the PARP pathway and thereby prevents replication-fork collapse. This conclusion is supported by a DNA-fiber assay demonstrating that ALC1 slows the progression of replication forks after CPT treatment. These data unveil the role played by ALC1 in the regulation of replication-fork progression following DNA damage. ALC1 contributes to cellular tolerance to DNA damage through multiple mechanisms: promotion of base-excision-repair pathways and prevention of DNA replication-fork collapse following DNA damage to template strands.

How ALC1 contribute to the regulation of DNA replication is not clear. It is possible that, during fork-slowing, some aspect of the PARP-ALC1 axis is under the control of the S-phase-checkpoint pathway that comprises ATR-Chk1 (Saldivar et al., 2017). Top1-cc interferes with DNA replication by avoiding origin firing and fork progression via the ATR-Chk1 signal pathway (Seiler et al., 2007). One possible scenario is that transient replication-fork arrest at Top1-cc sites activates the ATR-Chk1 checkpoint, which in turn activates the PARP-ALC1 axis, leading to fork reversal in which the newly synthesized strands are annealed to one another. This hypothesis is supported by previous reports that visualize fork reversal at Top1-cc and other DNA damage sites on template strands using an electronic microscope (Chaudhuri et al., 2012; Zellweger et al., 2015). Fork reversal might also require homologous

recombination mechanisms, including the RAD51-XRCC3 complex (Henry-Mowatt et al., 2003). As a result of fork reversal for the safe replication fork slowing, Top1-cc at the 3' SSB end might be efficiently excised by nucleases including TDP1. Besides, removal of CPT allows Top1-mediated re-ligation (Pommier, 2006, 2009). Loss of fork reversal and following lethal replication may result in one-end DSB at fork leading to fork collapse.

1-5-3 Overexpression of ALC1 and cancer development

The ALC1 gene is frequently amplified and overexpressed in human hepatocellular carcinoma and numerous solid tumors. This overexpression is associated with lymph node metastasis, tumor differentiation, and distant metastasis, suggesting that the ALC1 gene plays a role in invasion and metastasis of cancer cells. In contrast to the hypoxic microenvironment of solid tumors, malignant cells are exposed to a high concentration of oxygen during hematogenous metastasis. This study revealed that ALC1 induces chromatin remodeling around damaged bases. A liver is responsible for the metabolization process. Metabolization causes ROS. ROS activates ALC1. One possible explanation for the connection between overexpression of ALC1 and cancer development is that overexpressed ALC1 induces aberrant chromatin remodeling and thereby causes unscheduled enzymatic reactions, resulting in toxic chromosome rearrangement and cancer development.

Chapter 2:

Warsaw breakage syndrome DDX11 helicase acts jointly with RAD17 in the repair of bulky lesions and replication through abasic sites

2-1 Introduction

2-1-1 Warsaw Breakage Syndrome and DDX11

There are approximately 7,000 rare diseases reported. The definition of the rare disease depends on countries. In the US, it is defined as a condition that affects fewer than 200,000 people. 80% of rare diseases are considered to be related to genetic mutations on a specific gene (https://globalgenes.org/).

Warsaw breakage syndrome (WABS) is one of the rare diseases. There are only 14 cases have been reported by 2019 (Bottega et al., 2019). Because of a few numbers of the patients, molecular mechanisms underlying WABS have not been elucidated. Patients with this disease, however, have symptoms of severe growth retardation, microcephaly, intellectual disability, and deafness. WABS is caused by biallelic mutations in the *DDX11* gene (Bailey et al., 2015; Capo-Chichi et al., 2013).

DDX11 gene encodes DDX11 helicase (also known as CHDR1). Helicase enzyme catalyzes unwinding of duplex DNA. DDX11 is conserved from yeast to human (Figure 25). In addition to the role played by DDX11 as helicase enzyme, role(s) of DDX11 is suggested, since DDX11 directly interacts with replication factors, such as proliferating cell nuclear antigen (PCNA) and Ctf18-replication factor C (RFC) complex (Bharti et al., 2014a; Farina et al., 2008). PCNA is an essential protein for DNA replication. The main role of PCNA is to clamp replicative polymerases on duplex DNA for efficient DNA synthesis (Moldovan et al., 2007). When replication machinery encounters DNA damage and the replication is halted, the other polymerase sliding clamp, Rad9-Hus1-Rad1 (9-1-1) complex is loaded around DNA by the Rad17-RFC and Ctf18-RFC clamp loader (Karras et al., 2013; Lim et al., 2015).

9-1-1 complex promotes ATR-mediated phosphorylation and activation of checkpoint kinase 1 (Chk1) (Lim et al., 2015). Chk1 is responsible for checkpoint activation and stabilization of stalled replication fork. Although it has been suggested that DDX11 plays a role in the tolerance to DNA replication stress, the role of DDX11 in the replication has not been studied well. Moreover, the cells from WABS patients show a similar phenotype to that from Fanconi anemia patient (Bharti et al., 2014b; Eppley et al., 2017). However, the relationship between DX11 and Fanconi anemia associated protein is not uncovered yet.

	homology with DDX11 sequence in human
Homo sapience	
Mus musculus	71.0%
Gallus gallus	63.7%
Saccaromyces cerevisiae	20.2%

Figure 25 DDX11helicase is conserved in eukaryotic cells

DDX11 is well conserved from *S.cerevisiae* to *Homo sapience*

2-1-2 Fanconi anemia

Fanconi anemia (FA) is one of the hereditary disorders. FA patients tend to have bone marrow failure, developmental abnormalities and predisposition to cancer(Ceccaldi et al., 2012; Ceccaldi et al., 2016b). There are 22 proteins reported to complement FA disorder. Those proteins are referred to as Fanconi anemia complementation group (FANC) proteins. FANC proteins are essential to repair complicated DNA lesions such as Inter-strand cross-link (ICL) (Figure 26) (Ceccaldi et al., 2016b; Kottemann and Smogorzewska, 2013). The central components of the FA pathway, FANCD2 and FANCI interact with each other and are monoubiquitylated by the FA core complex(Ishiai et al., 2008). FANCD2–FANCI ubiquitylation promotes lesion unhooking, causing the formation of a gapped DNA molecule with the unhooked lesion in the gapped part and a double-strand break (DSB). The DNA damage is repaired subsequently by TLS and HR. The FA pathway is strongly linked to the intra-S phase checkpoint function of ATR, with ATR-mediated phosphorylation of FANCD2–

FANCI being required for the subsequent monoubiquitylation.

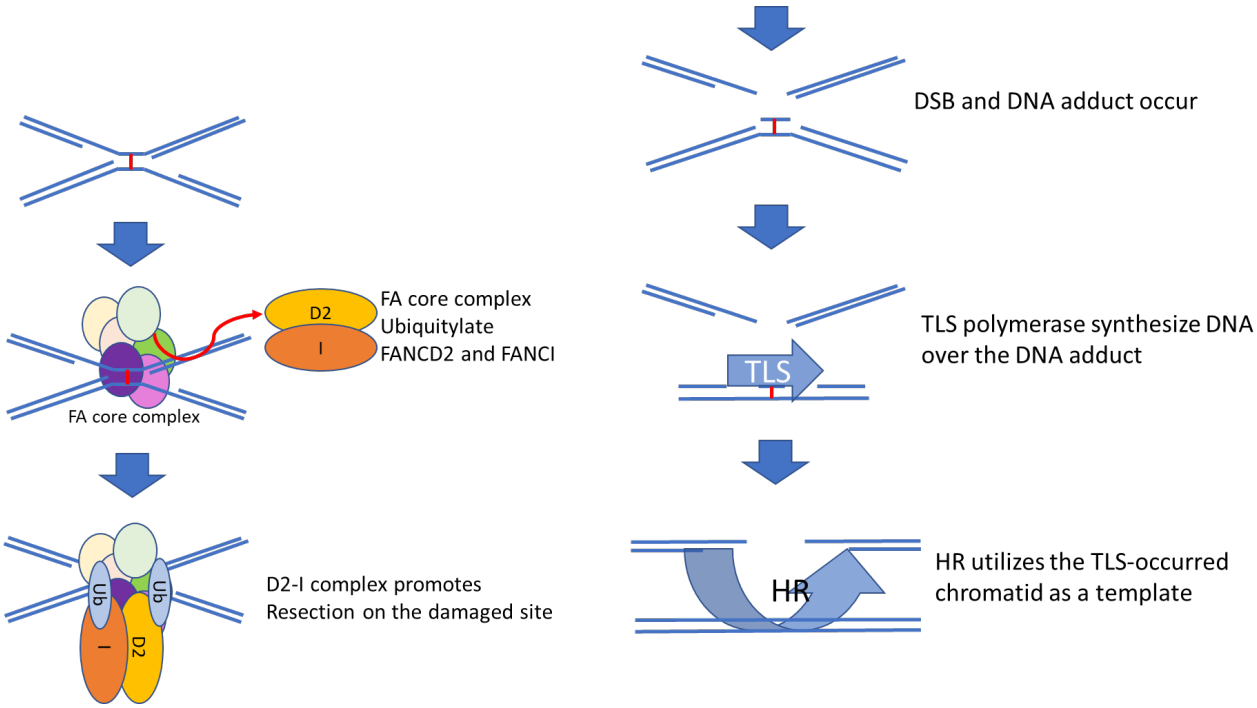

Figure 26 The role of FA-pathway in ICL repair

When DNA interstrand cross link occurs, FA core complex recognizes the damage and accumulates on the damage site. FANC D2/I complex is ubiquitylated by the complex. Ubiquitylated FANC D2-I complex promotes resection on the damaged site, leaving DNA double strand break on one strand and DNA adduct like damage on the other strand. DNA gap carrying DNA adduct like damage is filled-in by Translesion DNA synthesis. The DNA double strand break is repaired by homologous recombination by using newly synthesized DNA.

2-1-3 DNA damage during DNA replication

Maintaining genome information is very important for all livings. DNA lesions encountered during DNA replication may collapse the stability of replication forks and are an important source of DNA replication stress. For example, alkylation on DNA causes stalled replication

forks. To avoid replication fork collapse, cells are equipped with multiple tolerance mechanisms for replication stresses. One is translesion DNA synthesis (TLS). When replication machinery encounters damaged DNA, the replication polymerases are replaced with TLS polymerases. TLS polymerase can synthesize DNA over damaged DNA in return for accuracy. Another one is template switching. Template switching employs many HR-related proteins. Stalled newly synthesized DNA invades the sister chromatid and continues synthesizing by using sister chromatid as a template. Since the correct DNA sequence is used as a template in this process, TS is considered as an error-free pathway.
In addition to TLS and TS, cells have developed another tolerance mechanism called re-priming. In this process, DNA primer is generated right next to the damaged DNA. Cells can skip the replication on damaged DNA. DNA primase-polymerase (PrimPol) plays a central role in this process (Bailey and Doherty, 2017; Kobayashi et al., 2016).

In this study, I investigate the role of DDX11 in the tolerance to DNA replication stress, and the relationship between DDX11 and FA proteins, DDX11 and other proteins, which work to tolerate DNA replication stress.

2-2 Materials and Methods

Cell lines

WT
DDX11$^{-/-}$
Rad17$^{-/-}$
Brca2$^{-/-}$
FANCC$^{-/-}$
FANCJ$^{-/-}$
DDX11$^{-/-}$*/Rad17*$^{-/-}$
DDX11$^{-/-}$*/BRCA2*$^{-/-}$
DDX11$^{-/-}$*/FANCC*$^{-/-}$
DDX11$^{-/-}$*/FANCJ*$^{-/-}$

Assessment of Cell Growth and Sensitivity to DNA damaging Agents

Cells were cultured at 39.5 °C in D-MEM/F-12 medium (Gibco) supplemented with 10% fetal bovine serum, 2% chicken serum (Sigma), Penicillin/Streptomycin mix, and 10 μM 2-mercaptoethanol (Gibco). To plot growth curves, each cell line was cultured in three different wells of 24 well-plates and passaged every 24 h. The cell number was determined by flow cytometry using plastic microbeads (07313-5; Polysciences). Cell solutions were mixed with the plastic microbead suspension at a ratio of 10:1, and viable cells, determined by forward scatter and side scatter, were counted when a given number of microbeads was detected by flow cytometry. To assess drug sensitivity, 1 x 10^4 cells were cultured in 24-well plates containing various concentrations of DNA damaging agents in 1 ml of medium in duplicate. Cell viability was assessed after 48 h by flow cytometry using plastic microbeads. Percent survival was determined by considering the number of untreated cells as 100%. To determine CDDP and MMS sensitivity by Colony survival assay, 4×10^2 cells were inoculated into 60-mm dishes containing various concentrations of drug in a medium supplemented with 1.5% (wt/vol) methylcellulose, 15% fetal bovine serum, and 1.5% chicken serum. Colonies were counted after 7–14 days and the percent survival were determined relative to the number of colonies of untreated cells.

DNA Transfection and RT-PCR

DNA transfection and RT-PCR were performed as described previously. Drug-resistant colonies were selected in 96-well plates in medium containing 0.5 μg/ml puromycin, 30 μg/ml blasticidin, 1 mg/ml L-histidinol, 10 μg/ml mycophenolic acid, 2 mg/ml geneticin, 1 mg/mL bleomycin, or 2.5 mg/ml hygromycin B, as appropriate. Gene disruption was verified by genomic PCR and RT-PCR. The primers used for RTPCR are available upon request.

Visualization of RAD51 and γH2AX subnuclear foci

After MMC exposure (500 ng/mL, 1h), cells were harvested and spun onto glass slides using Cytospin. Cells were pre-permeabilized with 0.1% (v/v) Triton X-100 in in PBS, fixed with 4% paraformaldehyde and permeabilized with 0.5% (v/v)) Triton X-100 in PBS. Slides were then incubated with anti-Rad51 antibodies (Santacruz; sc-8349) and anti-γH2AX antibodies (Millipore; 05-636). Alexa-Fluor 488 goat anti-rabbit IgG (Invitrogen) and Cy3- conjugated donkey anti-mouse IgG (Jackson ImmunoResearch) were used as secondary antibody and 0.1 μg/mL DAPI was used for counterstaining. We only scored RAD51- and γH2AX-foci positive and negative cells with non-apoptotic nuclei. Images were captured with a fluorescent microscope (BX51, OLYMPUS).

AID overexpression by retrovirus infection

AID overexpression was carried out as described previously. Several single colonies were obtained from WT and each mutant. The cells which are overexpressing AID were cultured for 2 weeks. AID overexpression was carried out by infection of retrovirus containing the AID gene and the internal ribosomal entry site (IRES) followed by the Green fluorescent protein (GFP) gene. The efficiency of infection was about 60%, as measured by GFP expression.

sIgM gene conversion assay

The Ig gene conversion assay was carried out as described previously. DT40 has a frameshift in its rearranged V segment, which can be repaired by homologous pseudogene sequences. IgM negative cells from each genotype were cultured for 2 weeks. After collecting the cells, cells were treated with FITC-conjugated α-IgM antibody (BETHYL) and washed by SB (PBS containing 1% BSA). After that, cells were resuspended in SB. Cells were analyzed for surface-IgM (sIgM) expression by fluorescence-activated cell sorting (FACSCalibur, BD biosciences).

Analysis of IgVλ diversification

Genomic DNA was extracted at 14 days post-infection. Using primers CVLF6 5'-CAGGAGCTCGCGGGGCCGTCACTGATTGCCG and CVLR3 5'-GCGCAAGCTTCCCCAGCCTGCCGCCAAGTCCAAG, the rearranged V segments were PCR amplified, with Prime Star GXL DNA polymerase (Takarabio, Shiga, Japan), a high fidelity thermostable polymerase, cloned into pTOPOII-Zeroblunt (Invitrogen, CA) and sequenced with the M13 forward (−21) primer. Sequence alignment with clustalW (GenomeNet, Kyoto, Japan; https://www.genome.jp/) allowed identification of changes from the parental sequences in each clone. After the alignment, mutations were classified into Gene Conversion (GC) or Hypermutation (PM).

2-3 Results

2-3-1 DDX11 Helicase Facilitates Repair and Averts Genomic Instability Induced by ICLs

To explore the role of DDX11 in vertebrate cells, I established DT40 DDX11 knockout cell lines (*DDX11*$^{-/-}$). I tested the sensitivity to cisplatin (CDDP), which causes intra- and inter-strand crosslinks (ICLs). *DDX11*$^{-/-}$ cells are hypersensitive to cisplatin CDDP. The sensitivity of *DDX11*$^{-/-}$ mutants is complemented by expressing chicken and human *DDX11*, but not by expressing a helicase-dead, K87A variant of chicken *DDX11* (cDDX11) (Figure 27). In similar trends with FA mutants, such as *FANCC*$^{-/-}$ and *FANCJ*$^{-/-}$, *DDX11*$^{-/-}$ cells are defective in recovery from a transient exposure to mitomycin C (MMC) (Figure 27).

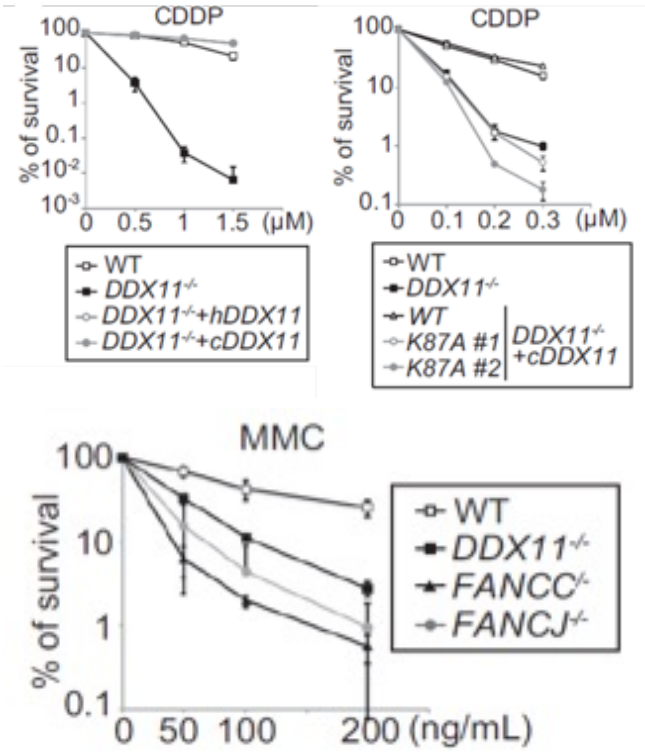

Figure 27

The sensitivity profile of indicated cell lines to CDDP and MMC. Y-axis indicates the survival % and x-axis indicates the dose.

Moreover, after exposure to MMC, the frequency of chromosome abnormalities was increased, especially regarding chromatid breaks (Figure 28). Thus, DDX11 might play pivotal role to avoid genome instability caused by ICLs.

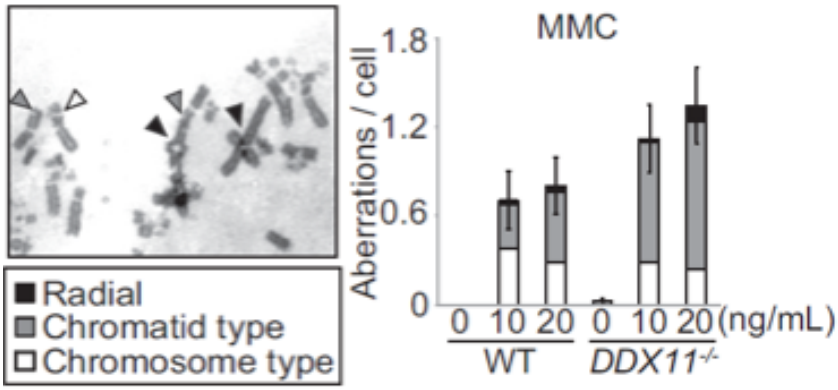

Figure 28

The representative picture of chromosome aberrations (Left). The number of chromosome aberrations after MMC treatment (Right).

2-3-2 DDX11 Functions as Backup to the FA Pathway in ICL Repair.

To examine the phenotypic relationship between DDX11 and the FA pathway, I carried out a sensitivity assay using double deletion mutant cell, in which both *DDX11* and *FANCC* are knocked-out. FANCC is an FA core component required for FANCD2–FANCI ubiquitylation. While *DDX11*$^{-/-}$ cells showed slight sensitivity, *FANCC*$^{-/}$ cells showed higher sensitivity than *DDX11*$^{-/-}$ cells. Moreover, *DDX11*$^{-/-}$*/FANCC*$^{-/}$ cells exhibited much greater sensitivity to cisplatin and MMC than either single mutant (Figure 29). Thus, DDX11 is important for ICL repair, acting in parallel with FA.

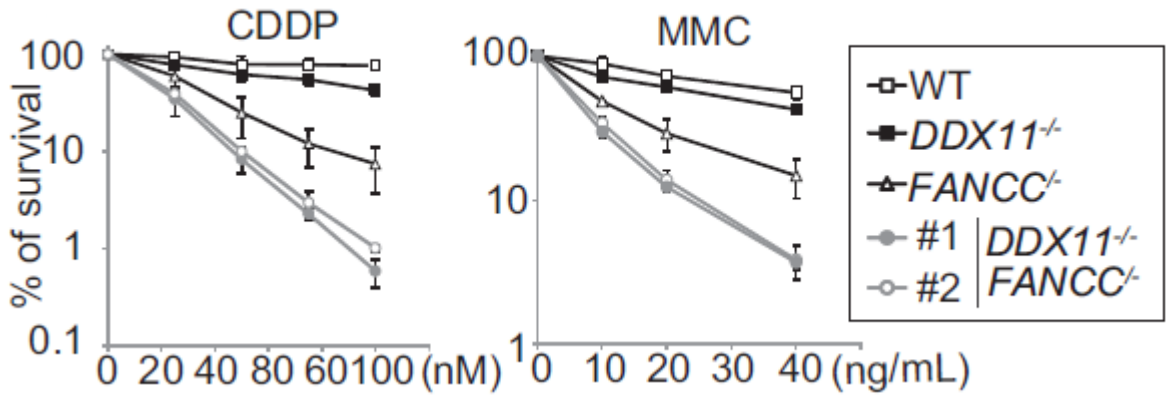

Figure 29

The sensitivity profile of indicated cell lines to CDDP and MMC. Y-axis indicates the survival % and x-axis indicates the dose.

2-3-3 DDX11 Facilitates DNA Repair by Homologous Recombination

The FA pathway is required for cellular tolerance to metabolic formaldehyde (Kottemann and Smogorzewska, 2013), which causes DNA adducts as well as ICLs. *DDX11*$^{-/-}$ cells showed slight sensitivity to formaldehyde but *DDX11*$^{-/-}$/*FANCC*$^{-/-}$ cells showed the much stronger sensitivity than *FANCC*$^{-/-}$ mutants did. I also tested double mutants between *DDX11* and *FANCJ*, as FANCJ is the main helicase associated with the FA pathway (Cota and Garcia-Garcia, 2012), and both DDX11 and FANCJ are orthologs of budding yeast Chl1. *DDX11*$^{-/-}$/*FANCJ*$^{-/-}$ cells showed slow proliferation and exhibited synergistic sensitivity to formaldehyde (Figure 30), suggesting compensatory functions of DDX11 and FANCJ in proliferation and DNA repair. Thus, DDX11 is dispensable for the FA pathway and acts as a backup to the FA pathway in ICL repair.

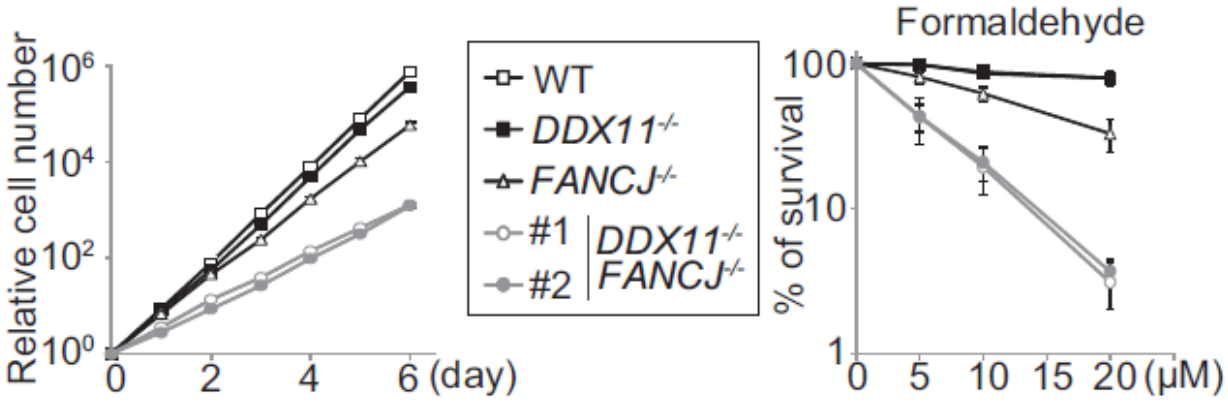

Figure 30

The cell proliferation curve of the indicated cell lines (Left). The sensitivity profile of indicated cell lines to Formaldehyde. Y-axis indicates the survival % and x-axis indicates the dose (Right).

In previous reports, DDX11 helicase is required to provide resistance against the PARP inhibitor, olaparib (Stoepker et al., 2015), which causes lesions that are repaired primarily by HR. To further investigate connections with HR, I carried out sensitivity assay using *DDX11*$^{-/-}$*/BRCA2*$^{-/-}$. BRCA2 is critical for HR and also implicated in FA (Prakash et al., 2015). *DDX11*$^{-/-}$*/BRCA2*$^{-/-}$ mutants showed additive sensitivity in regard to cellular tolerance to both cisplatin and olaparib (Figure 31).

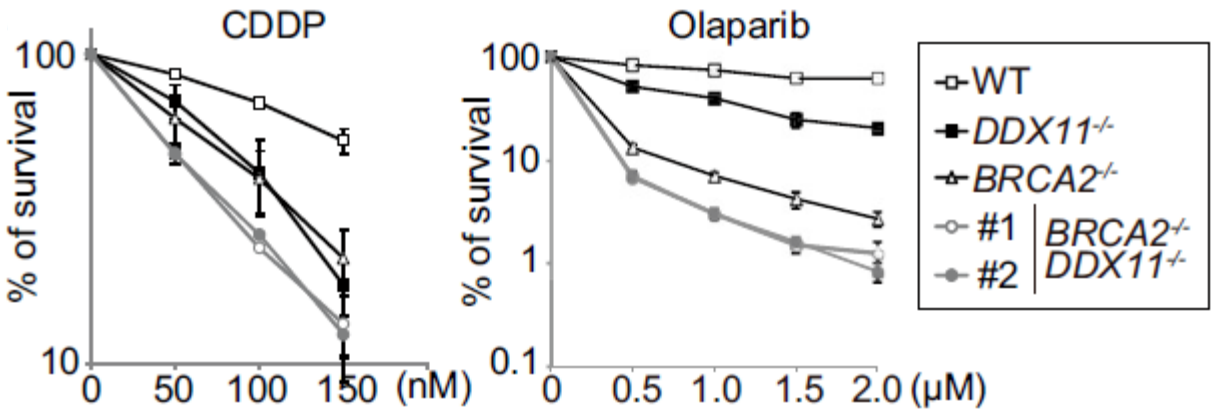

Figure 31

The sensitivity profile of indicated cell lines to CDDP and Olaparib. Y-axis indicates the survival % and x-axis indicates the dose

These results suggest a role for DDX11 in a repair mechanism that responds to olaparib but the role presents distinct features from the BRCA2- and FA core-mediated pathways. *DDX11*$^{-/-}$ cells are sensitive to the UV mimetic 4NQO (Figure 32), suggesting general roles of DDX11 in the repair of bulky lesions, rather than specificity toward ICLs.

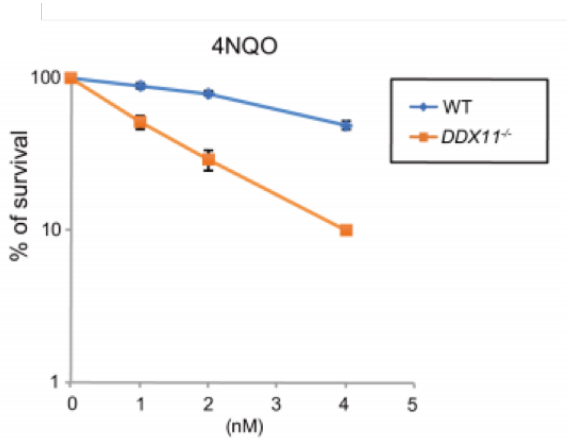

Figure 32

The sensitivity profile of indicated cell lines to 4NQO. Y-axis indicates the survival % and x-axis indicates the dose.

Since many HR-related FA factors contribute to DSB repair, I carried the sensitivity assay to DSB-inducing reagents. *DDX11*$^{-/-}$ cells display sensitivity toward drugs that cause topological stress and ultimately induce DSBs, such as Camptothecin (CPT), bleomycin, and etoposide, but are proficient in DSB-induced recombination (Figure 33).

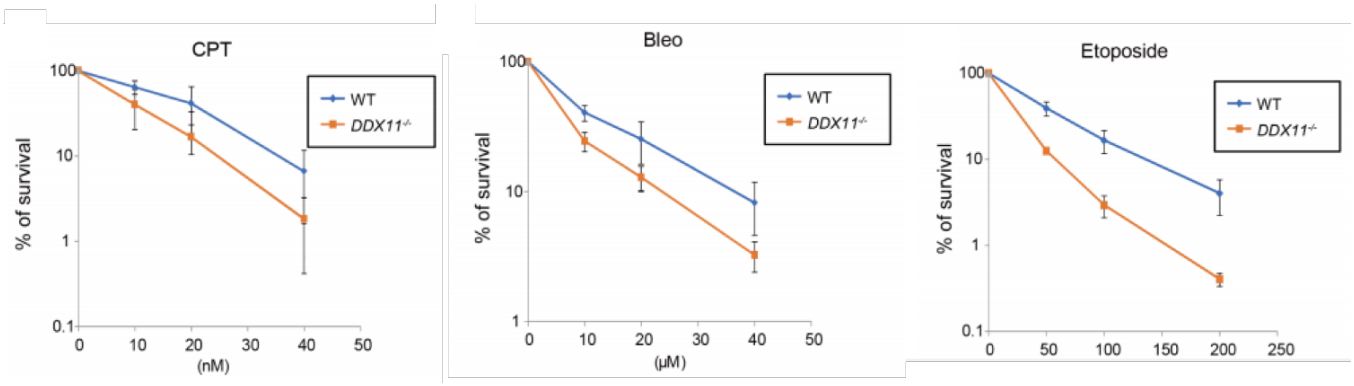

Figure 33
The sensitivity profile of indicated cell lines to CPT and bleomycin and etoposide. Y-axis indicates the survival % and x-axis indicates the dose.

To examine whether DDX11 may contribute to HR repair by affecting the recruitment of RAD51, I measured RAD51 foci after a short treatment with MMC, followed by recovery. Notably, RAD51 foci were decreased in *DDX11*$^{-/-}$ mutants compared with *wild-type* control cells (Figure 34).

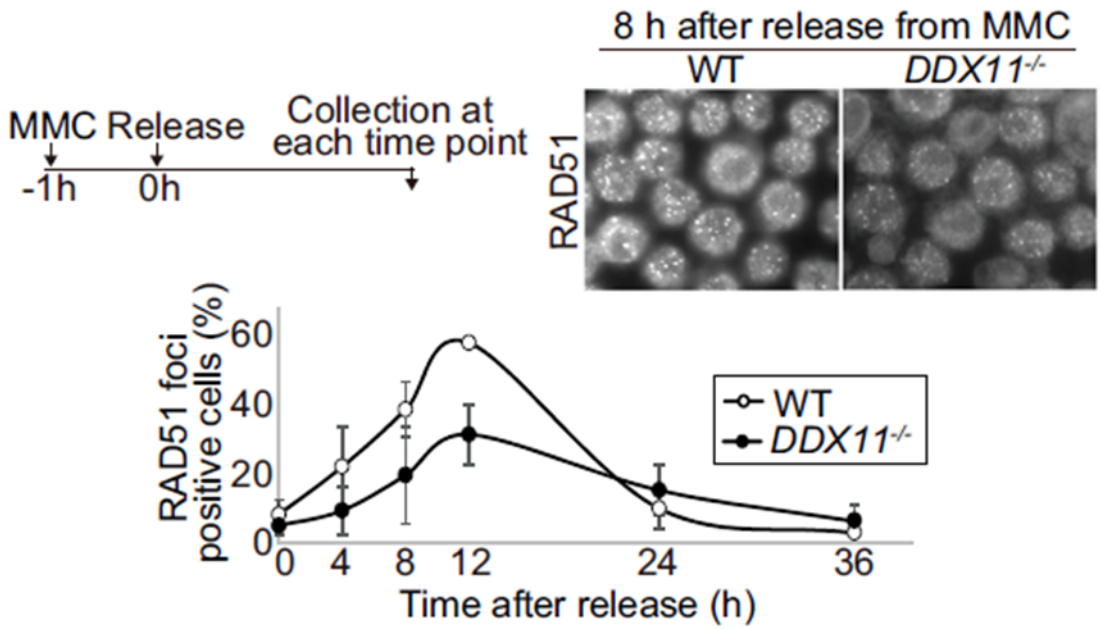

Figure 34

RAD51 focus formation after MMC treatment. The scheme for harvesting the cells (upper left). The representative image of the cells (upper right). Nuclei containing more than four bright foci were defined as foci positive and at least 200 cells were scored for each preparation (lower panel). The error bars indicate SD from three independent experiments.

To further address a possible role for DDX11 in endogenous recombination-mediated processes, I examined its role in Ig gene conversion, measured as the gain of surface IgM (sIgM) expression. DT40 cells carry a frameshift mutation in the Ig light-chain variable (IgVλ) segment, but gene conversion from pseudo-V segments removes the frameshift mutation, causing sIgM expression. WT and *DDX11*$^{-/-}$ clones were expanded for 14 d from single clones, in the absence or presence of trichostatin A (TSA), a histone deacetylase inhibitor that increases the frequency of Ig gene conversion in DT40 cells (Seo et al., 2005; Lin et al., 2008), thus allowing detection of rare gene-conversion events. In both spontaneous and TSA conditions, *DDX11*$^{-/-}$ mutants showed significant reduction in the frequency of Ig gene conversion events compared with WT cells (Figure 35).

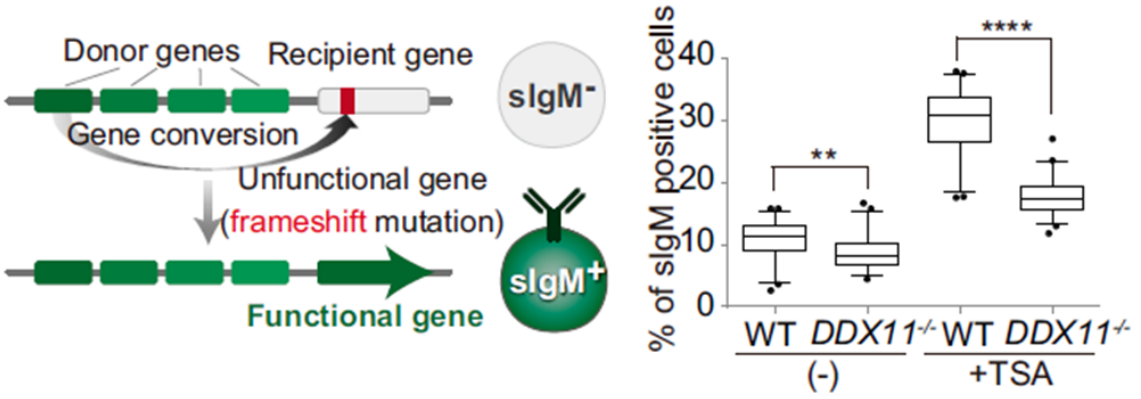

Figure 35

The scheme of sIgM assay of gene conversion (Left) and the rate of sIgM-positive cells (Right). In the box plots, the middle line indicates the median value; the box shows the 25th and 75th percentiles; the bars, the 5th and 95th percentiles. P values were calculated by Student's t test. **P ≤ 0.01, ****P ≤ 0.0001.

Taken together, these data suggest that DDX11 facilitates HR repair of PARP poison and ICL and gene conversion at the IgV region.

2-3-4 DDX11 Acts Jointly with 9-1-1 to Facilitate Post-replicative DNA Repair

To address whether DDX11 works at the replication fork, I tested the sensitivity of *DDX11*$^{-/-}$ mutant to aphidicolin and hydroxy urea (Figure 36). I did not observe significant differences between *wild-type* and *DDX11*$^{-/-}$ cells in either condition. Moreover, DDX11 is not essential for replication fork stability, as deduced from the lack of sensitivity of *DDX11*$^{-/-}$ cells to aphidicolin, a DNA polymerase inhibitor. Taken together, these results suggest that DDX11 may have a role in the post replicative DNA repair.

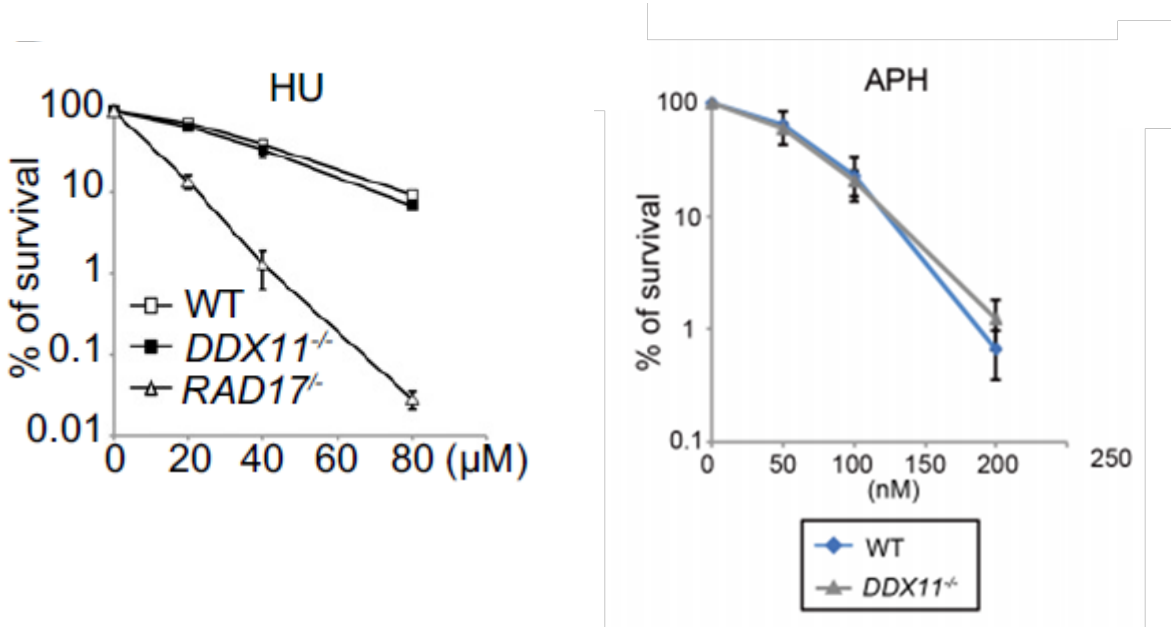

Figure 36

The sensitivity profile of indicated cell lines to Hydroxy Urea and Aphidicolin. Y-axis indicates the survival % and x-axis indicates the dose.

Because PrimPol has been implicated in reinitiating replication upon different types of replication lesions in eukaryotic cells (Bailey and Doherty, 2017; Kobayashi et al., 2016), I also generated *DDX11*$^{-/-}$*/PRIMPOL*$^{-/-}$ double mutants. These mutants showed additive sensitivity toward cisplatin and MMS (Figure 37), suggesting that DDX11 affects a step in DNA damage tolerance that is distinct from the replication restart step and TLS functions mediated by PrimPol.

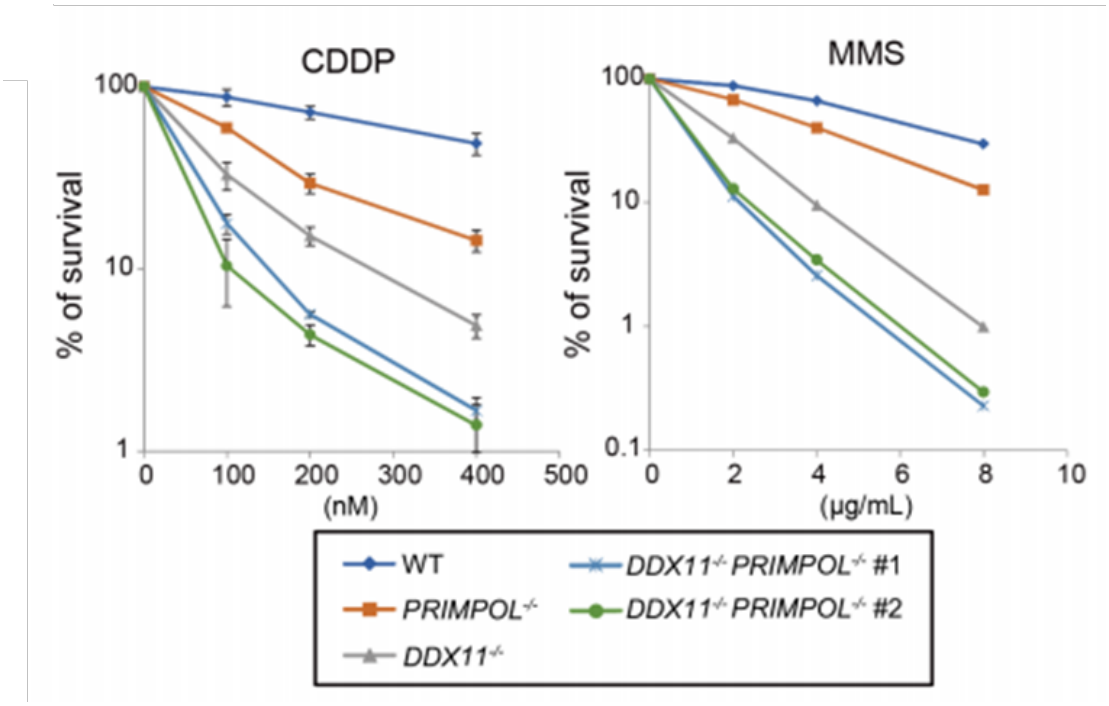

Figure 37

The sensitivity profile of indicated cell lines to CDDP and MMS. Y-axis indicates the survival % and x-axis indicates the dose.

The 9-1-1 checkpoint clamp promotes HR and facilitates repair of various types of replication lesions. The 9-1-1 checkpoint clamp is activated by ICLs, bulky adducts, and ssDNA gaps (Lim et al., 2015; Saberi et al., 2007). Because these features overlap what I found here for *DDX11*$^{-/-}$, I analyzed the functional interaction between DDX11 and 9-1-1. Strikingly, I found epistasis between DDX11 and the 9-1-1 checkpoint clamp loader, RAD17, regarding cisplatin and MMS sensitivity (Figure 38).

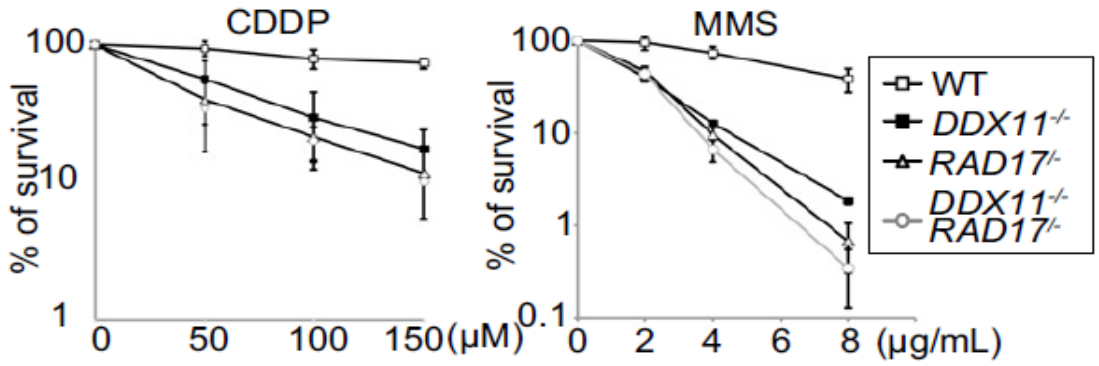

Figure 38

The sensitivity profile of indicated cell lines to CDDP and MMS. Y-axis indicates the survival % and x-axis indicates the dose.

Next, I tested whether the lesions remaining in *DDX11*$^{-/-}$ and *RAD17*$^{-/-}$ cells are amenable to post-replicative HR repair, a pathway induced by improving sister chromatid cohesion (SCC) in G2/M, after the bulk of DNA replication is complete. I improved post-replicative SCC by inhibiting a prophase pathway of cohesion release relying on Plk1-mediated phosphorylation of the cohesion subunit, SA2 (Hauf et al., 2005). SA2 has 12 serine/ threonine residues which are the targets of Plk1-mediated phosphorylation. The phosphorylation on the serine/ threonine residues are responsible for cohesion dissociation. The phosphorylation on SA2 is suppressed by mutating the serine/threonine residues to alanine (SA2-12A mutant) (Hauf et al., 2005). I found that expression of SA2-12A can partly rescue the sensitivity of *DDX11*$^{-/-}$ and *RAD17*$^{-/-}$ cells to cisplatin and MMS (Figure 39). Thus, the lesions accumulating in *DDX11*$^{-/-}$ and *RAD17*$^{-/-}$ cells can be repaired post-replicatively by alternate HR pathways.

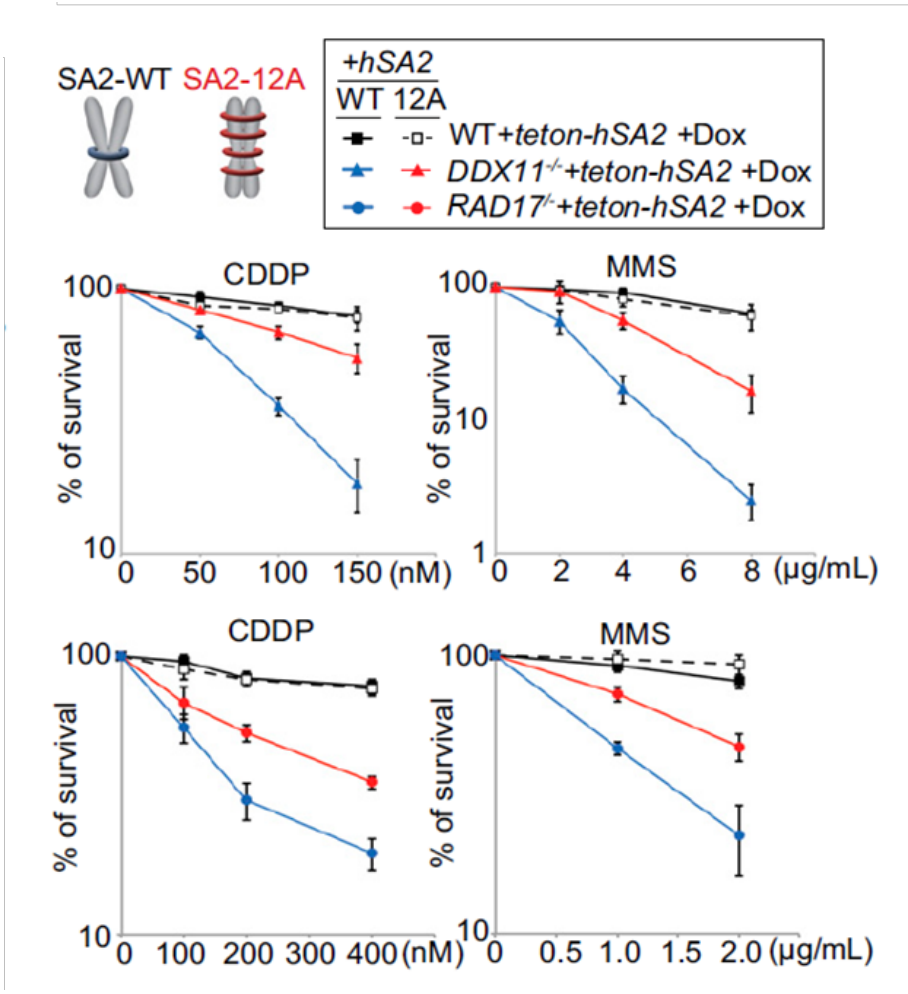

Figure 39

The sensitivity profile of indicated cell lines to CDDP and MMS. Y-axis indicates the survival % and x-axis indicates the dose.

Next, I tested whether DDX11 and 9-1-1 play similar or distinct roles in averting genome instability induced by MMC. Defects in RAD51 focus formation and accumulation of γH2AX foci following MMC treatment appeared similar in *DDX11*$^{-/-}$, *RAD17*$^{-/-}$, and *DDX11*$^{-/-}$/*RAD17*$^{-/-}$ double mutants (Figure 40). In all, these results indicate that DDX11 and 9-1-1 act jointly to mediate efficient HR mediated repair of ICLs.

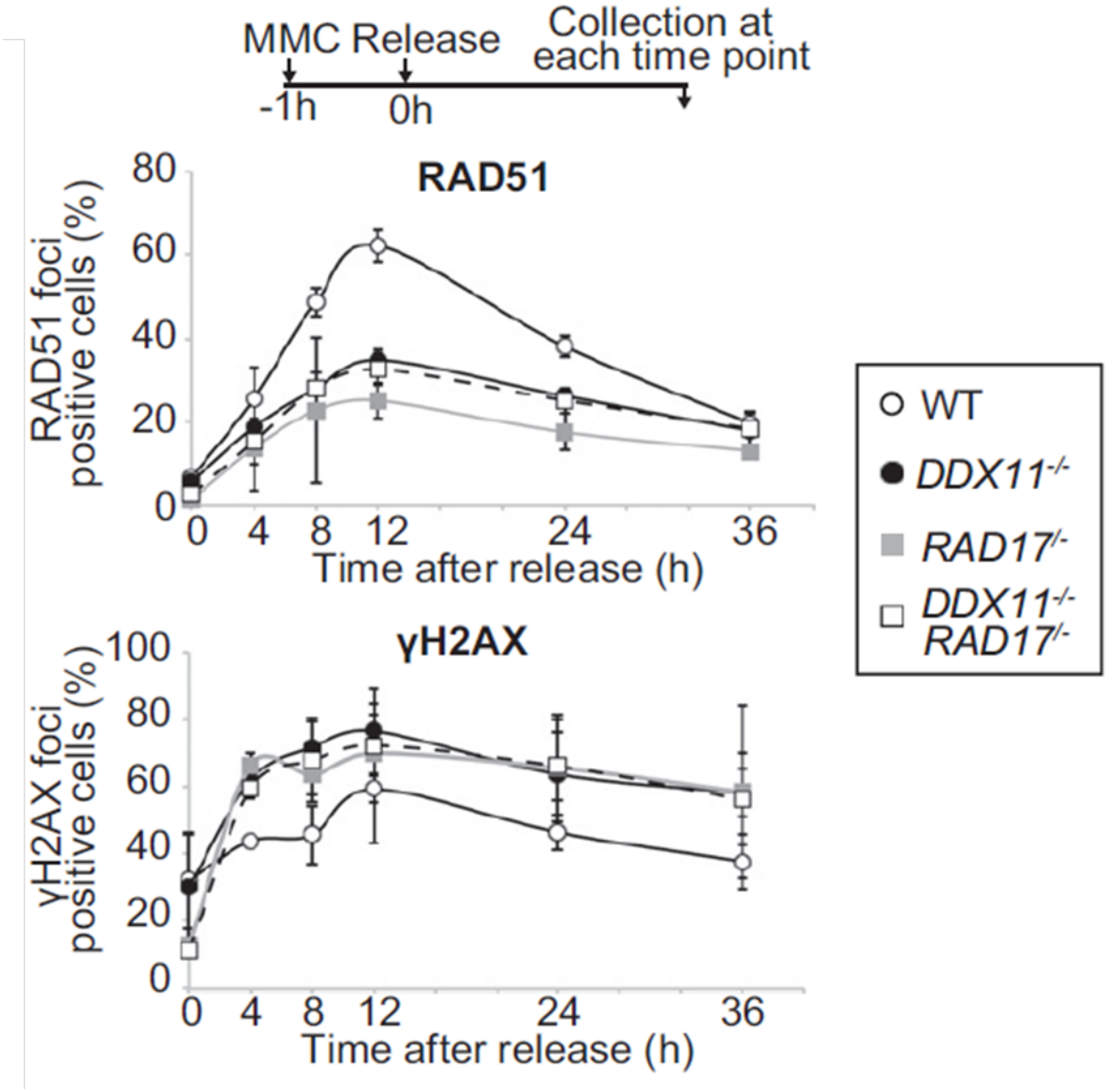

Figure40

RAD51 and γH2AX focus formation in cells of the indicated genotype following MMC treatment. The average values were plotted, and the bars indicate the values from two independent experiments.

2-3-5 DDX11 Facilitates Ig Hypermutation and Gene Conversion

To better analyze the *in vivo* role played by DDX11 at endogenous abasic sites, and its relationship with RAD17, I examined the diversification of the IgVλ region in WT, *DDX11*$^{-/-}$, *RAD17*$^{-/-}$, and *DDX11*$^{-/-}$/*RAD17*$^{-/-}$ mutants overexpressing AID, required for programmed induction of abasic sites at this locus (Figure 41) (Hirota et al., 2016; Kohzaki et al., 2010).

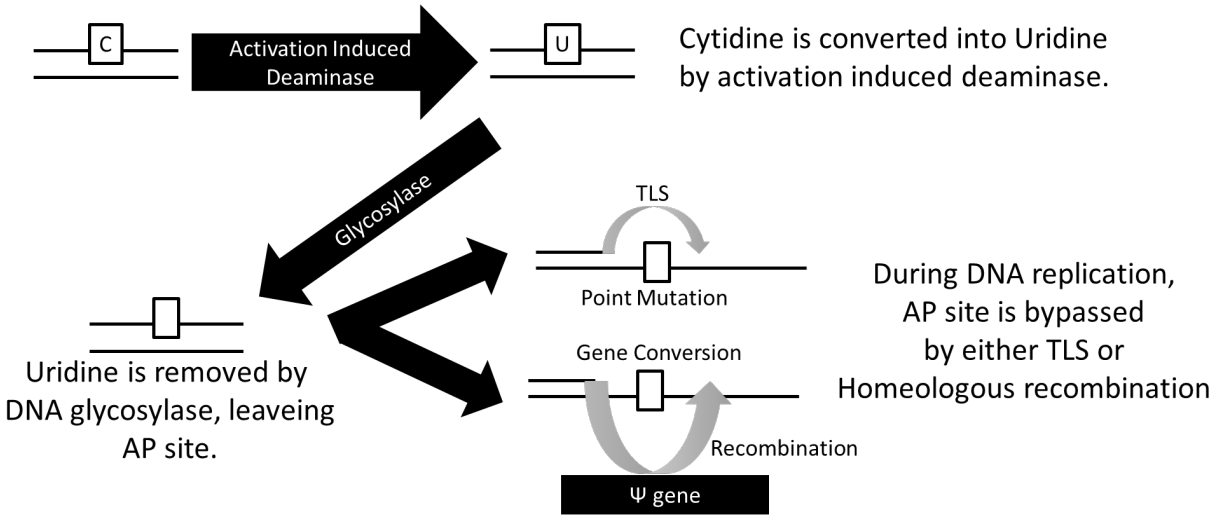

Figure 41
The scheme of IgVλ diversification assay.

I sequenced IgVλ gene libraries from expanded clones and analyzed the contributions of TLS-mediated hypermutation and HR-mediated gene conversion in this process. In a similar trend with *RAD17*$^{-/-}$, and in line with the sIgM assay of gene conversion, I found a reduction in gene conversion events in *DDX11*$^{-/-}$ cells compared with WT. The reduction in gene conversion events was stronger in *RAD17*$^{-/-}$ cells, and in line with previous reports (Saberi et al., 2008), and *DDX11*$^{-/-}$/*RAD17*$^{-/-}$ showed similar trends with *RAD17*$^{-/-}$ mutants (Figure 42). *RAD17*$^{-/-}$ mutants compensate for the reduction in gene conversion by increasing hypermutation, similarly with mutations in RAD51 paralogues. Interestingly, *DDX11*$^{-/-}$ mutants showed reduction in both hypermutation and gene conversion, and the strongly increased hypermutation events in *RAD17*$^{-/-}$ cells depended in large part on DDX11. These

results indicate that DDX11 promotes both gene conversion and TLS-mediated bypass of abasic sites.

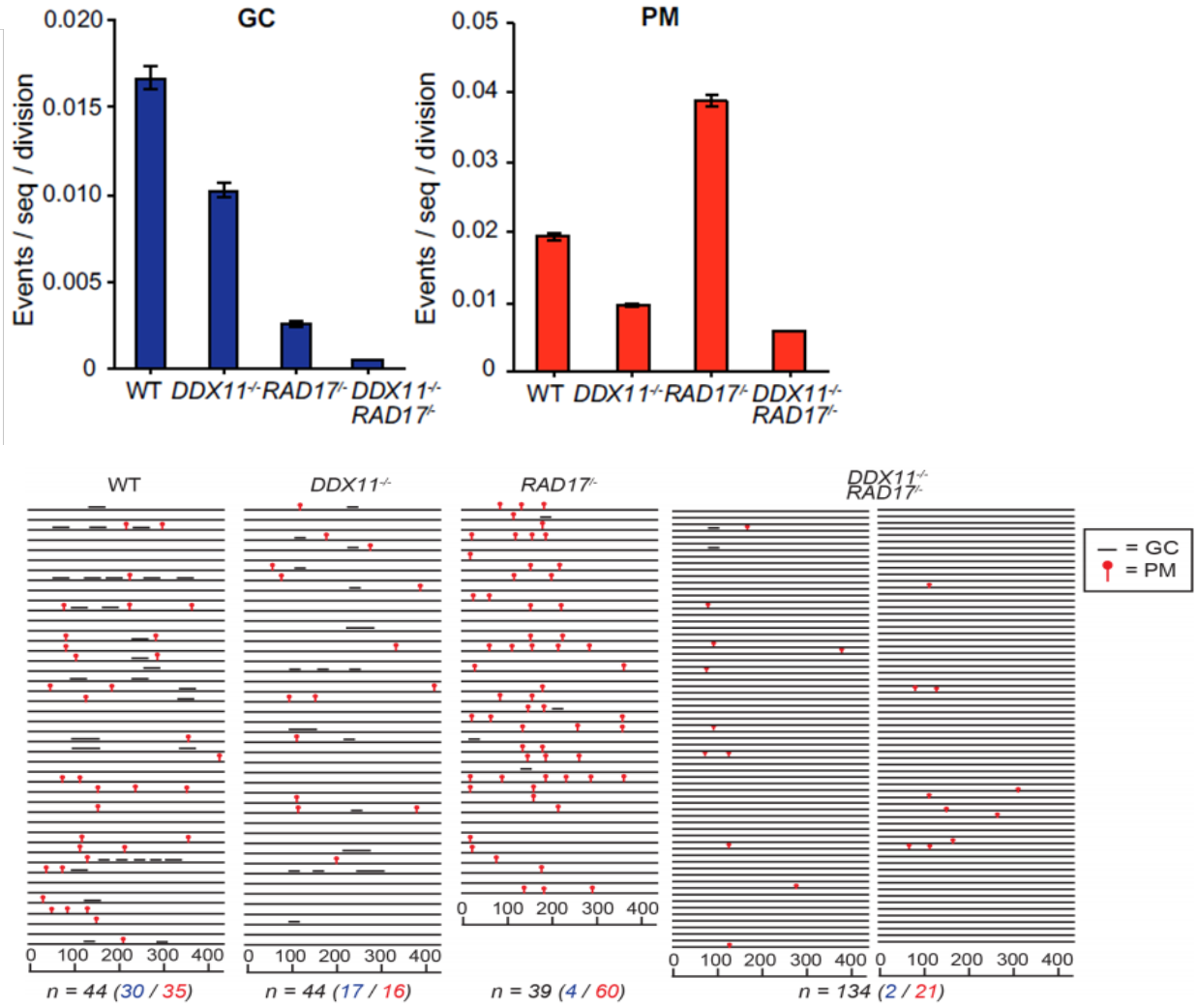

Figure 42

Rate of gene conversion (GC) and hypermutation (PM) (upper panel). The scheme of GC and PM. Lines indicate GC and red dots indicate PM (lower panel)

2-4 Discussion

2-4-1 DDX11 works as a backup for Fanconi anemia pathway in the repair of DNA inter strand crosslink

The importance of the FA pathway in repairing complex lesions such as ICLs is now well established. The existence of genetic disorders that have clinical and cellular overlaps with FA indicates the presence of pathways that can compensate in certain contexts for FA and/or act on other types of endogenous lesions. Our study highlighted that one such pathway is defined by the highly conserved DDX11/ChlR1 helicase mutated in the WABS genetic disorder. The cells deficient in DDX11 showed high sensitivity to ICL inducing reagent as well as FA protein mutant. However, the sensitivity was lower in DDX11 mutant than in FA mutant and knockout of DDX11 strongly enhanced the sensitivity in FA mutants, suggesting that DDX11 has a role in averting genome instability and in promoting DNA repair of ICLs, but this function is genetically distinct and secondary in importance to one of canonical FA components.

2-4-2 DDX11 facilitate DNA damage tolerance dependently on 9-1-1 check point clamp

Importantly, this study suggests that DDX11 also facilitates DNA damage tolerance of bulky lesions and replication through endogenous abasic sites, in a largely post-replicative manner and in collaboration with 9-1-1. Although previous studies reported accumulation of post-replicative gaps in human and mouse cells in response to UV damage (Buhl et al., 1973; Buhl et al., 1972; Lehmann, 1972; Lehmann et al., 1977) or upon RAD51 depletion in Xenopus egg extracts (Hashimoto et al., 2010), little is known about how post-replicative repair is carried out in vertebrate cells. This study indicates that DDX11 collaborates with the checkpoint clamp 9-1-1 and its loader, RAD17, in the post-replicative HR repair of bulky lesions, and in facilitating gene conversion induced by abasic sites, but without affecting checkpoint activation. Based on the current findings, 9-1-1, in addition to its role as lesion sensor and activator of ATR, may participate together with DDX11 in the post-replicative bypass of replication lesions that are not preferential substrates for the canonical FA pathway or other fork stabilization mechanisms. A noncanonical role for 9-1-1 in the post-replicative

HR-mediated repair of replication lesions was observed in budding yeast (Karras et al., 2013), and that 9-1-1 repair defects can be overcome by overexpressing RAD51(Shinohara et al., 2003). The data suggests a model in which the action of 9-1-1 favors the formation of the RAD51 filament on post-replicative gaps, while DDX11 promotes the unwinding of the stalled 3' end. The intermediate formed by the joint actions of 9-1-1 and DDX11 may be efficiently matured into an HR intermediate, while in the absence of 9-1-1, the 3' end exposed by the action of the DDX11 helicase may be more readily engaged by TLS polymerases (Figure 43).

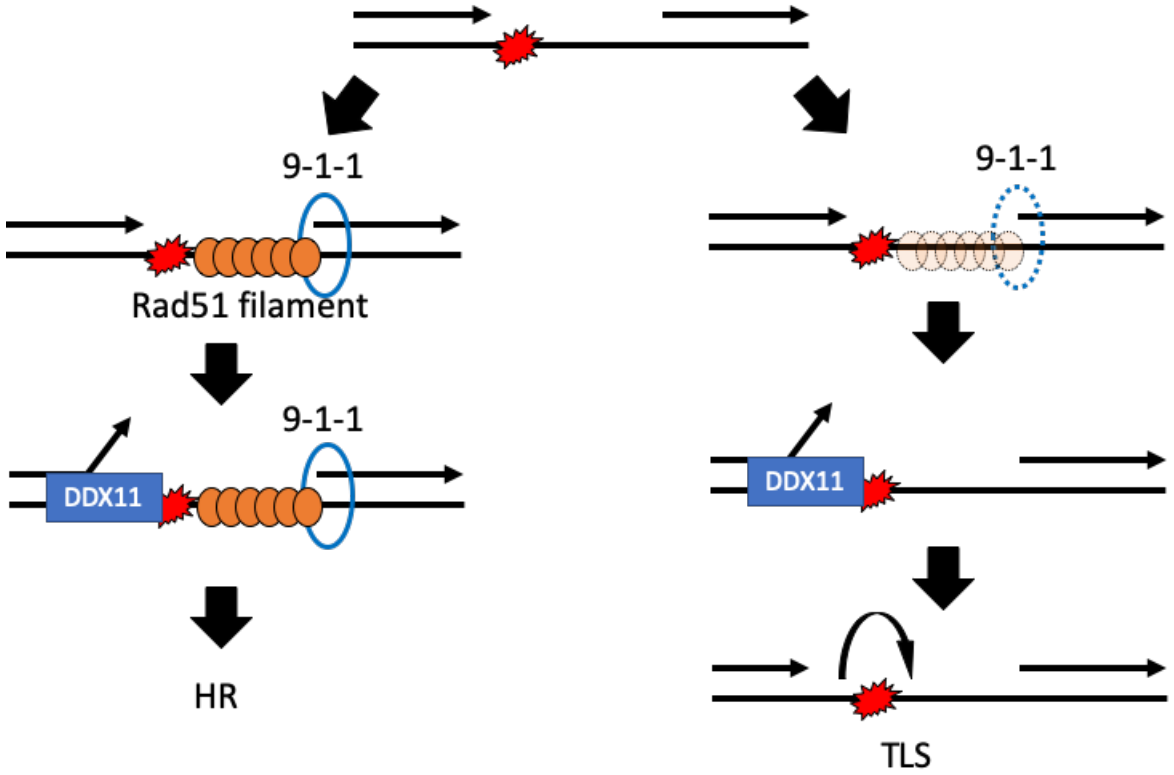

Figure 43
The model in the presence of RAD17 (Left) and in the absence of RAD17 (Right).

A joint role for DDX11 and 9-1-1 in the HR repair of replication lesions and abasic sites may explain why their individual depletion/knockout leads to very similar developmental defects in mouse, with the somitic mesoderm being especially sensitive to the genomic instability produced by their individual mutations (Cota and Garcia-Garcia, 2012; Weiss et al., 2000) and resembling the ones caused by mutations in *BRCA2* and *PALB2* (Rantakari et al., 2010;

Suzuki et al., 1997). These repair functions are likely critical in situations of fast proliferation, such as during early stages of development. I also found that DDX11 mitigates replication stress in FANCJ-defective cells and is critical for the repair of olaparib- and cisplatin-induced DNA damage in BRCA2 and FA-defective cells. Thus, another implication of our findings is that DDX11 is important for limiting replication stress in *FA* and *BRCA* mutated cells, and therefore it may be vital for the survival of these and other cancers, which often suffer from replication stress. Based on this study, I propose that the DNA repair pathway mediated by DDX11 has important functions related to replication of endogenous abasic sites and DNA damage tolerance of bulky lesions. This pathway is critical for human disease and may offer new opportunities for cancer treatment.

Chapter 3:

Molecular Mechanism-Based High Throughput Screening to Identify the Chemicals Which Cause DNA Double-Strand Break Through Estrogen Receptor Activation

3-1 Introduction

3-1-1 Translational Science

As shown in Chapter 2, synthetic effects of concurrent loss of DDX11 and FA factor on genome maintenance and cell proliferation. Thus, the rapid proliferation of FA cancer cells might be largely supported by the complementary working DDX11. Similarly, genes related to DNA damage repair pathways are generally mutated in cancer cells and thus the survival of the cancer cells is maintained by alternative and complementary DNA repair pathways (e.g. BRCA1 and PARP). The inhibition of such complementary system results in cell growth defect or cell death. To establish the novel cancer chemotherapy based on such genetic synthetic-relationship, I wish to establish a high throughput drug screening system based on imaging analysis of DNA damages in cells.

3-1-2 Nuclear hormone receptor and cancer therapy

Nuclear hormone receptors are ligand-activated transcription factors. When they bind to the ligand hormones, they move into the nucleus and regulate gene expression at their target sites. The target sites are called hormone response elements (HRE). The sequence of the site differs depending on the type of receptor. Each receptor has different HRE and regulates different cellular activities. Although nuclear hormone receptors are composed of several domains, two domains are differentially conserved in the various receptors. One is the DNA binding domain (DBD). The other is the ligand-binding domain (LBD) (Huang et al., 2018).

Hormones are produced in the hormone system (*i.e*. endocrine system), which is the network of glands and organs. The hormone system includes the pituitary gland, pineal gland, thyroid gland, adrenal gland, pancreas, testis, and ovary. Once the hormone system produces hormones, our bloodstream carries the hormones around the body. Each hormone has a different role as each hormone receptor has a different role. They control growth and development, sexual function, reproduction, *etc*. Since some of the hormone receptors control cell proliferation, hormone receptor is one of the targets for cancer therapies (Rossouw et al., 2002). Hormone therapy uses chemicals to prevent the hormone receptor from binding hormones to lower amount of hormone-receptor complex.

There are environmental compounds that disrupt the endocrine system by acting like hormones (Ji et al., 2009). Those compounds are called environmental hormones. The most famous environmental hormone is a bis-phenol A. It is used in many plastic products and is known to have estrogenic activity and genotoxic activity (Lee et al., 2013). However, how endocrine disruptor causes genotoxic effects had not been discovered.

3-1-3 Female organ cancer and Estrogen / Progesterone receptor

Breast cancer is the most frequently diagnosed cancer in females. Breast cancer is classified into 4 groups depending on the expression of 3 receptors (Table 2). Estrogen receptor and progesterone receptor is activated by estrogen and progesterone, respectively. Human Epidermal growth factor Receptor 2 (HER2) has a strong ability to promote cell proliferation. HER2 is frequently overexpressed in breast cancer cells. The expression of HER2 is regulated by the estrogen receptor and the ligand for HER2 has not been identified yet. Because the proliferation of breast cancer tumor is mostly controlled by those receptors, inhibitors for those receptors are used to suppress cancer cell proliferation. However, breast cancer classified in group-4 does not rely on those receptors for the proliferation. The prognosis for group-4 breast cancer is not good.

	Group1	Group2	Group3	Group4
Estrogen receptor	○	○	×	×
Progestorone receptor	○	×	×	×
HER2 receptor	×	○	○	×

Table 2
Classifying the breast cancer group according to the expression of three receptors.

Because more than 70% of breast cancer express the estrogen receptor and it regulates HER2 expression (Williamson and Lees-Miller, 2011), I focus on the estrogen receptor in this study. Once they are activated by estrogen, they translocate into the nucleus and bind to DNA to regulate transcription (Allred et al., 2004). There are two subtypes of ERs, (ER-α and ER-β). Both receptors promote transcription on their target genes. However, their roles in cells are different. While activation of ER-α promotes cell proliferation, activation of ER-β represses cell proliferation. Because ER-α is mainly expressed in breast, ER-α antagonist is used for preventing cancer cells from growing. Although ER-α is a common target for hormone therapy, there is a concern that the activation of ER can cause DNA damage (Stork et al., 2016). The activation of the ER is known to accelerate cancer cells. But the genotoxicity has not been studied very well.

3-1-4 Female organ cancer and BRCA1

BRCA1 is frequently mutated in breast and ovarian cancer (Nik-Zainal et al., 2019). Females who carry a mutation in BRCA1 genes have a lifetime risk for breast and ovarian cancer 75% and 65%, respectively (van der Kolk et al., 2010). BRCA1 is a multi-functional enzyme (*e.g.* DNA repair, checkpoint activation, apoptosis (Friedenson, 2005; Narod and Foulkes, 2004; Venkitaraman, 2002)). One of the well-known functions of BRCA1 is a key player in DNA Double-Strand Break (DSB) repair. DSB is a fatal DNA damage and can trigger genome instability (Khanna and Jackson, 2001). DSB is repaired mainly by two pathways. One is homologous recombination (HR) and the other is Non-Homologous End Joining (NHEJ). BRCA1 is involved in the HR pathway, which repairs DSB by using the sister chromosome

as a template (Farmer et al., 2005). Thus, BRCA1 deficiency results in less HR activity and the cells lacking BRCA1 show hypersensitivity to DSB-inducing agents, such as ionizing radiation. Although HR is activated in all kinds of cells mainly in the late-S/G2 phase (Takata et al., 1998), BRCA1 is strongly related to cancers in estrogen-regulated organs.

The relationship between the mutation in the BRCA1 gene and these cancers had not been uncovered for a long time. According to the report from Dr. Takeda's lab (Kyoto University, Japan), estrogen induces DSB depending on both ER-α activation and TOP2 (Sasanuma et al., 2018). TOP2 is the vital enzyme that resolves DNA supercoiling during transcription and replication. To resolve topological stress of DNA, TOP2 cuts and re-ligates DNA as well as Top1 (Pommier et al., 2016). A physiological concentration of estrogen activates ER-α and promotes ER-dependent transcription. During the transcription, TOP2 resolves DNA supercoiling by transiently generating DSB (Ju et al., 2006). TOP2 frequently fails to complete this process and remains on DNA, leading TOP2-cleavage complex (Top2cc). Remained unrepaired, Top2cc results in DSB. To remove this toxic Top2cc from DNA, MRE11 and TDP2 play an important role as a nuclease (Gómez-Herreros et al., 2013; Hoa et al., 2016). The amount of Top2cc increases in the absence of BRCA1. BRCA1 was found to be required to recruit MRE11 to the Top2cc damage site efficiently (Sasanuma et al., 2018) (Figure 44). This event occurs in the G0/G1 phase, suggesting BRCA1 has a role to repair Top2cc independent of HR. Moreover, BRCA1 has been believed to act only in S/G2 phase but not in the G1 phase. Cells with a mutation on BRCA1 fail to remove Top2cc, which is caused by ER activation, leading genome instability and promoting cancer development in female organs. This is how estrogen causes breast or ovarian cancer in females with mutations in the BRCA1 gene.

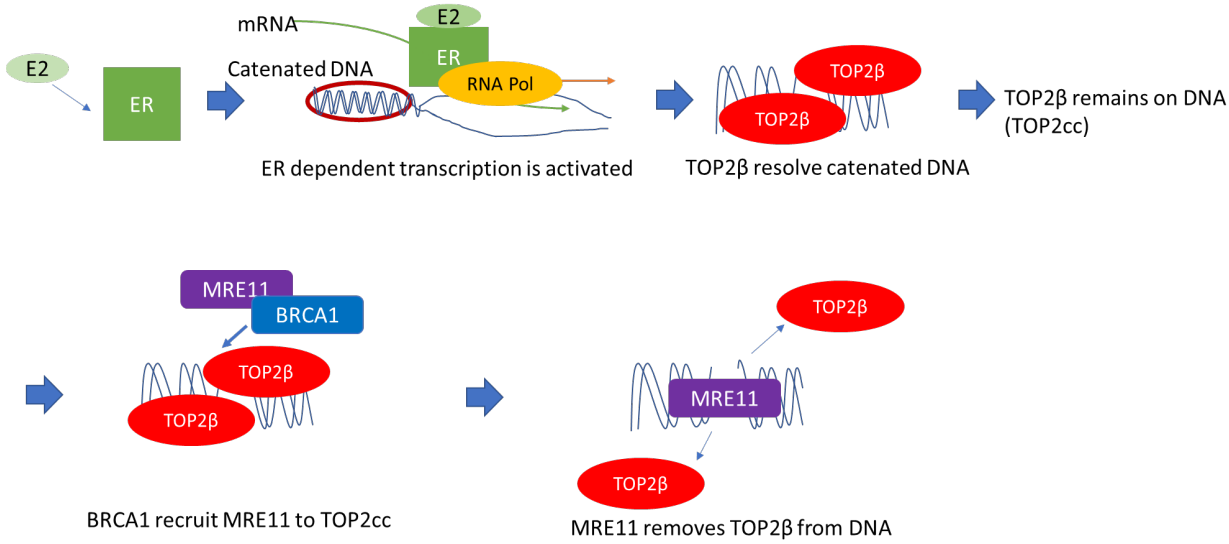

Figure 44
The scheme of the ER activation.

The loss of BRCA1 is embryonic lethal in the mouse model. This lethality is rescued by a disruption of 53BP1. 53BP1 protects DNA ends from resection to prevent unscheduled HR. BRCA1 removes 53BP1 from broken DNA ends. In the absence of BRCA1, 53BP1 remains on the DNA end and other repair machinery cannot access the damaged site, leading to cell death.

3-1-5 High content / High throughput screening

In this study, I aimed to identify environmental compounds that cause DNA damage through the activation of estrogen receptor as well as estrogen. To achieve this goal, I optimized high throughput / high content imaging screening system to measure DNA double-strand breaks. High content screening is an imaging-based assay (Li et al., 2018). It allows us to analyze the event in every single cell. On the other hand, we only can see the cellular events as a population in classical high throughput screenings. For this reason, high content screening gives us more about the cellular event compared to classical high throughput screening. Because DNA damaging activity of estrogen is not as strong as other DNA damaging agents (e.g. ionizing radiation), high content screening is needed.

3-2 Materials and methods

Cell lines

MCF7

WT

BRCA1$^{-/-}$/*53BP1*$^{-/-}$

53BP1$^{-/-}$

DNA-PKcs$^{-/-}$

T47D

WT

TDP2$^{-/-}$

CHO

WT

Ku80$^{-/-}$

Cell culture

TK6

TK6 cells were cultured in RPMI 1640 medium (Sigma) supplemented with 10% heat-inactivated horse serum (HS) (Sigma), 0.1 mM sodium pyruvate (Sigma), L-glutamine (Sigma), 50 U/mL penicillin, and 50 μg/mL streptomycin (Sigma).

MCF7

MCF7 cells were cultured in DMEM medium supplemented with 10% heat-inactivated Fatal Bovine Serum (FBS), 0.01 mg/ml insulin, 50 U/mL penicillin, and 50 μg/mL streptomycin.

For assay, MCF7 cells were cultured in a phenol red-free DMEM medium supplemented with 1% charcoal stripped FBS, 50 U/mL penicillin, and 50 μg/mL streptomycin

CHO (WT)

CHO WT cells were cultured in F12K medium supplemented with 10% heat-inactivated Fatal Bovine Serum (FBS), 50 U/mL penicillin, and 50 μg/mL streptomycin.

CHO (*Ku80*$^{-/-}$)

CHO WT cells were cultured in α-MEM medium supplemented with 10% heat-inactivated Fatal Bovine Serum (FBS), 50 U/mL penicillin, and 50 μg/mL streptomycin.

Homogeneous Time Resolved Fluorescence: phospho-H2AX quantification assay (HTRF assay)

I plated the cells at 2,000 cells/well in 5nl of culture medium into white solid bottom 1536-well plates. I incubated the assay plate for 18 hours. The next day, I added 23nl of compounds and DMSO by pin tool, then incubated it for 3 hours. After the incubation, I added 1 μl of lysis mixture into each well and incubated it for 30min RT. Next, I added the antibody mixture solution and incubated it for 24 hours. Finally, I read the plate in Envision plate reader (excitation 320nm and emissions at 665nm and 620nm).

Lysis mixture

a, Lysis buffer was diluted 4-fold with distilled water.

b, Blocking reagent was diluted 100-fold into prepared lysis buffer.

Antibody mixture

Stock antibody solutions were diluted 20-fold with detection buffer.

Solution A: Anti H2A.X-d2

Solution B: Anti pH2A.X (S139)-K

Solution A and Solution B mixed at 1:1 ratio with gentle mixing.

Immunostaining

I plated MCF7 cells at 1,500 cells / well in 5 μl of the medium into a black wall/ clear bottom

1536 well plate. I incubated the assay plate for 18 hours. The next day, I added 23 nl of compounds and DMSO by pin tool, then incubated it for 3 hours. Next, I added 5µl of 8% paraformaldehyde (final concentration: 4%) and incubate for 20 minutes. After a wash with PBS, I added a blocking/ permeabilization buffer and incubated for 30 min. Then, I treated the cells with the primary antibody for 45minutes at RT, followed by the incubation with the secondary antibody for 30 minutes at RT. I read the plates in the operetta plate reader.

Data analysis

I counted the foci per cell using operetta. Analysis of compound concentration–response data was performed as previously described. Briefly, raw plate reads for each titration point were first normalized relative to the positive control compound (sunitinib) and DMSO only wells (0%) as follows:

$$\%\text{Activity} = [(V_{compound} - V_{DMSO}) / (V_{pos} - V_{DMSO})] \times 100$$

where $V_{compound}$ denotes the compound well values, V_{pos} denotes the median value of the positive control wells, and V_{DMSO} denotes the median values of the DMSO-only wells. The data set was then corrected using the DMSO-only compound plates at the beginning and end of the compound plate stack by applying an in-house pattern correction algorithm. The half maximum effective values (IC50) for each compound and maximum response (efficacy) values were obtained by fitting the concentration–response curves of each compound to a four-parameter Hill equation. Compounds were designated as class 1–4 according to the type of concentration–response curve observed (Figure 45). In the present study, antagonists were defined as compounds that inhibited angiogenesis activity. Compounds with class 1.1, 1.2, 2.1, 2.2, 3 curves were considered active, compounds with class 4 curves were considered inactive, and compounds with all other curve classes were defined as inconclusive. Data were analyzed and depicted using OriginPro 2015 (OriginLab Corp., Northampton, MA) and GraphPad Prism 5 (GraphPad Software, Inc., La Jolla, CA).

CV value, Signal/ Background (S/B) ratio, and Z'- factor was calculated as below.

CV value:

The coefficient of variation (CV) is a measure of relative variability. It is the ratio of the standard deviation to the mean (average)

Coefficient of Variation (CV) = (Standard Deviation / Mean) * 100.

Signal/ Background (S/B) ratio:

S/B ratio is the ratio of the signal to the background signal.

Z' factor:

The Z-factor is a measure of statistical effect size.

Z'- factor = $1 - 3(\sigma_p + \sigma_n)/|\mu_p - \mu_n|$

Mean(μ) and standard deviations (σ) in positive(p) and negative(n).

Curve class	Asymptotes	r^2	Efficacy	Description
1	Higher and lower	≥ 0.9	> 80%	1.1: Complete curve; high efficacy
			Min - 80%	1.2: Complete curve; partial efficacy
		< 0.9	> 80%	1.3: Complete curve; high efficacy; poor fit
			Min - 80%	1.4: Complete curve; partial efficacy; poor fit
2	Lower only	≥ 0.9	> 80%	2.1: partial curve; high efficacy
			Min - 80%	2.2: partial curve; partial efficacy
		< 0.9	> 80%	2.3; partial curve; high efficacy; poor fit
			Min - 80%	2.4; partial curve; partial efficacy; poor fit
3	Lower only		≥ Min	3: Single point of activity
4			< Min	4: Inactive
5			≥ Min	5: Inconclusive

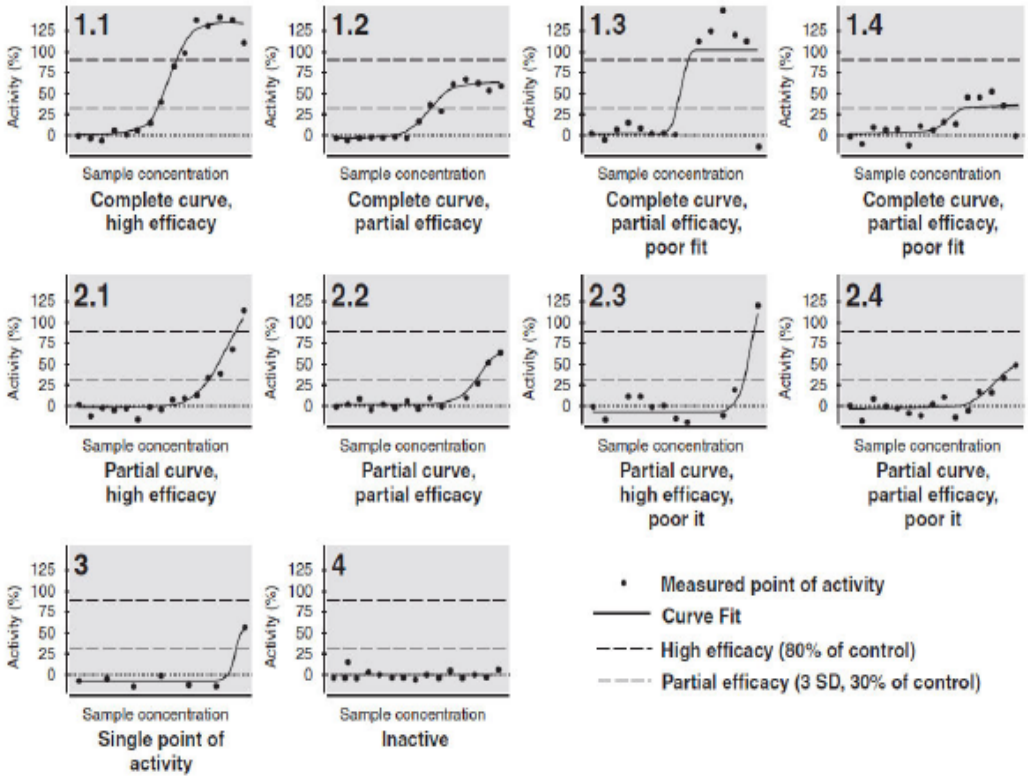

Figure 45

The classification for the dose response curves.

3-3 Results

3-3-1 Development of the assay system to identify DNA double strand inducers

Molecular biological studies allow us to develop molecular targeting chemotherapy. We need high throughput assay system to identify the compounds with a certain activity. I aimed to utilize antibody reaction in 1536 plate format, because antibody reaction can focus specific protein. From great number of antibodies, once I optimize the assay, it can be very versatile. I picked the DNA double strand break (DSB) as the model target for the assay development. I chose phospho-H2AX as a biomarker for DSB.

First, I tested if the Homogeneous Time Resolved Fluorescence: phospho-H2AX quantification assay (HTRF assay) is available for MCF7 or TK6 cells. Phosphor-H2AX is used as a biomarker for DSB. H2AX HTRF assay is a fluorescence resonance energy transfer (FRET)-based technology. FRET is a distance-dependent physical process, by which energy is transferred nonradiatively from an excited molecular fluorophore (the donor) to another fluorophore (the acceptor) by means of intermolecular long-range dipole–dipole coupling (Sekar and Periasamy, 2003). In HTRF assay, cells were lysed after the chemical treatment, followed by incubation with HTRF antibodies. One of the antibodies is conjugated with the donor and recognizes the phosphorylated H2AX. The other antibody is conjugated with the acceptor and recognizes H2AX independent of its phosphorylation state. The performance of HTRF assay depends on cell types. I treated *BRCA1*$^{-/-}$*/53BP1*$^{-/-}$ deficient MCF7 and TK6 with H_2O_2, Camptothecin, Actinomycin, and Bleomycin. None of them showed phospho-H2AX induction (Figure 46).

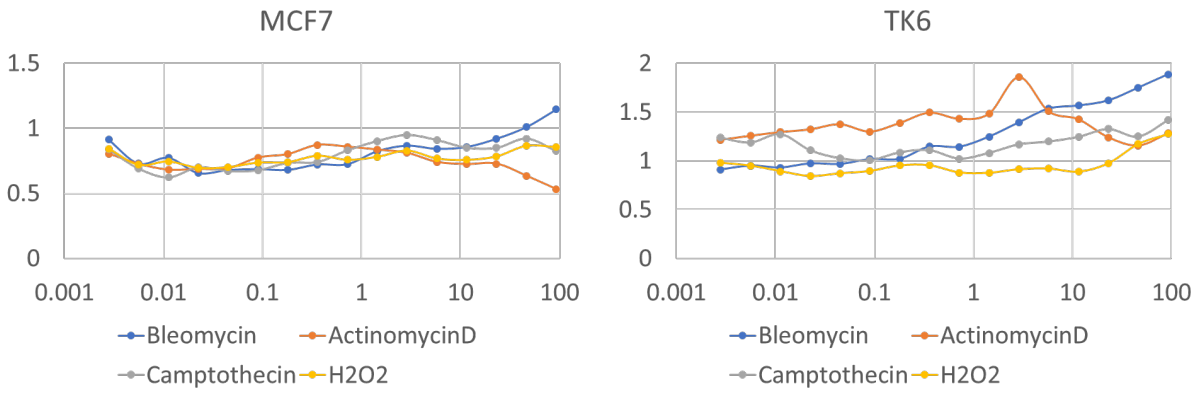

Figure 45

The result of HTRF assay. Y axis indicates the fold change compared to DMSO treated cells. X axis indicates the dose.

To find a better cell-based high-throughput assay system to quickly identify compounds that induce DNA double-strand break, I optimized and validated an immunostaining assay using a quantitative high-throughput and high-content imaging method. To validate this assay, MCF7 cells were plated in a 1536-well plate. Bleomycin, a known DNA damage inducer, caused phosphorylation of H2AX in a concentration-dependent manner in a 1536-well plate using the number of nuclei count and the number of spot count measurements (Figure 46). In the screening, “the number of foci per cell” was used for the quantitative image analysis of phospho-H2AX induction. The immunostaining assay was validated in 1536-well formats using Bleomycin with average signal-to-background (S/B) ratio, coefficient of variation (CV) value, and Z’ factor of 26.7, 10.1%, and 0.62, respectively.

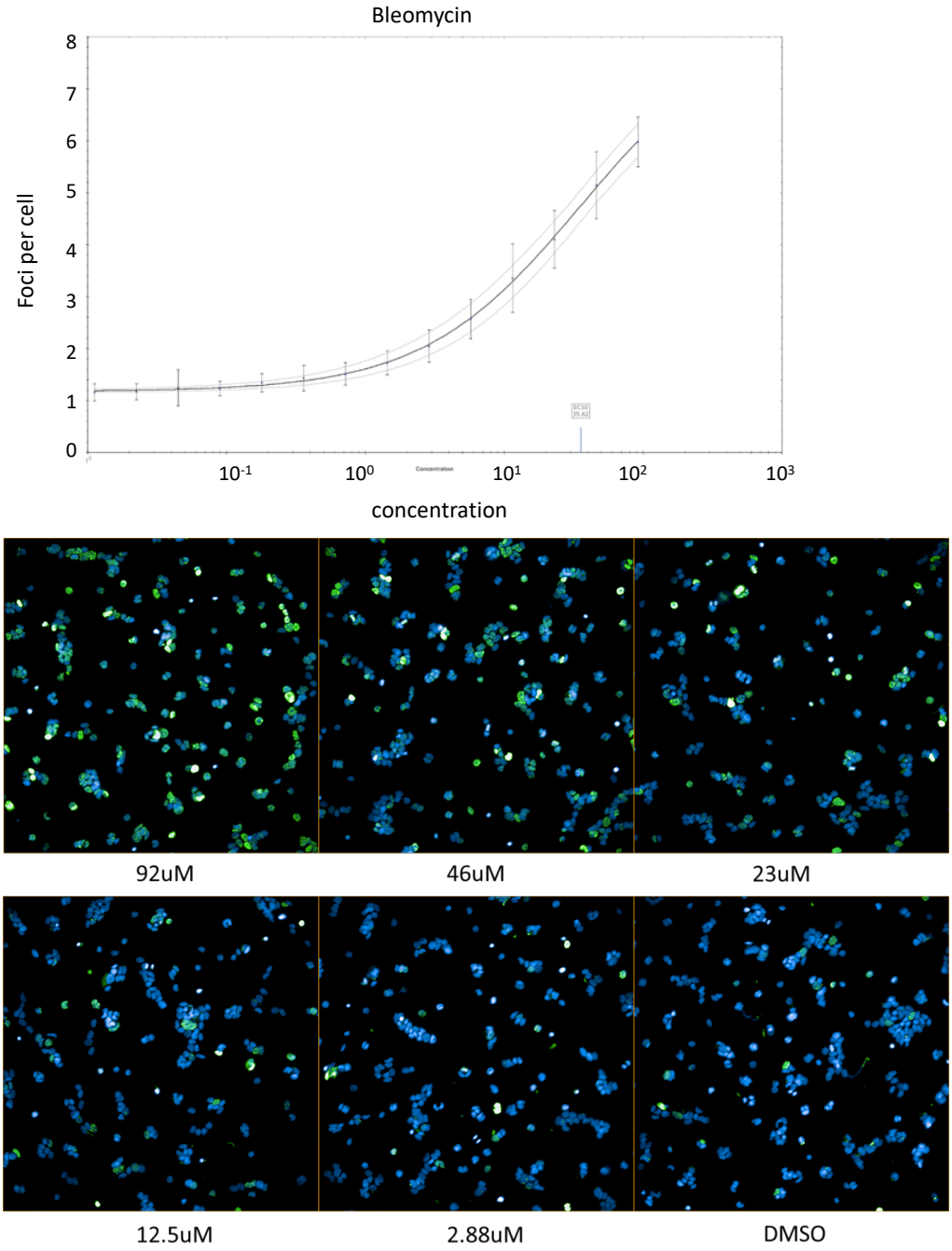

Figure 46

The dose response curves (upper panel) and the representative image for each dose point (lower panel). Blue: nuclei stained with DAPI. Green : γ H2AX stained with antibody

3-3-2 Identification of phospho-H2AX inducer using high content imaging analysis

I examined DSB inducers in a tiered testing approach (Figure 45). I have selected 907 compounds that potentially induce DSB, based on previous screening using the Tox21 10K chemical library (Huang et al., 2016). I used bleomycin as a positive control. These compounds are directly or indirectly related to DSBs.

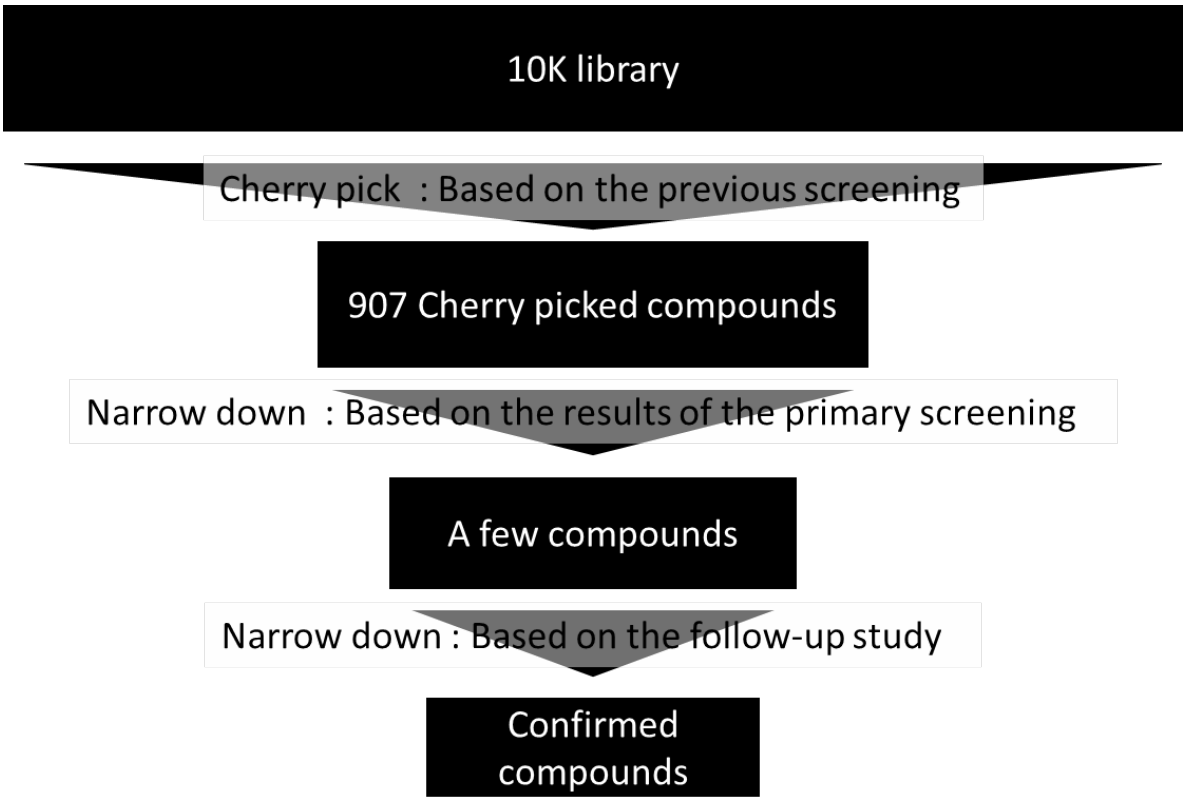

Figure 47
The strategy for the identification.

The average CV value, S/B ratio, and Z′ factor from the primary screen of 21 assay plates were 14.85 ± 5.77%, 5.53 ± 2.02, and 0.32 ± 0.14, respectively. The compounds in the curve classes of 1.1, 1.2, 2.1, 2.2 were considered active and potential phospho-H2AX inducer. The

number of foci per cell by positive control (bleomycin) is defined as 100% activity of the compounds. The number of foci per cell by negative control (DMSO) is defined as 0% activity of the compounds. The activity was calculated for each compound in each dose point. The half-maximal activity concentration (AC50) is the concentration in which the compound shows 50% activity compared to the control compounds. Efficacy is the maximum activity of each compound. From the primary screening, 128 potential inducers were identified and selected for the follow-up study (Table 3).

Sample Name	AC50(mM)	Efficacy(%)	Curve Class
Oxyphenisatin acetate	0.1 ± 0.0	59.5 ± 9.1	1.1
Carminomycin	0.2 ± 0.1	110.8 ± 19.2	2.1
8-Quinolinol Salicylic acid (1:1)	6.5 ± 2.4	71.3 ± 5.0	2.1
NSC-12155 (surfen)	24.5 ± 3.1	112.3 ± 49.8	1.1
Topotecan hydrochloride	14.9 ± 1.7	93.4 ± 4.0	1.1
Mitoxantrone	0.7 ± 0.1	101.7 ± 10.8	1.1
Raloxifene hydrochloride	22.1 ± 10.2	80.2 ± 17.1	1.1
Sanguinarine	10.8 ± 5.1	77.2 ± 20.8	1.1
Disulfiram	0.6 ± 0.3	85.3 ± 7.0	1.1
Bisacodyl	0.6 ± 0.1	47.7 ± 6.6	1.1
Curcumin	34.8 ± 18.6	58.9 ± 16.8	1.1
Resveratrol	2.1 ± 0.8	120.4 ± 25.5	1.1
Podofilox	1.1 ± 0.1	121.5 ± 6.8	1.1
Daunorubicin	0.5 ± 0.0	118.6 ± 23.8	1.1
Actinomycin D	0.3 ± 0.0	75.6 ± 7.7	1.1
N,N-Diethyl-p-phenylenediamine	4.6 ± 4.1	46.8 ± 15.9	1.1
4-(2-Methylbutan-2-yl)phenol	1.7 ± 0.9	50.7 ± 0.5	1.1
4-Chloro-1,2-diaminobenzene	27.7 ± 19.2	60.1 ± 9.6	1.1
2,3,4-Trichlorophenol	5.3 ± 0.6	122.4 ± 15.9	2.1
Amsacrine	11.9 ± 6.7	125.2 ± 25.0	1.1
Semaxanib	6.6 ± 5.6	38.6 ± 9.5	1.1
Chloroxine	3.6 ± 0.6	68.0 ± 26.7	1.1
Gramicidin	1.5 ± 1.1	63.5 ± 33.5	1.1

Ethacridine lactate	15.2 ± 12.5	92.6 ± 28.3	1.1
Tetramethylthiuram monosulfide	1.4 ± 0.3	83.9 ± 8.5	1.1
Testosterone decanoate	3.2 ± 3.0	116.8 ± 30.3	2.1
Nitroxoline	3.0 ± 3.1	63.2 ± 14.2	1.1
1,4-NAPHTHOQUINONE	9.5 ± 2.0	57.4 ± 20.9	1.1
Tiliquinol	1.9 ± 0.7	74.8 ± 9.5	2.1
Rubitecan	8.3 ± 3.0	53.2 ± 7.2	1.1
Pirarubicin	10.2 ± 7.4	96.1 ± 20.0	1.1
Dithiazanine iodide	18.4 ± 11.4	46.8 ± 15.1	1.1
Carboquone	13.9 ± 2.5	74.6 ± 8.0	1.1
Dicyclopentamethylenethiuram disulfide	0.7 ± 0.3	100.3 ± 21.0	1.1
Peplomycin sulfate	17.3 ± 1.2	39.3 ± 5.6	1.1
Eprinomectin B1a	21.5 ± 8.4	69.4 ± 14.2	2.1
Lestaurtinib	18.0 ± 5.9	45.5 ± 9.2	2.1
Gimatecan	2.1 ± 1.8	96.0 ± 25.0	2.1
Menadiol	8.7 ± 0.6	88.6 ± 22.2	1.1
2,3-Diaminotoluene	35.4 ± 17.7	64.2 ± 11.7	1.2
Sodium (2-pyridylthio)-N-oxide	5.5 ± 3.4	83.7 ± 6.8	2.1
2,4-Bis(1-methyl-1-phenylethyl)phenol	28.9 ± 8.5	64.8 ± 21.0	2.1
Sodium dimethyldithiocarbamate	8.7 ± 3.3	88.1 ± 8.2	1.1
Ziram	1.4 ± 0.8	89.1 ± 18.9	2.1
Captafol	13.8 ± 3.2	86.1 ± 2.2	2.1
Dazomet	6.4 ± 1.1	87.5 ± 4.2	1.1
4-Dodecylphenol	27.7 ± 14.8	45.8 ± 17.2	2.1
Methylene bis(thiocyanate)	41.1 ± 2.7	55.6 ± 17.9	2.1
2-(Thiocyanomethylthio)benzothiazole	46.6 ± 6.4	103.9 ± 56.5	1.1
3,4,5,6-Tetrachloro-2-pyridinecarbonitrile	37.5 ± 9.4	79.7 ± 10.2	1.1
3,3'-Diaminobenzidine	39.8 ± 2.7	62.6 ± 28.2	2.1
Dipentaerythritol pentaacrylate	20.5 ± 1.3	84.2 ± 10.3	2.1

Dithianon	6.6 ± 1.1	116.1 ± 15.9	1.1
3-Hydroxy-2-naphthoic o-anisidide	19.7 ± 20.1	99.4 ± 63.8	2.1
Potassium dicyanoaurate	3.9 ± 1.3	82.6 ± 7.5	2.1
Phenylarsine oxide	1.4 ± 0.3	85.8 ± 7.4	1.1
2,3,4,5-Tetrachloro-6-(trichloromethyl)pyridine	6.5 ± 4.9	82.9 ± 17.5	2.1
1,1,2-Trimethyl-1H-benzo[e]indole	6.1 ± 0.7	64.6 ± 9.2	1.1
6-Nitrobenzimidazole	5.9 ± 2.8	93.7 ± 12.3	2.1
Rhodamine 6G	12.7 ± 4.8	70.1 ± 16.0	1.1
2,4-Diaminoanisole sulfate hydrate	30.5 ± 3.9	94.6 ± 14.2	1.1
2-Aminoanthracene	6.5 ± 2.7	51.3 ± 9.5	2.1
Oxyphenisatin	0.3 ± 0.0	64.7 ± 3.1	2.1
Nemorubicin	10.1 ± 0.7	84.6 ± 16.2	2.1
Teniposide	5.7 ± 4.4	128.9 ± 41.6	2.1
Etoposide	18.0 ± 1.2	105.3 ± 3.6	2.1
THIRAM	0.9 ± 0.1	77.6 ± 1.1	2.1
Idarubicin hydrochloride	0.1 ± 0.1	83.9 ± 6.0	1.1
Cloxyquin	5.8 ± 5.0	73.5 ± 34.2	1.1
Estradiol dipropionate	21.1 ± 3.4	81.9 ± 4.6	1.1
Geliomycin	18.8 ± 3.0	53.1 ± 2.6	1.1
1,4-dihydroxy-2-naphthoic acid	24.7 ± 7.9	125.4 ± 35.4	1.1
Dihydrotachysterol	24.9 ± 2.0	39.8 ± 12.2	2.1
Bismuth subgallate	12.7 ± 3.1	122.1 ± 9.0	1.1
Nitrovin	7.1 ± 1.7	55.7 ± 21.1	1.1
Estramustine phosphate	13.1 ± 11.1	75.0 ± 36.0	2.1
Nitromersol	22.5 ± 5.4	52.4 ± 22.0	1.1
Methyl 3-amino-5,6-dichloropyrazine-2-carboxylate	26.5 ± 4.3	45.7 ± 18.8	1.1
p,p'-DDD	48.4 ± 7.8	53.0 ± 14.4	1.1
PD 0343701	13.6 ± 0.0	102.8 ± 19.5	2.1
Barban	42.9 ± 0.0	59.9 ± 32.1	1.1
3,4,4'-Triaminodiphenyl ether	40.5 ± 3.3	74.4 ± 19.0	2.1
Tetraiodoethene	16.1 ± 1.3	49.2 ± 4.5	2.1

2,2'-Methylenebis(4-methyl-6-tert-butylphenol)	14.4 ± 1.2	71.3 ± 2.1	1.1
Dichlone	5.3 ± 2.1	71.6 ± 2.8	1.1
Pentaerythritol triacrylate	48.1 ± 0.0	100.5 ± 14.1	2.1
Manganese(II) acetate	36.1 ± 17.0	82.1 ± 52.7	1.1
2,2'-Methylenebis(ethyl-6-tert-butylphenol)	15.3 ± 2.5	33.1 ± 0.2	1.1
Proflavin hydrochloride	1.0 ± 1.3	67.6 ± 35.3	1.1
1-Decyl-3-methylimidazolium trifluoromethanesulfonate	37.1 ± 3.0	43.0 ± 4.1	2.1

Table 3
The positive compounds from the primary compounds with AC50, Efficacy, and curve class

12 compounds induce phosphorylation on H2AX depending on Estrogen receptor

I re-cherry picked 128 compounds. Because MCF7 is a breast cancer cell line with an expression of estrogen receptor, I focused on Estrogen receptor-dependent DNA double strand break. To test the induction of phospho-H2AX depends on the estrogen receptor, I exposed the cells to the compounds with or without tamoxifen, an inhibitor for estrogen receptor. For 12 out of 128 compounds, the amount of phospho-H2AX was reduced by tamoxifen (Figure 48), suggesting their DNA damaging activities depend on estrogen receptor. These 12 compounds include practical drugs and food chemicals.

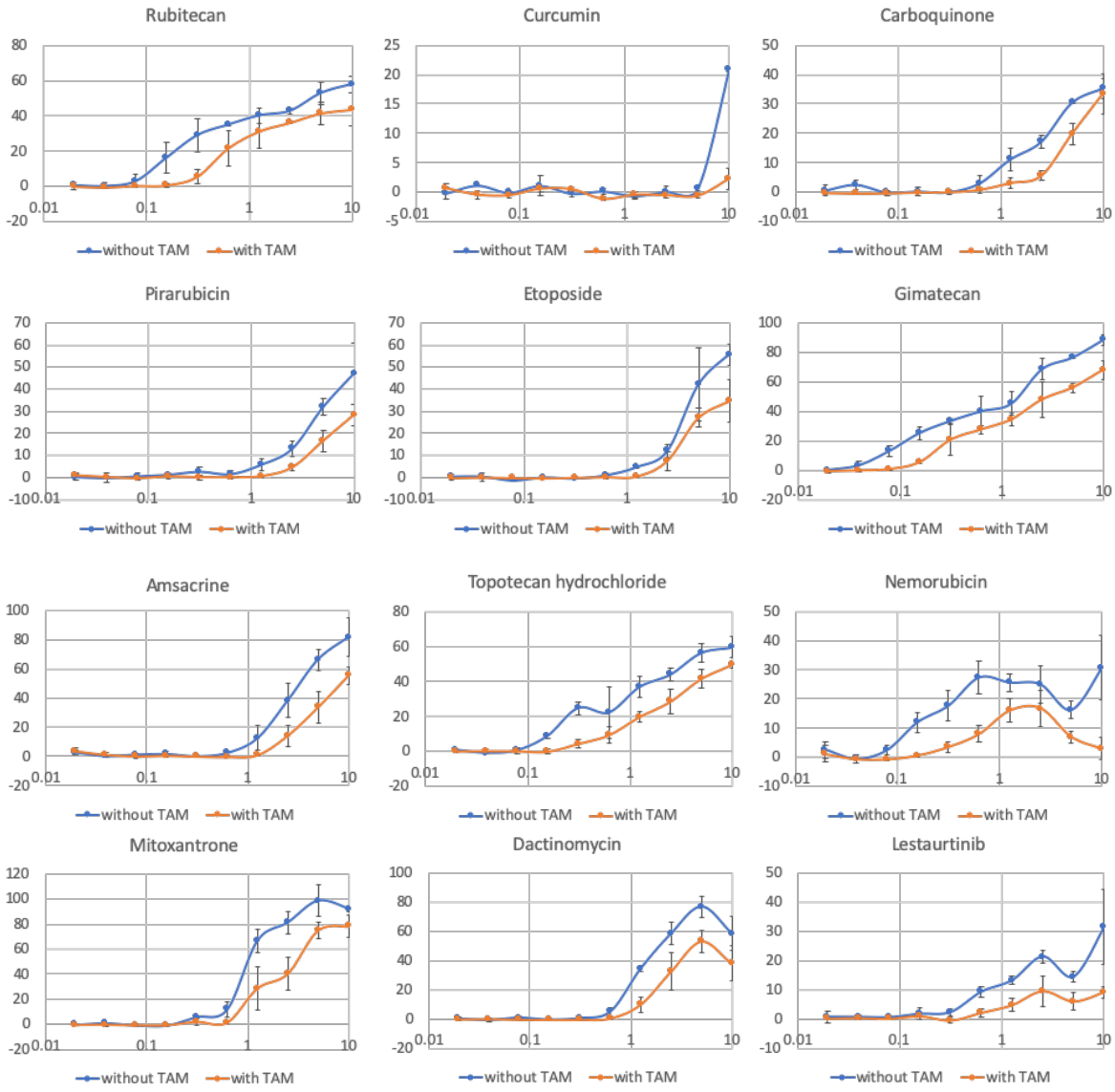

Figure 48

The dose response curve for the indicated compounds. Cells are exposed to the compounds with Tamoxifen (Orange line) or without Tamoxifen (Blue line). Y axis indicates the activity and X axis indicates the dose.

3-4 Discussion

In this study, I optimized the high throughput/ high content screening assay format to detect DNA double strand breaks in 1536 well plate format. In the previous cell-based screening system, the data was obtained from the population. Since high content screening applies imaging based data analysis, it can observe the event in each single cell. I identified 128 DSB inducers. I identified 14 compounds, which induce DNA double strand breaks via the activation of the estrogen receptor.

The new assay I optimized utilizes antibody reaction which allow us to identify the compounds that have specific activity in the cells. For example, this assay can be used to identify the disrupter of certain proteins. Current drug discovery focuses on molecular mechanism. Although many researches about molecular mechanism allow us to plan the strategy for the drug discovery, there was no efficient assay system to utilizes the molecular mechanism data. This assay helps us to efficiently identify molecular-targeting drug for chemotherapies, which reduce unexpected side effects.

General Discussion

In this study, I investigated the molecular mechanism related to ALC1 and DDX11 to maintain genome information. The information helps us to develop molecular targeting chemotherapy. In addition, I have created a high throughput drug screening system, based on the DNA repair mechanism in cells, to potentially create a novel cancer chemotherapy through synthetic lethality using specific inhibitors for DNA repair enzymes.

In chapter 1, I focused on the role of ALC1 in the repair of base damage and CPT-induced DNA damage. Base damage is the most common DNA damage. Although BER is well studied repair pathway, there still are many things unknown. PARP, XRCC1 and Polβ plays main role in BER (Sharbeen et al., 2015). Recently, ALC1 was found to have the PARP interacting domain in the structure (Ahel et al, 2010). However, the role played by ALC1 and interaction with PARP is largely unknown. I found the epistatic relationship between ALC1 and PARP. Moreover, ALC1 works as a chromatin remodeler independently of XRCC1 and Polβ. I also found ALC1 works with PARP in the repair of Camptothecin (CPT)-induced DNA damage. CPT is used for a cancer chemotherapy. CPT inhibits re-sealing step of DNA topoisomerase-I during DNA replication, and thereby induces SSBs associated with TopI-cc their 3' end. This data suggests that ALC1 works on DNA replication. BER pathway is independent of DNA replication. The data suggests ALC1's possible role on DNA replication. The over expression of ALC1 reduces 5-year survival after diagnosis of liver cancer (https://www.proteinatlas.org/). This may be because over expression of ALC1 induces unscheduled chromatin remodeling, leading to toxic translocation.

In chapter 2, I investigated the role of DDX11. DDX11 is mutated in Warsaw breakage syndrome (WABS). The cells from WABS patient shows similar phenotype to the cells from Fanconi Anemia patients. The cells are sensitive to DNA inter-strand crosslink (ICL). I found that DDX11 works as a backup pathway for Fanconi anemia pathway in the repair of ICL. I also found DDX11 works in the DNA replication. In the immunoglobulin diversification assay, DDX11 mutant shows less gene conversion rate and point mutation rate, suggesting DDX11 have a role in both homologous recombination-mediated template switch and translesion DNA synthesis. While DDX11 is known to work in homologous recombination

as a helicase, the role played by DDX11 in TLS has been unappreciated and this study newly identified this function.

Molecular biological studies, as I did in chapter 1 and 2, helps us to establish new approach for cancer chemotherapy. Inhibition of two proteins in a certain combination, as DDX11 and Fanconi anemia proteins, prevents cell proliferation. This effect is referred to as a synergistic effect. The most successful molecular targeting chemotherapy is olaparib. Olaparib inhibits PARP. PARP is in the synergistic relationship with BRCA1. Mutation on *BRCA1* increases the risk for breast cancer, which is why olaparib is widely used for breast cancer chemotherapy. However, not many molecular targeting drugs are used. One of the reasons is that the relationship between genes are largely unknown. Another reason is there are no appropriate methods to screen the drug.

In chapter 3, I aimed to establish the screening system focusing on molecular function. In the lab environment, there are many methods to test protein accumulation, but they are too low throughput to carry out drug screening. I optimized antibody-based screening system to detect protein accumulation in high throughput screening format. In this study, I used γH2AX (phosphorylated H2AX), which is used as a biomarker for DNA double strand break, as a model for assay development.

In the screening, I used MCF7 breast cancer cell line for the assay optimization. I screened 907 compounds from Tox21-10K chemical library at the National Center for Advancing Translational Science/ National Institutes of Health (NCATS/NIH). These compounds were directly or indirectly related to DSB from previous screenings done at NCATS/NIH (Hsieh et al., 2019). The average CV value, S/B ratio, and Z' factor from the primary screen of 21 assay plates were 14.85%, 5.53, and 0.32, respectively. The compounds, with efficacy of >3SD from the negative control (DMSO), were considered active and potential γH2AX inducers. A total of 128 potential inducers were identified from the primary screening. Since MCF7 express estrogen receptor, I sought to identify compounds, which cause DNA double strand breaks through estrogen receptor activation. I identified 12 compounds with the criteria. The result suggests that it is easy to modify the condition depending on the purpose.

In this study, I achieved three things. First, that ALC1 works as a chromatin remodeler together with PARP in BER. ALC1 also works in the repair of Camptothecin-induced DNA damage. Second, that DDX11 works as a backup of Fanconi anemia pathway in the repair of ICLs. Furthermore, I identified DDX11's role in DNA replication and the relationship

between DDX11 and other proteins which work to tolerate DNA replication stress. Finally, I optimized a high throughput imaging analysis to measure the amount of DNA damage in cells caused by environmental chemicals.

Publication list

1. “Two-dimensional cellular and three-dimensional bio-printed skin models to screen topical-use compounds for irritation potential” Wei, Z; Liu, X; **Ooka, M**; Zhang, L; Song, M.J.; Huang, R; Kleinstreuer, N.C.; Simeonov, A; Xia, M and Ferrer, M, 2020, *Frontier Bioengineering and Biotechnology*, fbioe.2020.00109
2. “PDIP38/PolDIP2 controls the DNA damage tolerance pathways by increasing the relative usage of translesion DNA synthesis over template switching” Tsuda, M; Ogawa, S; **Ooka, M**; Kobayashi, K; Hirota, K; Wakasugi, M, Matsunaga, T; Sakuma, T; Yamamoto, T; Chikuma, S; Sasanuma, H; Debatisse, M; Doherty, A.J.; Fuchs, R.P.; Takeda, S, 2019, *PLOS ONE* Vol.14 Issue.3 e0213383
3. “Warsaw breakage syndrome DDX11 helicase acts jointly with RAD17 in the repair of bulky lesions and replication through abasic sites” Abe, T; **Ooka, M(co-first)**; Kawasumi, R; Miyata, K; Takata, M; Hirota, K; Branzei, D, 2018, *PROCEEDINGS OF THE NATIONAL ACADEMY OF SCIENCES OF THE UNITED STATES OF AMERICA*, Vol.115, Issue.33 8412-8417
4. “SPARTAN promotes genetic diversification of the immunoglobulin-variable gene locus in avian DT40 cells” Nakazato, A; Kajita, K; **Ooka, M(co-first)**; Akagawa, R; Abe, T; Takeda, S; Branzei, D; Hirota, K, 2018, *DNA REPAIR*, Vol.68 50-57
5. “Chromatin remodeler ALC1 prevents replication-fork collapse by slowing fork progression” **Ooka, M**; Abe, T; Cho, K; Koike, K; Takeda, S; Hirota, K, 2018, *PLOS ONE*, Vol.13, Issue.2 e0192421
6. “ALC1/CHD1L, a chromatin-remodeling enzyme, is required for efficient base excision repair” Tsuda, M; Cho, K; **Ooka, M**; Shimizu, N; Watanabe, R; Yasui, A; Nakazawa, Y; Ogi, T; Harada, H; Agama, K; Nakamura, J; Asada, R; Fujiike, H; Sakuma, T; Yamamoto, T; Murai, J; Hiraoka, M; Koike, K; Pommier, Y; Takeda, S; Hirota, K, *PLOS ONE*, 2017, Vol.102, Issue.11 e0188320
7. “The dominant role of proofreading exonuclease activity of replicative polymerase epsilon in cellular tolerance to cytarabine (Ara-C)” Tsuda, M; Terada, K; **Ooka, M**; Kobayashi, K; Sasanuma, H; Fujisawa, R; Tsurimoto, T; Yamamoto, J; Iwai, S; Kadoda, K; Akagawa, R; Huang, SYN ; Pommier, Y; Sale, JE; Takeda, S; Hirota, K, 2017, *ONCOTARGET*, Vol.8 Issue.20 33457-22474
8. “Determination of genotoxic potential by comparison of structurally related azo dyes using DNA repair-deficient DT40 mutant panels” **Ooka, M**; Kobayashi, K; Abe, T; Akiyama, K; Hada, M; Takeda, S; Hirota, K, 2016, *CHEMOSPHERE*, Vol.164 106-112
9. “Cytotoxic and genotoxic profiles of benzo[a]pyrene and N-nitrosodimethylamine demonstrated using DNA repair deficient DT40 cells with metabolic activation” **Ooka, M**; Takazawa, H; Takeda, S; Hirota, K, 2016, *CHEMOSPHERE*, Vol.144 1901-1907

10. “Distinct DNA Damage Spectra Induced by Ionizing Radiation in Normoxic and Hypoxic Cells” Shimizu, N; **Ooka, M(co-first)**; Takagi, T; Takeda, S; Hirota, K, 2015, *Radiation Research*, Vol.184, Issue.4, 442-448
11. “Development of a Targeted Flip-in System in Avian DT40 Cells” Kobayashi, K; Fujii, T; Asada, R; **Ooka, M**; Hirota, K, 2015, *PLOS ONE*, Vol.10, Issue.3, e0122006

References

Abe, T., Branzei, D., and Hirota, K. (2018). DNA Damage Tolerance Mechanisms Revealed from the Analysis of Immunoglobulin V Gene Diversification in Avian DT40 Cells. Genes *9*, 18.

Ahel, D., Horejsi, Z., Wiechens, N., Polo, S.E., Garcia-Wilson, E., Ahel, I., Flynn, H., Skehel, M., West, S.C., Jackson, S.P*., et al.* (2009). Poly(ADP-ribose)-Dependent Regulation of DNA Repair by the Chromatin Remodeling Enzyme ALC1. Science *325*, 1240-1243.

Allred, D.C., Brown, P., and Medina, D. (2004). The origins of estrogen receptor alpha-positive and estrogen receptor alpha-negative human breast cancer. Breast Cancer Res *6*, 240-245.

Arakawa, H., Moldovan, G.L., Saribasak, H., Saribasak, N.N., Jentsch, S., and Buerstedde, J.M. (2006). A role for PCNA ubiquitination in immunoglobulin hypermutation. Plos Biology *4*, 1947-1956.

Bailey, C., Fryer, A.E., and Greenslade, M. (2015). Warsaw Breakage Syndrome - A further report, emphasising cutaneous findings. European Journal of Medical Genetics *58*, 235-237.

Bailey, L.J., and Doherty, A.J. (2017). Mitochondrial DNA replication: a PrimPol perspective. Biochem Soc Trans *45*, 513-529.

Bharti, S.K., Khan, I., Banerjee, T., Sommers, J.A., Wu, Y., and Brosh, R.M., Jr. (2014a). Molecular functions and cellular roles of the ChlR1 (DDX11) helicase defective in the rare cohesinopathy Warsaw breakage syndrome. Cellular and Molecular Life Sciences *71*, 2625-2639.

Bharti, S.K., Khan, I., Banerjee, T., Sommers, J.A., Wu, Y.L., and Brosh, R.M. (2014b). Molecular functions and cellular roles of the ChlR1 (DDX11) helicase defective in the rare cohesinopathy Warsaw breakage syndrome. Cellular and Molecular Life Sciences *71*, 2625-2639.

Bottega, R., Napolitano, L.M.R., Carbone, A., Cappelli, E., Corsolini, F., Onesti, S., Savoia, A., Gasparini, P., and Faletra, F. (2019). Two further patients with Warsaw breakage syndrome. Is a mild phenotype possible? Mol Genet Genom Med *7*, 6.

Braafladt, S., Reipa, V., and Atha, D.H. (2016). The Comet Assay: Automated Imaging Methods for Improved Analysis and Reproducibility. Scientific Reports *6*.

Buerstedde, J.M., and Takeda, S. (1991). INCREASED RATIO OF TARGETED TO RANDOM INTEGRATION AFTER TRANSFECTION OF CHICKEN B-CELL LINES. Cell *67*, 179-188.

Buhl, S.N., Setlow, R.B., and Regan, J.D. (1973). RECOVERY OF ABILITY TO SYNTHESIZE DNA IN SEGMENTS OF NORMAL SIZE AT LONG TIMES AFTER ULTRAVIOLET-IRRADIATION OF HUMAN CELLS. Biophysical Journal *13*, 1265-1275.

Buhl, S.N., Stillman, R.M., Setlow, R.B., and Regan, J.D. (1972). DNA CHAIN ELONGATION AND JOINING IN NORMAL HUMAN AND XERODERMA PIGMENTOSUM CELLS AFTER ULTRAVIOLET-IRRADIATION. Biophysical Journal *12*, 1183-&.

Bunting, S.F., Callen, E., Wong, N., Chen, H.-T., Polato, F., Gunn, A., Bothmer, A., Feldhahn, N., Fernandez-Capetillo, O., Cao, L*., et al.* (2010). 53BP1 Inhibits Homologous Recombination in Brca1-Deficient Cells by Blocking Resection of DNA Breaks. Cell *141*, 243-254.

Burkle, A. (2001). Physiology and pathophysiology of poly(ADP-ribosyl)ation. Bioessays *23*, 795-806.

Capo-Chichi, J.-M., Bharti, S.K., Sommers, J.A., Yammine, T., Chouery, E., Patry, L., Rouleau, G.A., Samuels, M.E., Hamdan, F.F., Michaud, J.L*., et al.* (2013). Identification and Biochemical Characterization of a Novel Mutation in DDX11 Causing Warsaw Breakage Syndrome. Human Mutation *34*, 103-107.

Ceccaldi, R., Parmar, K., Mouly, E., Delord, M., Kim, J.M., Regairaz, M., Pla, M., Vasquez, N., Zhang, Q.S., Pondarre, C*., et al.* (2012). Bone Marrow Failure in Fanconi Anemia Is Triggered by an

Exacerbated p53/p21 DNA Damage Response that Impairs Hematopoietic Stem and Progenitor Cells. Cell Stem Cell *11*, 36-49.
Ceccaldi, R., Rondinelli, B., and D'Andrea, A.D. (2016a). Repair Pathway Choices and Consequences at the Double-Strand Break. Trends Cell Biol *26*, 52-64.
Ceccaldi, R., Sarangi, P., and D'Andrea, A.D. (2016b). The Fanconi anaemia pathway: newyplayers and new functions. Nature Reviews Molecular Cell Biology *17*, 337-349.
Chaudhuri, A.R., Hashimoto, Y., Herrador, R., Neelsen, K.J., Fachinetti, D., Bermejo, R., Cocito, A., Costanzo, V., and Lopes, M. (2012). Topoisomerase I poisoning results in PARP-mediated replication fork reversal. Nature Structural & Molecular Biology *19*, 417-423.
Cong, L., Ran, F.A., Cox, D., Lin, S.L., Barretto, R., Habib, N., Hsu, P.D., Wu, X.B., Jiang, W.Y., Marraffini, L.A*., et al.* (2013). Multiplex Genome Engineering Using CRISPR/Cas Systems. Science *339*, 819-823.
Cota, C.D., and Garcia-Garcia, M.J. (2012). The ENU-induced cetus mutation reveals an essential role of the DNA helicase DDX11 for mesoderm development during early mouse embryogenesis. Developmental Dynamics *241*, 1249-1259.
Daley, J.M., and Sung, P. (2014). 53BP1, BRCA1, and the choice between recombination and end joining at DNA double-strand breaks. Mol Cell Biol *34*, 1380-1388.
Eppley, S., Hopkin, R.J., Mendelsohn, B., and Slavotinek, A.M. (2017). Clinical Report: Warsaw Breakage Syndrome with small radii and fibulae. American Journal of Medical Genetics Part A *173*, 3075-3081.
Farina, A., Shin, J.-H., Kim, D.-H., Bermudez, V.P., Kelman, Z., Seo, Y.-S., and Hurwitz, J. (2008). Studies with the human cohesin establishment factor, ChlR1 - Association of ChlR1 with Ctf18-RFC and Fen1. Journal of Biological Chemistry *283*, 20925-20936.
Farmer, H., McCabe, N., Lord, C.J., Tutt, A.N., Johnson, D.A., Richardson, T.B., Santarosa, M., Dillon, K.J., Hickson, I., Knights, C*., et al.* (2005). Targeting the DNA repair defect in BRCA mutant cells as a therapeutic strategy. Nature *434*, 917-921.
Friedenson, B. (2005). BRCA1 and BRCA2 pathways and the risk of cancers other than breast or ovarian. MedGenMed *7*, 60.
Ganem, N.J., and Pellman, D. (2012). Linking abnormal mitosis to the acquisition of DNA damage. Journal of Cell Biology *199*, 871-881.
Gómez-Herreros, F., Romero-Granados, R., Zeng, Z., Alvarez-Quilón, A., Quintero, C., Ju, L., Umans, L., Vermeire, L., Huylebroeck, D., Caldecott, K.W*., et al.* (2013). TDP2-dependent non-homologous end-joining protects against topoisomerase II-induced DNA breaks and genome instability in cells and in vivo. PLoS Genet *9*, e1003226.
Hashimoto, Y., Chaudhuri, A.R., Lopes, M., and Costanzo, V. (2010). Rad51 protects nascent DNA from Mre11-dependent degradation and promotes continuous DNA synthesis. Nature Structural & Molecular Biology *17*, 1305-U1268.
Hauf, S., Roitinger, E., Koch, B., Dittrich, C.M., Mechtler, K., and Peters, J.M. (2005). Dissociation of cohesin from chromosome arms and loss of arm cohesion during early mitosis depends on phosphorylation of SA2. Plos Biology *3*, 419-432.
Henry-Mowatt, J., Jackson, D., Masson, J.Y., Johnson, P.A., Clements, P.M., Benson, F.E., Thompson, L.H., Takeda, S., West, S.C., and Caldecott, K.W. (2003). XRCC3 and Rad51 modulate replication fork progression on damaged vertebrate chromosomes. Molecular Cell *11*, 1109-1117.
Hirota, K., Miyoshi, T., Kugou, K., Hoffman, C.S., Shibata, T., and Ohta, K. (2008). Stepwise chromatin remodelling by a cascade of transcription initiation of non-coding RNAs. Nature *456*, 130-U115.
Hirota, K., Tsuda, M., Mohiuddin, Tsurimoto, T., Cohen, I.S., Livneh, Z., Kobayashi, K., Narita, T., Nishihara, K., Murai, J*., et al.* (2016). In vivo evidence for translesion synthesis by the replicative

DNA polymerase delta. Nucleic Acids Research *44*, 7242-7250.
Hoa, N.N., Shimizu, T., Zhou, Z.W., Wang, Z.Q., Deshpande, R.A., Paull, T.T., Akter, S., Tsuda, M., Furuta, R., Tsutsui, K.*, et al.* (2016). Mre11 Is Essential for the Removal of Lethal Topoisomerase 2 Covalent Cleavage Complexes. Mol Cell *64*, 580-592.
Huang, R., Xia, M., Sakamuru, S., Zhao, J., Shahane, S.A., Attene-Ramos, M., Zhao, T., Austin, C.P., and Simeonov, A. (2016). Modelling the Tox21 10 K chemical profiles for in vivo toxicity prediction and mechanism characterization. Nat Commun *7*, 10425.
Huang, W., Peng, Y., Kiselar, J., Zhao, X., Albaqami, A., Mendez, D., Chen, Y.H., Chakravarthy, S., Gupta, S., Ralston, C.*, et al.* (2018). Multidomain architecture of estrogen receptor reveals interfacial cross-talk between its DNA-binding and ligand-binding domains. Nature Communications *9*.
Ishiai, M., Kitao, H., Smogorzewska, A., Tomida, J., Kinomura, A., Uchida, E., Saberi, A., Kinoshita, E., Kinoshita-Kikuta, E., Koike, T.*, et al.* (2008). FANCI phosphorylation functions as a molecular switch to turn on the Fanconi anemia pathway. Nature Structural & Molecular Biology *15*, 1138-1146.
Ji, K., Kogame, T., Choi, K., Wang, X., Lee, J., Taniguchi, Y., and Takeda, S. (2009). A Novel Approach Using DNA-Repair-Deficient Chicken DT40 Cell Lines for Screening and Characterizing the Genotoxicity of Environmental Contaminants. Environ Health Perspect *117*, 1737-1744.
Ju, B.G., Lunyak, V.V., Perissi, V., Garcia-Bassets, I., Rose, D.W., Glass, C.K., and Rosenfeld, M.G. (2006). A topoisomerase IIbeta-mediated dsDNA break required for regulated transcription. Science *312*, 1798-1802.
Karras, G.I., Fumasoni, M., Sienski, G., Vanoli, F., Branzei, D., and Jentsch, S. (2013). Noncanonical Role of the 9-1-1 Clamp in the Error-Free DNA Damage Tolerance Pathway. Molecular Cell *49*, 536-546.
Karras, G.I., Kustatscher, G., Buhecha, H.R., Allen, M.D., Pugieux, C., Sait, F., Bycroft, M., and Ladurner, A.G. (2005). The macro domain is an ADP-ribose binding module. Embo Journal *24*, 1911-1920.
Kelley, M.R., and Fishel, M.L. (2016). OVERVIEW OF DNA REPAIR PATHWAYS, CURRENT TARGETS, AND CLINICAL TRIALS BENCH TO CLINIC. In DNA Repair in Cancer Therapy: Molecular Targets and Clinical Applications, 2nd Edition, M.R. Kelley, and M.L. Fishel, eds. (London: Academic Press Ltd-Elsevier Science Ltd), pp. 1-54.
Khanna, K.K., and Jackson, S.P. (2001). DNA double-strand breaks: signaling, repair and the cancer connection. Nat Genet *27*, 247-254.
Kobayashi, K., Guilliam, T.A., Tsuda, M., Yamamoto, J., Bailey, L.J., Iwai, S., Takeda, S., Doherty, A.J., and Hirota, K. (2016). Repriming by PrimPol is critical for DNA replication restart downstream of lesions and chain-terminating nucleosides. Cell Cycle *15*, 1997-2008.
Kohzaki, M., Nishihara, K., Hirota, K., Sonoda, E., Yoshimura, M., Ekino, S., Butler, J.E., Watanabe, M., Halazonetis, T.D., and Takeda, S. (2010). DNA polymerases nu and theta are required for efficient immunoglobulin V gene diversification in chicken. Journal of Cell Biology *189*, 1117-1127.
Kottemann, M.C., and Smogorzewska, A. (2013). Fanconi anaemia and the repair of Watson and Crick DNA crosslinks. Nature *493*, 356-363.
Lee, S., Liu, X., Takeda, S., and Choi, K. (2013). Genotoxic potentials and related mechanisms of bisphenol A and other bisphenol compounds: A comparison study employing chicken DT40 cells. Chemosphere *93*, 434-440.
Lehmann, A.R. (1972). POSTREPLICATION REPAIR OF DNA IN ULTRAVIOLET-IRRADIATED MAMMALIAN-CELLS. Journal of Molecular Biology *66*, 319-&.
Lehmann, A.R., Kirkbell, S., Arlett, C.F., Harcourt, S.A., Weerdkastein, E.A.D., Keijzer, W., and Hallsmith, P. (1977). REPAIR OF ULTRAVIOLET-LIGHT DAMAGE IN A VARIETY OF HUMAN FIBROBLAST CELL STRAINS. Cancer Research *37*, 904-910.
Li, S., Hsu, C.W., Sakamuru, S., Zou, C., Huang, R., and Xia, M. (2018). Identification of

Angiogenesis Inhibitors Using a Co-culture Cell Model in a High-Content and High-Throughput Screening Platform. SLAS Technol *23*, 217-225.
Lim, P.X., Patel, D.R., Poisson, K.E., Basuita, M., Tsai, C., Lyndaker, A.M., Hwang, B.-J., Lu, A.L., and Weiss, R.S. (2015). Genome Protection by the 9-1-1 Complex Subunit HUS1 Requires Clamp Formation, DNA Contacts, and ATR Signaling-independent Effector Functions. Journal of Biological Chemistry *290*, 14826-14840.
Lin, W., Hashimoto, S.I., Seo, H., Shibata, T., and Ohta, K. (2008). Modulation of immunoglobulin gene conversion frequency and distribution by the histone deacetylase HDAC2 in chicken DT40. Genes Cells *13*, 255-268.
Liu, Y.A., Prasad, R., Beard, W.A., Kedar, P.S., Hou, E.W., Shock, D.D., and Wilson, S.H. (2007). Coordination of steps in single-nucleotide base excision repair mediated by apurinic/apyrimidinic endonuclease 1 and DNA polymerase beta. Journal of Biological Chemistry *282*, 13532-13541.
Maya-Mendoza, A., Moudry, P., Merchut-Maya, J.M., Lee, M., Strauss, R., and Bartek, J. (2018). High speed of fork progression induces DNA replication stress and genomic instability. Nature *559*, 279-+.
Murai, J., Huang, S.-y.N., Das, B.B., Renaud, A., Zhang, Y., Doroshow, J.H., Ji, J., Takeda, S., and Pommier, Y. (2012). Trapping of PARP1 and PARP2 by Clinical PARP Inhibitors. Cancer Research *72*, 5588-5599.
Narod, S.A., and Foulkes, W.D. (2004). BRCA1 and BRCA2: 1994 and beyond. Nat Rev Cancer *4*, 665-676.
Nik-Zainal, S., Davies, H., Staaf, J., Ramakrishna, M., Glodzik, D., Zou, X.Q., Martincorena, I., Alexandrov, L.B., Martin, S., Wedge, D.C.*, et al.* (2019). Landscape of somatic mutations in 560 breast cancer whole-genome sequences (vol 534, pg 47, 2016). Nature *566*, E1-E1.
Pines, A., Vrouwe, M.G., Marteijn, J.A., Typas, D., Luijsterburg, M.S., Cansoy, M., Hensbergen, P., Deelder, A., de Groot, A., Matsumoto, S.*, et al.* (2012). PARP1 promotes nucleotide excision repair through DDB2 stabilization and recruitment of ALC1. Journal of Cell Biology *199*, 235-249.
Pommier, Y. (2006). Topoisomerase I inhibitors: camptothecins and beyond. Nature Reviews Cancer *6*, 789-802.
Pommier, Y. (2009). DNA Topoisomerase I Inhibitors: Chemistry, Biology, and Interfacial Inhibition. Chemical Reviews *109*, 2894-2902.
Pommier, Y., Sun, Y., Huang, S.N., and Nitiss, J.L. (2016). Roles of eukaryotic topoisomerases in transcription, replication and genomic stability. Nat Rev Mol Cell Biol *17*, 703-721.
Prakash, R., Zhang, Y., Feng, W.R., and Jasin, M. (2015). Homologous Recombination and Human Health: The Roles of BRCA1, BRCA2, and Associated Proteins. Cold Spring Harbor Perspectives in Biology *7*.
Rantakari, P., Nikkila, J., Jokela, H., Ola, R., Pylkas, K., Lagerbohm, H., Sainio, K., Poutanen, M., and Winqvist, R. (2010). Inactivation of Palb2 gene leads to mesoderm differentiation defect and early embryonic lethality in mice. Hum Mol Genet *19*, 3021-3029.
Rossouw, J.E., Anderson, G.L., Prentice, R.L., LaCroix, A.Z., Kooperberg, C., Stefanick, M.L., Jackson, R.D., Beresford, S.A.A., Howard, B.V., Johnson, K.C.*, et al.* (2002). Risks and benefits of estrogen plus progestin in healthy postmenopausal women - Principal results from the Women's Health Initiative randomized controlled trial. JAMA-J Am Med Assoc *288*, 321-333.
Saberi, A., Hochegger, H., Szuts, D., Lan, L., Yasui, A., Sale, J.E., Taniguchi, Y., Murakawa, Y., Zeng, W., Yokomori, K.*, et al.* (2007). RAD18 and poly(ADP-ribose) polymerase independently suppress the access of nonhomologous end joining to double-strand breaks and facilitate homologous recombination-mediated repair. Molecular and Cellular Biology *27*, 2562-2571.
Saberi, A., Nakahara, M., Sale, J.E., Kikuchi, K., Arakawa, H., Buerstedde, J.M., Yamamoto, K., Takeda, S., and Sonoda, E. (2008). The 9-1-1 DNA clamp is required for immunoglobulin gene

conversion. Molecular and Cellular Biology *28*, 6113-6122.
Saha, L.K., Kim, S., Kang, H., Akter, S., Choi, K., Sakuma, T., Yamamoto, T., Sasanuma, H., Hirota, K., Nakamura, J.*, et al.* (2018). Differential micronucleus frequency in isogenic human cells deficient in DNA repair pathways is a valuable indicator for evaluating genotoxic agents and their genotoxic mechanisms. Environmental and Molecular Mutagenesis *59*, 529-538.
Saldivar, J.C., Cortez, D., and Cimprich, K.A. (2017). The essential kinase ATR: ensuring faithful duplication of a challenging genome. Nature Reviews Molecular Cell Biology *18*, 622-636.
Sasanuma, H., Tsuda, M., Morimoto, S., Saha, L.K., Rahman, M.M., Kiyooka, Y., Fujiike, H., Cherniack, A.D., Itou, J., Callen Moreu, E.*, et al.* (2018). BRCA1 ensures genome integrity by eliminating estrogen-induced pathological topoisomerase II-DNA complexes. Proc Natl Acad Sci U S A *115*, E10642-E10651.
Schiewer, M.J., and Knudsen, K.E. (2014). Transcriptional Roles of PARP1 in Cancer. Mol Cancer Res *12*, 1069-1080.
Seiler, J.A., Conti, C., Syed, A., Aladjem, M.I., and Pommier, Y. (2007). The intra-S-phase checkpoint affects both DNA replication initiation and elongation: Single-cell and -DNA fiber analyses. Molecular and Cellular Biology *27*, 5806-5818.
Sekar, R.B., and Periasamy, A. (2003). Fluorescence resonance energy transfer (FRET) microscopy imaging of live cell protein localizations. Journal of Cell Biology *160*, 629-633.
Shinohara, M., Sakai, K., Ogawa, T., and Shinohara, A. (2003). The mitotic DNA damage checkpoint proteins Rad17 and Rad24 are required for repair of double-strand breaks during meiosis in yeast. Genetics *164*, 855-865.
Stoepker, C., Faramarz, A., Rooimans, M.A., van Mil, S.E., Balk, J.A., Velleuer, E., Ameziane, N., te Riele, H., and de Winter, J.P. (2015). DNA helicases FANCM and DDX11 are determinants of PARP inhibitor sensitivity. DNA Repair *26*, 54-64.
Stork, C.T., Bocek, M., Crossley, M.P., Sollier, J., Sanz, L.A., Chedin, F., Swigut, T., and Cimprich, K.A. (2016). Co-transcriptional R-loops are the main cause of estrogen-induced DNA damage. eLife *5*, 21.
Sugimura, K., Takebayashi, S.-i., Taguchi, H., Takeda, S., and Okumura, K. (2008). PARP-1 ensures regulation of replication fork progression by homologous recombination on damaged DNA. Journal of Cell Biology *183*, 1203-1212.
Suzuki, A., delaPompa, J.L., Hakem, R., Elia, A., Yoshida, R., Mo, R., Nishina, H., Chuang, T., Wakeham, A., Itie, A.*, et al.* (1997). Brca2 is required for embryonic cellular proliferation in the mouse. Genes & Development *11*, 1242-1252.
Takata, M., Sasaki, M.S., Sonoda, E., Morrison, C., Hashimoto, M., Utsumi, H., Yamaguchi-Iwai, Y., Shinohara, A., and Takeda, S. (1998). Homologous recombination and non-homologous end-joining pathways of DNA double-strand break repair have overlapping roles in the maintenance of chromosomal integrity in vertebrate cells. EMBO J *17*, 5497-5508.
Tutt, A., Robson, M., Garber, J.E., Domchek, S.M., Audeh, M.W., Weitzel, J.N., Friedlander, M., Arun, B., Loman, N., Schmutzler, R.K.*, et al.* (2010). Oral poly(ADP-ribose) polymerase inhibitor olaparib in patients with BRCA1 or BRCA2 mutations and advanced breast cancer: a proof-of-concept trial. Lancet *376*, 235-244.
Vaisman, A., and Woodgate, R. (2017). Translesion DNA polymerases in eukaryotes: what makes them tick? Crit Rev Biochem Mol Biol *52*, 274-303.
van der Kolk, D.M., de Bock, G.H., Leegte, B.K., Schaapveld, M., Mourits, M.J., de Vries, J., van der Hout, A.H., and Oosterwijk, J.C. (2010). Penetrance of breast cancer, ovarian cancer and contralateral breast cancer in BRCA1 and BRCA2 families: high cancer incidence at older age. Breast Cancer Res Treat *124*, 643-651.
Venkatesh, S., and Workman, J.L. (2015). Histone exchange, chromatin structure and the regulation

of transcription. Nat Rev Mol Cell Biol *16*, 178-189.
Venkitaraman, A.R. (2002). Cancer susceptibility and the functions of BRCA1 and BRCA2. Cell *108*, 171-182.
Wang, M.L., Wu, W.Z., Wu, W.Q., Rosidi, B., Zhang, L.H., Wang, H.C., and Iliakis, G. (2006). PARP-1 and Ku compete for repair of DNA double strand breaks by distinct NHEJ pathways. Nucleic Acids Research *34*, 6170-6182.
Weiss, R.S., Enoch, T., and Leder, P. (2000). Inactivation of mouse Hus1 results in genomic instability and impaired responses to genotoxic stress. Genes & Development *14*, 1886-1898.
Williamson, L.M., and Lees-Miller, S.P. (2011). Estrogen receptor α-mediated transcription induces cell cycle-dependent DNA double-strand breaks. Carcinogenesis *32*, 279-285.
Zellweger, R., Dalcher, D., Mutreja, K., Berti, M., Schmid, J.A., Herrador, R., Vindigni, A., and Lopes, M. (2015). Rad51-mediated replication fork reversal is a global response to genotoxic treatments in human cells. Journal of Cell Biology *208*, 563-579.

Acknowledgement

I would like to express the greatest appreciation to my supervisor, professor Kouji Hirota, for the instruction of this research, providing me a great research environment, teaching me how joyful science is. I'm grateful to Associate Professor Masato Taoka, Assistant professor Takuya Abe and Professor Takehiko Shibata for giving me many advises and the opportunity of discussion. I really thank Makiko Nakagawa for purchasing and managing my research grant. I really appreciate to Professor Shunichi Takeda (Kyoto University, Japan) and Professor Dana Branzei (IFOM, Italy) and Professor Menghang Xia (National Institutes of Health, America) for valuable discussion and helping in preparation of the publication. I also thank to Ryuta Asada, Toshihiko Fujii, Hironori Takazawa, Ryotaro Kawasumi, Kaori Kobayashi, Tokiyo Takagi, Satoshi Senmatsu, Keiji Miyata, Kinumi Kajita, Arisa Nakazato, Shinji Koyama, Koji Kobayashi, Yuya Suzuki, Koume Umemura, Chiaki Tsunekawa, Shota Sakaba, Yui Yoshimoto, Yuka Yamaki and all other Dr. Hirota's lab members and Hiroyuki Sasanuma, Remi Akagawa, Taiki Niki and all other Dr. Takeda's lab members and Ivan Psakhye, Weber Barzagli, Romeo Francesco, Beatrice Toia, Chinnu Rose Joseph, Clarisse Reyes, Mio Sumie and all other Dr. Branzei's lab members and Li Zhang, Zhengxi Wei and all Dr. Xia's lab members and Anne Lee Baskin for giving me the fun research life. Finally, I specially appreciate to my family for giving me the great environment I can concentrate to the research.